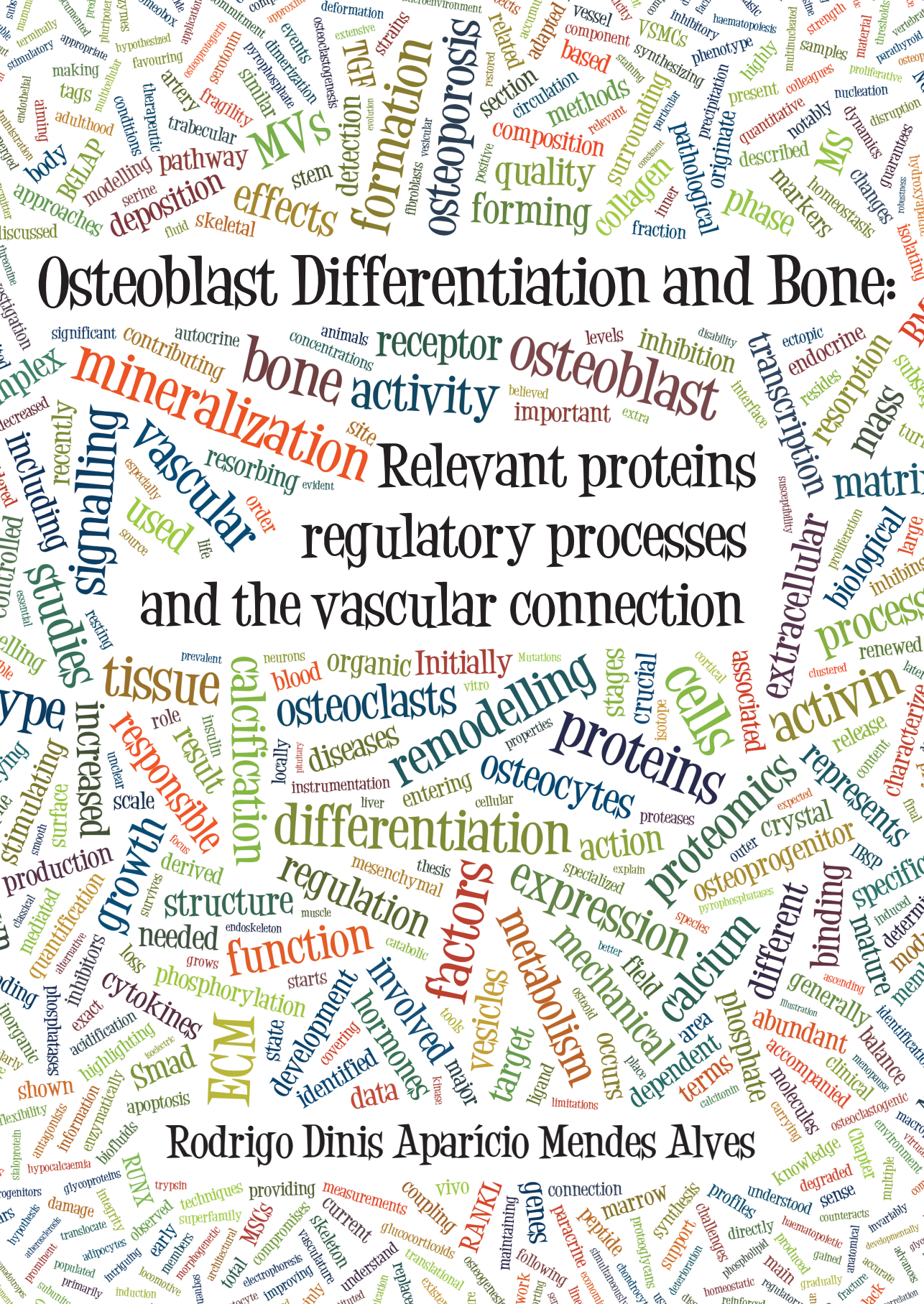
Osteoblast Differentiation and Bone:
Relevant proteins
regulatory processes
and the vascular connection
Rodrigo Dinis Aparício Mendes Alves

Osteoblast Differentiation and Bone: Relevant proteins, regulatory processes and the vascular connection

Osteoblast Differentiatie en Bot:
Belangrijke eiwitten, regulerende processen
en de vasculaire verbinding

Rodrigo Dinis Aparício Mendes Alves

Publication of this thesis was supported by:

Erasmus University
Nederlandse Vereniging voor Calcium- en Botstofwisseling (NVCB)

Cover: Thesis word cloud. Greater prominence is given to words that appear more frequently in this thesis. Created using Tagxedo (http://www.tagxedo.com).

Layout and design by Rodrigo D.A.M. Alves
Printed by Ipskamp Drukkers

ISBN: 978-94-6191-354-8

Osteoblast Differentiation and Bone: Relevant proteins, regulatory processes and the vascular connection

Osteoblast Differentiatie en Bot: Belangrijke eiwitten, regulerende processen en de vasculaire verbinding

Thesis

to obtain the degree of Doctor from the
Erasmus University Rotterdam
by command of the
rector magnificus

Prof. dr. H.G. Schmidt

and in accordance with the decision of the Doctorate Board.

The public defense shall be held on
Wednesday 5 September 2012 at 13.30 hrs

by

Rodrigo Dinis Aparício Mendes Alves
born in Loriga, Portugal

DOCTORAL COMMITTEE

Promotor:	Prof.dr. J.P.T.M. van Leeuwen
Co-Promotor:	Dr. M. Eijken
Other members:	Prof. dr. G. Carmeliet Dr. J.A.A. Demmers Prof. dr. D.J. Duncker Dr. G. Jenster Prof. dr. P.J. van der Spek Prof. dr. ir. H.H. Weinans
Paraninfs:	Dr. Bram C. J. van der Eerden Dr. Jeroen van de Peppel

The research here described was conducted at the Department of Internal Medicine in the Erasmus MC, Rotterdam, The Netherlands. All the studies described in this thesis were supported by ZonMW. The studies described in Chapter 2 were performed in collaboration with the Department of Neurology and Department of Bioinformatics of the Erasmus MC. The studies presented in Chapter 3 were done in close collaboration with the Proteomics Center of the Erasmus MC and supported by the European Calcified Tissue Society (ECTS). The studies presented in Chapter 4 were performed in collaboration with the Department of Orthopedics and the Proteomics Center of the Erasmus MC. The studies presented in Chapter 5 were supported by the ECTS. The unpublished data discussed in Chapter 6 results from a collaboration with the Proteomics Center of the Erasmus MC and was supported by the Netherlands Proteomics Centre.

To my family, to Leticia…

Sempre chegamos ao sítio aonde nos esperam.

José Saramago *in* A Viagem do Elefante

Contents

Osteoblast Differentiation and Bone: Relevant proteins, regulatory processes and the vascular connection

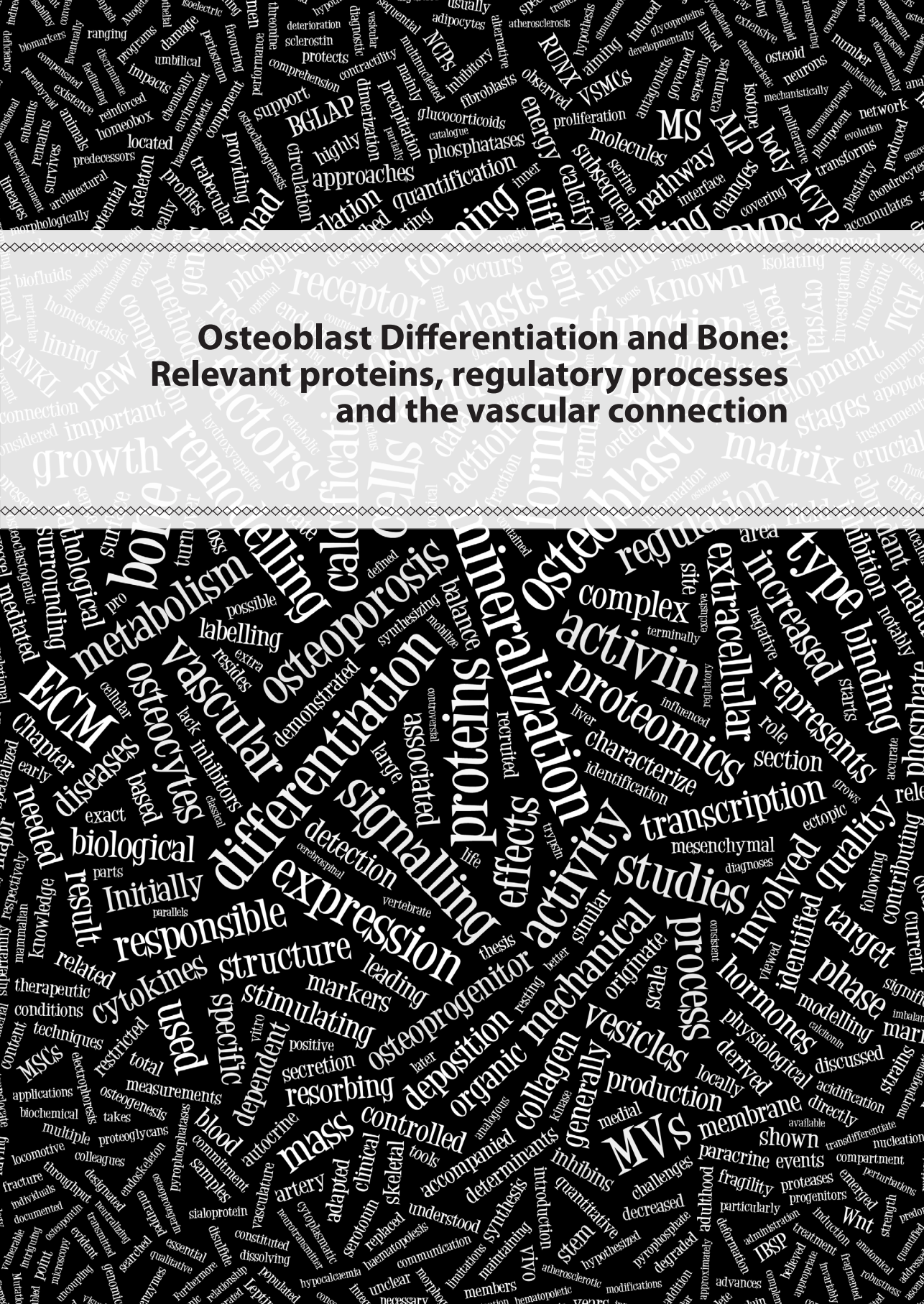

Chapter 1

General Introduction

1.1 BONE TISSUE

Bone is a highly specialized form of connective tissue present in most vertebrate animals as part of the endoskeleton. Structurally speaking, bone is mainly constituted by an organic extracellular matrix (ECM) hardened by deposited mineral. The blending between the organic and inorganic parts originates two main types of osseous tissue. The outer part of the tissue, the cortex, is hard compact bone and surrounds the inner trabecular bone, a spongy-like structure. In terms of function, bone provides mechanical support for the body, being a key component of the locomotive system, and protects vital organs, such as brain, spinal cord, heart and lungs from harmful impacts that could result in damage. Bone houses the bone marrow cavity as well as an extensive network of blood vessels. The interface between bone and these surrounding tissues is associated to its metabolic functions, such as supporting haematopoiesis and maintaining the blood calcium levels[1]. Besides the storage of calcium important for the body, the bone ECM is also a rich reservoir of cytokines and growth factors involved in autocrine, paracrine and endocrine[2] signaling.

1.2 BONE CELLS

The bone tissue is populated by four different cell types: osteoclasts, osteoblasts, osteocytes and bone lining cells (Figure 1). Osteoclasts are multinucleated cells derived form haematopoietic progenitors and responsible for degradation of bone (Figure 1). During bone resorption osteoclasts attach to the bone surface isolating the area to be degraded. The acidification of this area is responsible for dissolving the

inorganic ECM part while the subsequent action of different proteases guarantees the disassembling of the organic matrix[3]. The cells with opposite function to the bone resorbing osteoclasts are the osteoblasts. These bone forming cells are of mesenchymal origin and responsible for the production of new bone tissue (Figure 1), synthesizing first the organic matrix (i.e. the osteoid) and later on contributing to its mineralization[4]. At the end of this bone-forming phase, the majority of osteoblasts enter apoptosis. The remainder either survives entrapped in the mineralized ECM as terminally differentiated osteoblasts, now designated osteocytes, or covering the resting bone surface as bone lining cells[5] (Figure 1).

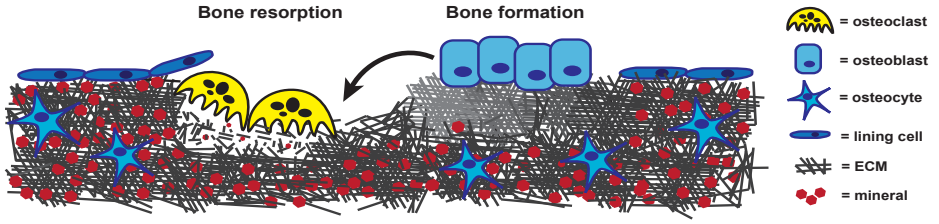

Figure 1. Bone cells and bone remodeling. Four functionally different types of cells reside in bone, 1) osteoclasts responsible for bone resorption, 2) osteoblasts responsible for bone formation, 3) osteocytes that sense mechanical strains and 4) lining cells covering a resting bone surface. The bone remodeling starts when osteoclasts are recruited and resorb bone by acidification of the ECM combined with the release of several proteases. The bone lost is then replaced with new bone matrix and mineralized by the action of osteoblasts.

1.3 OSTEOBLAST DIFFERENTIATION

Mesenchymal stem cells (MSCs) are pluripotent stem cells found at an increasing number of sites throughout the body, including bone marrow, fat, vasculature, liver and umbilical cord blood[6-9]. As stem cells, MSCs have the plasticity to commit into multiple cell lineages, giving rise to osteoblasts but also to chondrocytes, adipocytes, fibroblasts, myocytes, and neurons[10]. The osteoblast differentiation process is controlled by osteoblast specific transcription factors, runt-related transcription factor 2 (RUNX2)[11-13] and osterix (SP7)[14], in coordination with other transcription mediators, including distal-less homeobox-5 (DLX5) and msh homeobox homologue-2 (MSX2)[4, 15]. Osteoblast development begins with the proliferation and commitment of MSCs residing in the bone marrow and periosteum[16] into osteoprogenitor cells (Figure 2).

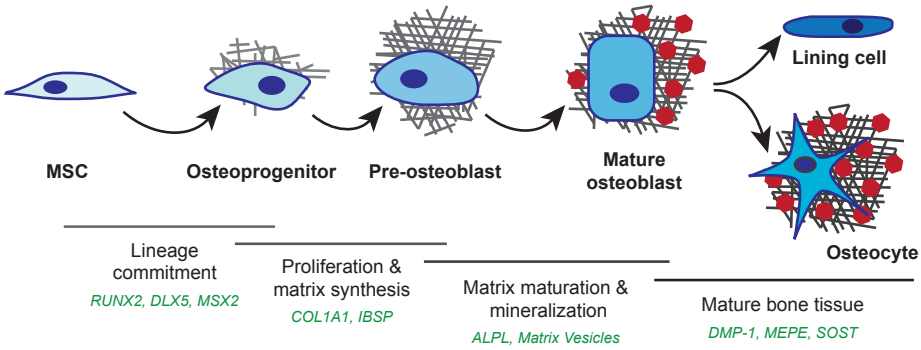

Figure 2. Osteoblast differentiation. Osteoblasts originate from mesenchymal stem cells in a sequential order of events governed by different transcription factors, cytokines, growth factors and ECM proteins. The different stages of osteoblast differentiation are accompanied by the expression of specific genes/proteins and matrix vesicles.

Little is known about the osteoprogenitor cell identity and what regulates their cellular fate. Despite having restricted proliferative profile, they are neither morphologically different from their MSCs predecessors nor express osteoblast markers[17]. In the subsequent phase of development the osteoprogenitor cells become pre-osteoblasts (Figure 2) and start the ECM synthesis expressing first collagen type I α1 (COL1A1) and bone sialoprotein (IBSP). The pre-osteoblasts differentiate further into mature osteoblasts with increasing levels of alkaline phosphatase (ALP) activity[4, 18] (Figure 2). At this point the ECM produced by the osteoblasts is mature and mineralization is soon initiated within specialized vesicles (discussed in section 1.5.2). In the final stages of osteoblasts differentiation only a fraction of mature osteoblasts survive, as osteocytes or as bone lining cells[4] (Figure 2). The latter are usually localized at the interface of bone with bone marrow but their exact function is not known[4, 19]. Entombed in the mineralized ECM, osteocytes represent the most abundant cellular component in mammalian bone, representing up to 95% of the total cells[5]. They are characterized by their long cytoplasmatic processes that keep them in communication with the surrounding cells and the expression of a new set of genes, including dentin matrix protein-1 (DMP-1) and matrix extracellular phosphoglycoprotein (MEPE)[20-21]. Osteocytes also express sclerostin (SOST), a bone morphogenetic protein (BMP) and Wnt signaling antagonist[22] with potent inhibitory effects on bone formation[23] (Figure 2). In terms of function, osteocytes have long been known by the mechano-sensing properties, translating mechanical

strain into biochemical signals of resorption or formation[24]. Signals for resorption were recently highlighted in osteocytes with the expression of high levels of receptor activator of NF-kB ligand (RANKL) an important osteoclastogenic cytokine[25]. Also recently, osteocytes emerged as endocrine cells, due to the expression of fibroblast growth factor 23 (FGF23) and other factors involved in phosphate homeostasis[26].

1.4 REGULATION OF OSTEOBLAST DIFFERENTIATION AND BONE METABOLISM

Osteoblast differentiation is controlled by a plethora of molecules, including morphogens, growth factors, cytokines and hormones all contributing to an intricate network of signaling cascades, from autocrine/paracrine to endocrine. Bone is exposed to these factors from circulation, surrounding cells and also notably the ECM when bone resorption releases factors from this compartment.

Some of the most prominent regulators of bone formation are the transforming growth factor beta (TGF-β) superfamily members, including TGF-β itself, BMPs and activins. Skeletal and extra-skeletal tissues synthesize BMPs and within the skeleton osteoblasts is the major source. These autocrine/paracrine factors are responsible for the induction of osteoprogenitor cells and their regulation throughout the entire osteoblast differentiation process[27]. In the early stages of differentiation the pro-osteoblastic effect of BMPs is reinforced by the action of TGF-β stimulating the expansion of the osteoprogenitor cell pool[28]. However, later in osteoblast development TGF-β counteracts the effects of BMPs by acting as an inhibitor of osteoblast differentiation and mineralization[29-30]. Activins also modulate bone formation by inhibiting osteoblast differentiation. Their role in this process is discussed in greater detail in section 1.8.

Another signaling pathway involved in osteoblast differentiation is the Wnt signaling pathway. Mutations in genes associated to this pathway are associated to changes in bone mass and skeletal fragility[31-34] demonstrating the importance of this pathway in bone metabolism. The exact function of Wnt signaling in osteoblast differentiation remains unclear and needs further investigation. Several studies support a stimulatory role of Wnt signaling in osteoblast differentiation[35-36] while others point to an inhibitory function of this pathway during osteogenesis[37-38].

Several classical hormones, parathyroid hormone (PTH), calcitonin, glucocorticoids, vitamin D_3 and sex steroids, are known to regulate osteoblast

differentiation. The effect of these hormones on osteoblast differentiation is generally considered as positive[4] but bone catabolic actions can be observed depending on the type of study (*in vivo* or *in vitro*), animal species, dosage, mode of administration and bone type (trabecular or cortical), like observed for glucocorticoids and PTH[4, 39]. Recent studies have increased the number of hormones targeting osteogenesis. Leptin and serotonin are the best examples of molecules whose effects have been described in relation to osteoblast differentiation[40] and in a broader view with respect to bone metabolism[41] (discussed in section 1.6).

1.5 EXTRACELLULAR MATRIX

1.5.1 Synthesis and maturation phase

The formation of an ECM by osteoblasts is a complex and only partially understood process. The ECM synthesis and maturation phase is mainly controlled by RUNX2 and SP7. These transcription factors are responsible for the regulation of several bone ECM genes, including COL1A1, IBSP, osteopontin (OPN) and osteocalcin (BGLAP)[42]. COL1A1 and IBSP are among the first proteins assembled into the matrix being determinant to the expression of other differentiation related proteins[43-44]. OPN and BGLAP are markers of late osteoblast differentiation and thought to be negative regulators of the mineralization process[45-46]. After collagens, representing up to 90% of the total bone protein content[4], BGLAP is the most abundant protein found in the ECM making up to 10-20% of the known non-collagenous proteins (NCPs)[47-49]. BGLAP is the most studied NCP and a specific product of osteoblast activity used clinically as a marker for bone turnover. Exciting new data has demonstrated its action as an energy metabolism hormone, stimulating insulin production, improving insulin sensitivity and glucose tolerance[2, 50]. This data opens new horizons in the bone field for other ECM proteins with potentially relevant regulatory functions. To this end, it is crucial to characterize the bone tissue beyond the few NCPs presently documented.

1.5.2 Mineralization phase: role of matrix vesicles

The inorganic mineral, mostly hydroxyapatite, is a characteristic feature of the bone tissue. During the final stages of osteoblast differentiation the ECM is mature and ready to become mineralized in a complex and far from understood mechanism.

The initial hydroxyapatite crystal formation occurs within extracellular membrane-invested vesicles highly enriched in ALP activity called matrix vesicles (MV)[51]. Initially identified as the mineralization precursors in cartilage[52], these vesicles are nowadays associated with virtually any type of biomineralization, either physiologic, in bone[53], tendon[54] and teeth[55] or pathological in calcifying vasculature[56]. Data from electron microscopy revealed that these extracellular vesicles are ~50-200nm in diameter and arise by polarized budding and pinching-off from the outer cell membranes as single MVs or in sacs of clustered MVs[57-58]. However, the conditions and molecular determinants for production and release of the MVs are currently unclear.

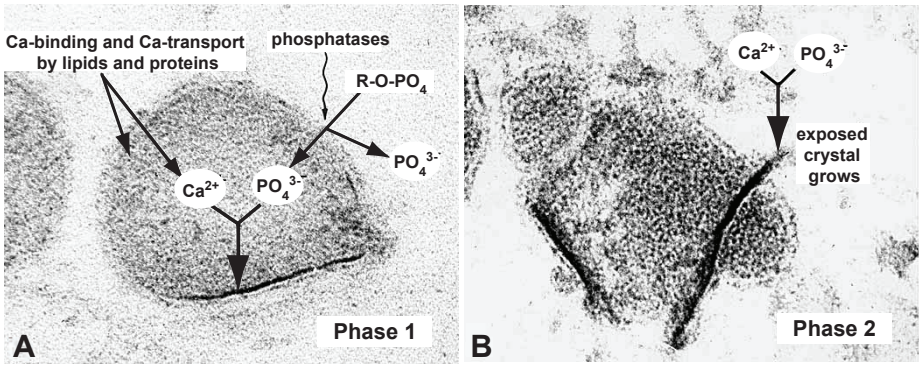

Figure 3. Matrix vesicle (MV)-induced mineralization. The MV-dependent biomineralization is a biphasic process. In the first phase **(A)**, calcium and phosphate are accumulated within the lumen of the MVs favouring mineral precipitation and crystal formation. In this period the action of calcium-binding/transporting proteins and (pyro)phosphatases contained within the MVs is crucial. In the second phase **(B)**, the preformed crystals grow further, leading to the disruption of the MV membrane with exposure to the extracellular environment and formation of a mineral nucleation site. Image adapted from Anderson[59].

The MV-mediated mineralization mechanism is a biphasic process (Figure 3). Initially, calcium and phosphate accumulates inside the vesicles favouring precipitation and crystal formation (Figure 3A). In a second phase mineral grows further, leading to the disruption of the MV membrane and exposure of the crystals to the extracellular fluid forming a mineral nucleation site[59] (Figure 3B). The rate of mineral growth within the MVs is dependent on several factors, both intra- and extra-vesicular. Calcium/phosphate concentrations and the pH are among the latter. The ECM composition, particularly due to anionic proteoglycans, calcium- and phosphate-

binding proteins, is also believed to control crystal formation and growth[4, 60-61]. In terms of the internal MV milieu, different types of proteins have been described with roles in mineralization[51, 58]. Calcium-dependent phospholipid binding proteins (annexins) are responsible for the calcium influx into the MVs by forming calcium channels in their membranes[62-64]. Within the MVs, ALP is the most abundant of the phosphatases, a class of enzymes involved in the mobilization of phosphate from substrates like pyrophosphate and ATP that can inhibit mineralization[65-66] (Figure 3A).

Recent studies have confirmed the existence of proteins within the MVs that are not directly involved in mineralization. Nahar and colleagues[67] have identified significant amounts of BMPs and detected vascular endothelial growth factor (VEGF). The presence of cytokines and growth factors in MVs is intriguing and raises the idea that these vesicles are not solely responsible for the mineralization, carrying as well signaling information to the surrounding cells.

1.6 BONE METABOLISM: MODELING AND REMODELING

The bone tissue changes dynamically throughout life, accompanying the body growth to define the appropriate skeletal structure or renewing compromised parts of the tissue upon injury. Bone modeling is the adaptation of the skeleton to mechanical usage during the growth phase, leading to optimal bone geometry and strength[68-69]. This process involves either osteoclast activation to resorb bone or osteoblast activation to form new bone, but never both at the same location. The coupling of osteoclast and osteoblast activities at one specific bone area is known as bone remodeling (Figure 1). In contrast to bone modeling, remodeling takes place during adulthood, being responsible for tissue renewal, contributing for the stability, integrity and quality of the bone tissue[70-71].

The remodeling process occurs constantly in bone and is carried out within temporary anatomical structures of osteoclasts and osteoblasts arranged in basic multicellular units (BMUs)[69]. BMUs are encased by a canopy of cells that create a unique microenvironment for the bone remodeling[72-73]. It is within this environment that bone remodeling is initiated and osteoclasts are activated by RANKL and macrophage colony-stimulating factor (M-CSF) to resorb bone[74]. The positive stimulus for osteoclastogenesis via RANKL, a crucial cytokine for osteoclast formation, can be originated by osteoblasts or even strongly by osteocytes[25]. The

inhibition of osteoclastogenesis is also dependent on the actions of these two cell types. Osteoblasts secrete a soluble RANKL decoy receptor osteoprotegerin (OPG) [75] and the osteocyte sense the mechanical strains to enter or not in apoptosis[76].

The coupling of bone resorption to bone formation is not fully understood but while osteoclasts undergo apoptosis, osteoblasts are recruited to the resorption site where they form new bone and complete the remodeling cycle. This coupling can occur indirectly, via release of ECM-derived osteoblast stimulating factors (such as BMPs; Insulin growth factor I, IGF1; TGF-β1)[77-78] or directly, via osteoclast secretion products (such as sphingosine-1-phosphate, S1P; platelet-derived growth factor β, PDGFβ; hepatocyte growth factor, HGF)[79]. SOST, secreted by the osteocytes represents another modulator of bone formation, controlling the proliferation/ differentiation of osteoprogenitor cells and the activity of mature osteoblasts[80].

The regulation of bone remodeling is not only made locally in bone. Endocrine signaling represents a strong conditioning factor for bone metabolism (see also section 1.4). Recent studies on this field demonstrated that bone remodeling is regulated by energy metabolism (reviewed by[81]). Leptin, a satiety hormone, and serotonin, best known as a neurotransmitter, are two molecules found to be involved in the regulation of bone mass[40, 82-84]. These data has drawn a bone–energy metabolism paradigm in the bone field, with BGLAP possibly representing the feedback loop signaling from the bone controlling energy metabolism[50].

During adulthood approximately 10% of the bone material is renewed every year by bone remodeling[85]. Bone diseases, most notably osteoporosis are the result of a remodeling imbalance due to uncoupling bone resorbing and bone formation activities. The net effect of osteoporosis in bone remodeling is an increased bone turnover that compromises bone tissue composition and quality[86]. Understanding how bone metabolism is integrated within the whole body system may become crucial for the development of new therapies for bone disorders affecting the balance of bone remodeling. This was recently shown for serotonin and its potential as an anabolic target for the treatment of osteoporosis[87].

1.7 BONE COMPOSITION, BONE TISSUE QUALITY AND OSTEOPOROSIS

The bone tissue has to be simultaneously stiff, to resist deformation, and elastic, to absorb energy by deformation without breaking[88]. These quality parameters of

bone are determined by the composition, structure and balance of its two main fractions, the organic ECM and the mineral deposited. The organic ECM is responsible for tissue flexibility, especially collagens that represent up to 90% of the total protein content[4]. Oriented in the same direction, collagen fibers are the bone building blocks where the ground substance, glycoproteins and proteoglycans, and other NCPs anchor facilitating the mineral deposition[89-90]. The flexibility of bone is tempered by varying degrees of mineral deposition, matching tissue properties with function. Cortical bone is 80-90% calcified in volume, which confers to this tissue the solidity and rigidity necessary for its predominant mechanical/protective functions. This value decreases to only 15-25% in trabecular bone providing this type of bone tissue with adequate plasticity to perform its main metabolic function[91].

The mineralization degree of bone tissue is also influenced by the dynamics of bone remodeling activities. In areas where bone remodeling takes place, old highly mineralized bone is replaced by new bone tissue, composed primarily of non-mineralized osteoid and lowly mineralized ECM. Several factors account for the bone remodeling balance and consequently for overall bone tissue quality. Among these factors are calcium homeostasis, disease and aging.

Calcium concentrations in blood need to be maintained within a narrow homeostatic range due to the importance of this cation in different extracellular physiologic events[92]. This need to buffer systemic calcium concentrations overrules the regulation of bone mass. During hypocalcaemia, bone resorption is increased to mobilize calcium from bone and restore extracellular calcium homeostasis[93].

Disease and aging are invariably related to bone architectural changes leading to bone fragility. In adulthood, after reaching peak bone mass the bone balance reverses gradually to negative due to a decreased bone formation[94]. This negative bone balance is accompanied by bone architectural loss and structural damage in both women and men[88]. Eventually the bone tissue deterioration reaches pathological thresholds defined as osteoporosis, low bone mass (i.e. quantity and quality) resulting in increased fracture susceptibility, disability and morbidity[95-96]. Osteoporosis is the most prevalent of all bone diseases with 50% of women and 20% of men older than 50 years having a fragility fracture in their remaining lifetime. Women are more vulnerable to osteoporosis than man due to a lower peak bone mass. In addition, menopause-derived estrogen deficiency compromises further the bone quality as a result of a higher bone turnover with increased osteoclast activity that can not be compensated by bone formation[97].

In terms of impact for the society, osteoporosis represents a major burden both economically, with costs ascending up to 25 billion euros only in Europe[98] and socially, with the decrease on the quality of life of the patients. In the years to come the toll of osteoporosis is expected to worsen as a result of an increased life expectancy[99]. In order to minimize these effects, new diagnostic tools for early detection of osteoporosis and accurate risk prediction are needed. Bone mineral density (BMD) measurements, the current method to detect osteoporosis, only diagnoses half of the patients[100], a poor performance highlighting the need for more accurate detection methods. These detection methods should aim at identifying osteoporosis in its early stages, i.e. osteopenia, in order to prevent loss of significant bone mass, which can not be effectively restored with the current treatment methods. To accomplish this task a better comprehension of the bone tissue is needed, especially of the ECM composition and its relationship to bone quality.

1.8 ACTIVIN SIGNALING

Activins are members of the TGF-β superfamily. In structural terms, activins are the result of homo-dimerization of two inhibin ß subunits linked by a disulfide bond[101] (Figure 4A. These protein dimers exert their action via TGF-β signaling, that starts with the binding of the ligands to type I and II serine/threonine kinase receptors located on the cell surface. Activins signal using the type II receptors ACVR2A or ACVR2B (also known as ActRII or ActRIIB) and the type I receptor ACVR1B (Figure 4B). Upon ligand binding the type II receptor phosphorylates serine residues of the type I receptor, activating the receptor complex. The signal is transmitted further through Smad proteins, Smad2/3 and Smad4 in the case of activin[102-103]. Once phosphorylated, the active Smad proteins translocate to the nucleus binding to transcription factors and modulating the expression of target genes[104-105] (Figure 4B).

Functionally, activins were initially characterized as antagonists of inhibins in follicule stimulating hormone (FSH) secretion from pituitary gonadotropes[106-107]. Since then, activins (and inhibins) have shown to target many other cell types and tissues, including hematopoietic[108] and monocyte/macrophage[109] cell lineages, adrenal gland, liver and neurons[110-112]. Activins are also present in bone tissue[113-114] with effects on both the osteoblasts and osteoclasts. While the action of activin in the bone resorbing cells is generally viewed as pro-osteoclastogenic[109, 115-116], the

effects on osteoblasts are more controversial. *In vitro*, activins have been shown to stimulate or inhibit osteoblast differentiation and mineralization, depending on the cell system used[113, 117-118]. Regarding to *in vivo* studies the effect of activins appears to be catabolic. In mice, the blockage of activin signaling, using a decoy receptor for activin, resulted in increased bone formation, bone mass and bone strength[119]. Similar effects have been observed in monkeys and humans, where the use of an antibody neutralizing activin resulted in a significant improvement in BMD[120-121]. These studies have renewed the interest in the activin signaling to bone, converting it in a potential therapeutic target for osteoporosis[122].

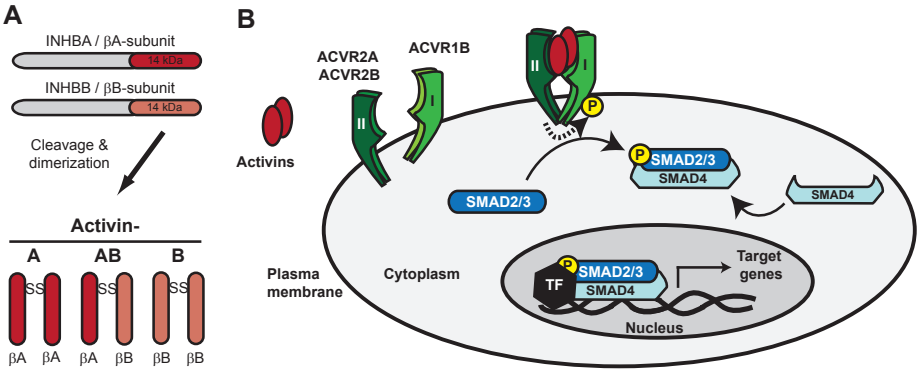

Figure 4. Activin structure and activin signaling pathway. **(A)** Activins are a formed by dimerization of two inhibin ß subunits linked by a disulfide bond. **(B)** Activins from the circulation or produced locally in bone by the osteoblasts binds to a TGF-β type II serine/threonine kinase activity receptor (ACVR2A or ACVR2B). This binding leads to the recruitment and subsequent phosphorylation of a type I receptor (ACVR1B). The receptor complex is now active and phosphorylates Smad2 or 3 proteins (Smad2/3). Upon phosphorylation, Smad2/3 binds to Smad 4 and the Smad protein complex translocate into the nucleus where it binds transcription factors (TF) to regulate the expression of target genes.

1.9 ECTOPIC VASCULAR CALCIFICATION: THE BONE CONNECTION

Tissue mineralization is a physiological capacity restricted to the skeleton and the inner ear. However, in pathological conditions tissue mineralization can also occur ectopically and vascular calcification is arguably the most relevant example (Figure 5A). Pathological vascular calcifications have evolved from considered passive precipitation to become seen as an active cell-mediated process[123]. Medial

artery calcification is in fact hypothesized to be analogous to physiological bone mineralization[124].

Vascular smooth muscle cells (VSMCs) are contractile cells located at the medial layer of the vessel wall. Despite their differentiated state, VSMC can be triggered to loose smooth muscle cell contractility markers entering a synthetic state with abundant production of ECM proteins[123, 125-127] followed by MV-mediated calcification[56, 62]. In general terms, osteoblast differentiation and mineralization follows similar events (see section 1.5). Other lines of evidence for analogous vascular calcification and osteoblast mineralization come from observations that atherosclerotic plaques express bone specific transcription factors (RUNX2 and SP7), BMPs[128-130] (Figure 5B) as well as M-CSF, RANKL or OPG[131].

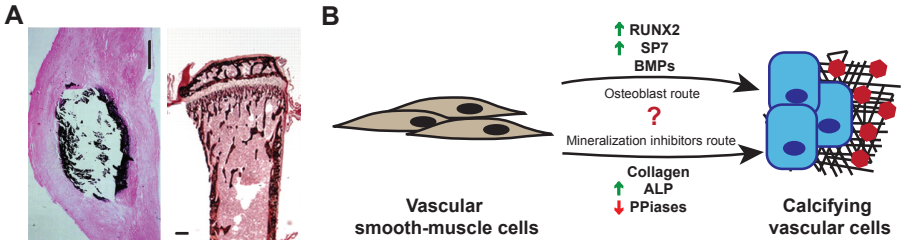

Figure 5. Pathological vascular calcification. **(A)** Calcifications of artery (left; scale bar = 100 µm) and bone (right; scale bar = 200 µm) visualized by von Kossa staining (black = mineral deposited). **(B)** Illustration of the most debated hypothetical routes to explain calcification in the tunica media of arteries. VSMCs transdifferentiate into calcifying vascular cells (CVCs) entering an osteoblast differentiation program governed by osteoblast specific transcription factors (RUNX2 and SP7) and pro-osteogenic cytokines (BMPs). Alternatively, vascular cells calcify due to the lack of mineralization inhibitors such as pyrophosphatases (PPiases) while co-expressing proteins essential for mineral deposition, including collagens and ALP. Artery and bone tissue staining images were adapted from Bini *et al.*[132] and Douni *et al.*[133] respectively.

An alternative hypothesis to explain ectopic vascular calcification contemplates the lack of inhibitors of mineralization in the ECM (Figure 5B). Murshed and colleagues[134] have explored this hypothesis and have shown that mineralization can occur in any tissue, providing that a fibrillar collagen ECM is deposited and pyrophosphatases, most notably ALP, are expressed to cleave the mineralization inhibitor pyrophosphate. The co-expression of type I collagen and ALP is restricted to mineralizing tissues. VSMC do not normally express ALP but calcifying vascular

cells (CVCs) show increased expression and activity of this enzyme[56, 135] capable to induce calcification in rat models of medial calcification[136].

The exact mechanism behind vascular calcification is largely unknown. More studies are needed to test the two most consistent hypotheses here described which do not seem to be mutually exclusive. It is possible that *in vivo* vascular calcification involves as well others cell types, such as osteoprogenitor cells from circulation or pericytes from the vessel wall[137]. If mechanistically the connection between vascular and bone calcifications needs further elucidation, the clinical parallels between the two are more evident. Several studies have shown an inverse correlation between BMD and vascular calcium deposition associating osteoporosis with increased risk of atherosclerosis and *vice versa*[138-140].

1.10 PROTEOMICS: THE NEW RESEARCH TOOLBOX

Proteomics represents the study of proteins within their biological system, i.e. the proteome, from structure to biological function. The proteomics field complements functional genomic approaches (e.g. microarray-based expression profiles and systematic phenotypic profiles)[141] with the advantage that proteins are a particularly rich source of biological information being directly involved in almost all biological activities.

Proteomics has benefited tremendously from technology innovations that enable large-scale identification of proteins and a better comprehension of the biological questions under investigation. These large-scale studies emerged initially with two-dimensional gel electrophoresis[142] and were renovated with the coupling of liquid chromatography (LC) techniques to mass spectrometry (MS) measurements[143] (Figure 6). With the introduction of MS into proteomics, the field also gained the robustness and high-throughput necessary to become amenable for clinical applications[141] using tissue biopsies or biofluids (plasma, serum, cerebrospinal fluid, urine). The evolution in the instrumentation was accompanied by tailored protein quantification solutions, isotope-labelling methods involving tagging of proteins, either chemically (isotope-coded affinity tags, ICAT; isobaric tags for relative and absolute quantitation, iTRAQ; tandem mass tags, TMT)[144-146], enzymatically (^{18}O water for trypsin digestion)[147] or metabolically (stable isotope labelling of amino acids in cell culture, SILAC; ^{15}N-labeling)[148-149] (Figure 6). Label-free quantification techniques (e.g. spectrum counting and emPAI scores)[151-152] are becoming popular

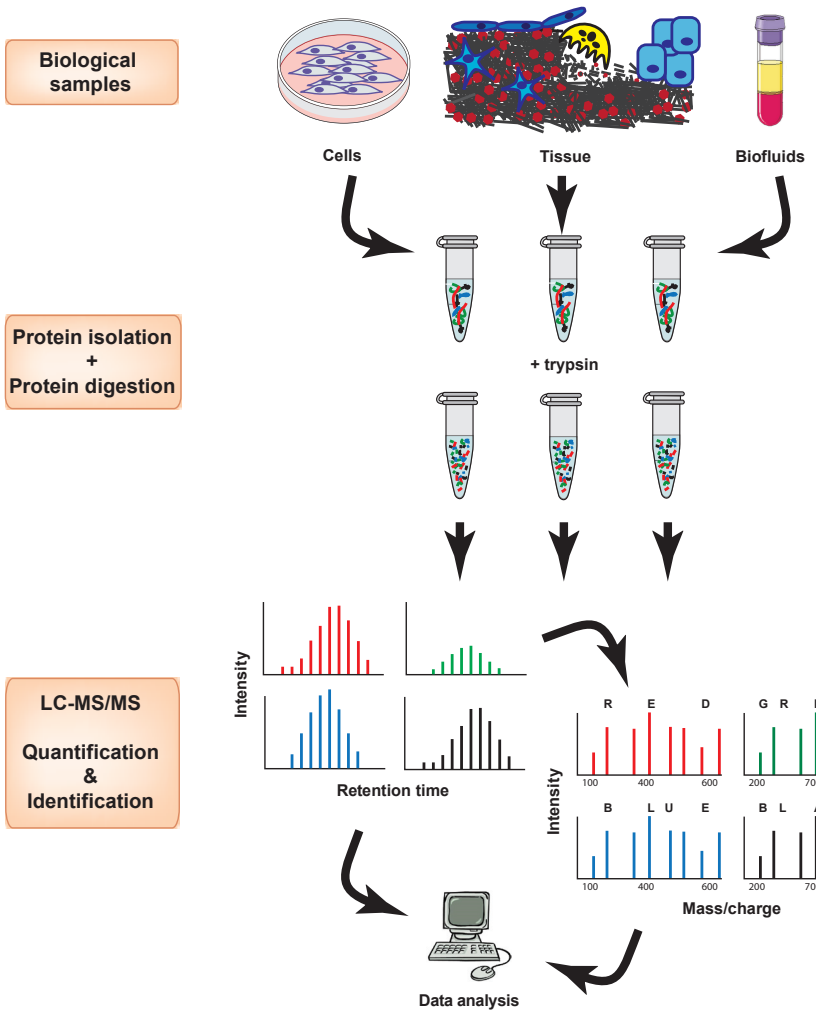

Figure 6. Workflow of a mass spectrometry-based proteomics approach. Initially, proteins are isolated from the biological material of interest, cells, tissue or biofluids. For quantification purposes biological samples can be metabolically labelled. After isolation, proteins are enzymatically digested, most commonly using trypsin. At this stage chemical or enzymatic labelling methods can be used for protein quantification. Fractionation methods aiming at reducing sample complexity, e.g. gel electrophoresis or isoelectric focusing, are also possible at this stage. The peptide mixture of the samples is resolved LC and subsequently measured by MS. The detected peptides generate MS signal intensities that can be used for quantification. Peptides are fragmented (MS/MS) and the spectra obtained are searched against protein sequence databases to determine peptide and protein identifications. Scheme was adapted from Mallick and Kuster[150].

as well following advances in instrumentation, computing power and software development.

The variety of approaches available at the moment transforms proteomics suitable for any application with 100s-1000s of proteins being routinely identified and quantified[150] from cells, tissues or biofluids. Despite these advances, MS-based proteomics has its own limitations and faces several challenges. The major challenge is the complexity of the proteomes and their elaborated dynamics. Cells are believed to contain over 100.000 proteins species spanning 7-10 orders of magnitude in abundance[153] hampering the detection of low abundant molecules by current MS-based approaches. Additional complexity in proteome analysis resides in the existence of multiple splice variants and post-translational modifications (PTM; e.g. phosphorylation and glycosilation), factors that are temporal and developmentally specific but also influenced by disease states and drug perturbations[141]. One way to tackle these challenges is to diminish the limitations of MS-based proteomics approaches, ranging from sub-optimal instrumentation[141] to the yet lengthy data analysis for quantitative and PTM studies[150].

Proteomics has already made its contribution to the bone field as demonstrated by several studies in osteoblasts[58, 154-155] and osteoclasts[156-158]. Despite the substantial biological data delivered by these studies, the absence of a complete proteome identification demands further characterization of the osteoblast and osteoclast differentiation programs. This information is crucial, not only to know how to modulate the action of these cells *in vivo* but also to develop new diagnostic and therapeutic tools for the management of bone diseases such as osteoporosis.

1.11 SCOPE OF THIS THESIS

The process of bone formation is a key element to guarantee the quality of the bone tissue, during bone growth, bone maintenance and in bone diseases such as osteoporosis. To be able to target and modulate bone formation, it is essential to understand how osteoblasts differentiate and what occurs when this process is stimulated or inhibited. In this thesis, the osteoblast differentiation (**Chapter 2**) and the effects elicited by activin A during osteoblast differentiation was studied (**Chapter 3**). The inhibition of osteoblast differentiation by activin A was studied with a focus on extracellular proteomes, suggested as a primary target of activin[113]. The state-of-the-art MS-based proteomics techniques were used to generate large-scale qualitative and

quantitative protein data, highlighting important biological functions and changes in osteoblast behaviour during differentiation. High-throughput proteomics tools were used as well to characterize human bone composition (**Chapter 4**), a complex tissue described usually by a handful of proteins and the high mineral content. More than making a catalogue of proteins, this work is of particular interest in the search for novel (protein) markers of bone turnover, potentially valuable in the clinic to diagnose bone loss and prevent osteoporosis.

The pathological vascular calcification is often associated to other disease states, including osteoporosis. Besides being considered similar to the osteoblast differentiation and mineralization, not much is known about the mechanism of vascular calcification. This lack of knowledge was addressed using genome-wide gene expression arrays to investigate how and what make vascular cells convey into a similar osteoblast-mineralized phenotype (**Chapter 5**).

Altogether this thesis aims to gain knowledge about bone biology with a particular focus on the bone formation process, the osteoblast differentiation and mineralization. This knowledge forms a basis to identify therapeutic targets for bone diseases. Furthermore, it will be crucial to identify candidate biomarkers for bone loss that whenever altered in the blood stream might discriminate osteoporotic from healthy individuals. Our knowledge about bone formation and osteoblasts differentiation will guide us as well in the study of vascular calcification to understand how different cells develop a common phenotype.

REFERENCES

[1] Marks SC, *et al.* In *Principles of bone biology.*; 2nd ed.; Bilezikian JP, *et al.*, Eds.; Academic Press: 2002.

[2] Lee NK, *et al.* Endocrine regulation of energy metabolism by the skeleton *Cell* 2007, *130*, 456-69.

[3] Ross FD In *Primer on the metabolic bone diseases and disorders of mineral metabolism.*; 6th ed.; Favus MJ, Ed.; The American Society for Bone and Mineral Research: Washington D.C., 2006.

[4] Aubin JE, *et al.* In *Primer on the metabolic bone diseases and disorders of mineral metabolism.*; 6th ed.; Favus MJ, Ed.; The American Society for Bone and Mineral Research: Washington D.C., 2006.

[5] Franz-Odendaal TA, *et al.* Buried alive: how osteoblasts become osteocytes *Dev Dyn* 2006, *235*, 176-90.

[6] Campagnoli C, *et al.* Identification of mesenchymal stem/progenitor cells in human first-trimester fetal blood, liver, and bone marrow *Blood* 2001, *98*, 2396-402.

[7] Crisan M, *et al.* A perivascular origin for mesenchymal stem cells in multiple human organs *Cell Stem Cell* 2008, *3*, 301-13.

[8] Erices A, *et al.* Mesenchymal progenitor cells in human umbilical cord blood *Br J Haematol* 2000, *109*, 235-42.

[9] Zuk PA, *et al.* Human adipose tissue is a source of multipotent stem cells *Mol Biol Cell* 2002, *13*, 4279-95.

[10] Chamberlain G, *et al.* Concise review: mesenchymal stem cells: their phenotype, differentiation capacity, immunological features, and potential for homing *Stem Cells* 2007, *25*, 2739-49.

[11] Komori T, *et al.* Targeted disruption of Cbfa1 results in a complete lack of bone formation owing to maturational arrest of osteoblasts *Cell* 1997, *89*, 755-64.

[12] Ducy P, *et al.* Osf2/Cbfa1: a transcriptional activator of osteoblast differentiation *Cell* 1997, *89*, 747-54.

[13] Otto F, *et al.* Cbfa1, a candidate gene for cleidocranial dysplasia syndrome, is essential for osteoblast differentiation and bone development *Cell* 1997, *89*, 765-71.

[14] Nakashima K, *et al.* The novel zinc finger-containing transcription factor osterix is required for osteoblast differentiation and bone formation *Cell* 2002, *108*, 17-29.

[15] Komori T Regulation of osteoblast differentiation by transcription factors *J Cell Biochem* 2006, *99*, 1233-9.

[16] De Bari C, *et al.* Mesenchymal multipotency of adult human periosteal cells demonstrated by single-cell lineage analysis *Arthritis Rheum* 2006, *54*, 1209-21.

[17] Franceschi RT The developmental control of osteoblast-specific gene expression: role of specific transcription factors and the extracellular matrix environment *Crit Rev Oral Biol Med* 1999, *10*, 40-57.

[18] Aubin JE Regulation of osteoblast formation and function *Rev Endocr Metab Disord* 2001, *2*, 81-94.

[19] Parfitt AM The bone remodeling compartment: a circulatory function for bone lining cells *J Bone Miner Res* 2001, *16*, 1583-5.

[20] Nampei A, *et al.* Matrix extracellular phosphoglycoprotein (MEPE) is highly expressed in osteocytes in human bone *J Bone Miner Metab* 2004, *22*, 176-84.

[21] Toyosawa S, *et al.* Dentin matrix protein 1 is predominantly expressed in chicken and rat osteocytes but not in osteoblasts *J Bone Miner Res* 2001, *16*, 2017-26.

[22] ten Dijke P, *et al.* Osteocyte-derived sclerostin inhibits bone formation: its role in bone morphogenetic protein and Wnt signaling *J Bone Joint Surg Am* 2008, *90 Suppl 1*, 31-5.

[23] van Bezooijen RL, *et al.* Sclerostin is an osteocyte-expressed negative regulator of bone formation, but not a classical BMP antagonist *J Exp Med* 2004, *199*, 805-14.

[24] Lanyon LE Osteocytes, strain detection, bone modeling and remodeling *Calcif Tissue Int* 1993, *53 Suppl 1*, S102-6; discussion S106-7.

[25] Nakashima T, *et al.* Evidence for osteocyte regulation of bone homeostasis through RANKL expression *Nat Med* 2011, *17*, 1231-4.
[26] Cheng F, *et al.* The osteocyte--a novel endocrine regulator of body phosphate homeostasis *Maturitas* 2010, *67*, 327-38.
[27] Canalis E, *et al.* Bone morphogenetic proteins, their antagonists, and the skeleton *Endocr Rev* 2003, *24*, 218-35.
[28] Janssens K, *et al.* Transforming growth factor-beta1 to the bone *Endocr Rev* 2005, *26*, 743-74.
[29] Alliston T, *et al.* TGF-beta-induced repression of CBFA1 by Smad3 decreases cbfa1 and osteocalcin expression and inhibits osteoblast differentiation *EMBO J* 2001, *20*, 2254-72.
[30] Spinella-Jaegle S, *et al.* Opposite effects of bone morphogenetic protein-2 and transforming growth factor-beta1 on osteoblast differentiation *Bone* 2001, *29*, 323-30.
[31] Boyden LM, *et al.* High bone density due to a mutation in LDL-receptor-related protein 5 *N Engl J Med* 2002, *346*, 1513-21.
[32] Gong Y, *et al.* LDL receptor-related protein 5 (LRP5) affects bone accrual and eye development *Cell* 2001, *107*, 513-23.
[33] Kubota T, *et al.* Wnt signaling in bone metabolism *J Bone Miner Metab* 2009, *27*, 265-71.
[34] van Meurs JB, *et al.* Large-scale analysis of association between LRP5 and LRP6 variants and osteoporosis *JAMA* 2008, *299*, 1277-90.
[35] Bain G, *et al.* Activated beta-catenin induces osteoblast differentiation of C3H10T1/2 cells and participates in BMP2 mediated signal transduction *Biochem Biophys Res Commun* 2003, *301*, 84-91.
[36] Rawadi G, *et al.* BMP-2 controls alkaline phosphatase expression and osteoblast mineralization by a Wnt autocrine loop *J Bone Miner Res* 2003, *18*, 1842-53.
[37] Boland GM, *et al.* Wnt 3a promotes proliferation and suppresses osteogenic differentiation of adult human mesenchymal stem cells *J Cell Biochem* 2004, *93*, 1210-30.
[38] de Boer J, *et al.* Wnt signaling inhibits osteogenic differentiation of human mesenchymal stem cells *Bone* 2004, *34*, 818-26.
[39] Jüppner H, *et al.* In *Primer on the metabolic bone diseases and disorders of mineral metabolism.*; 6th ed.; Favus MJ, Ed.; The American Society for Bone and Mineral Research: Washington D.C., 2006.
[40] Thomas T, *et al.* Leptin acts on human marrow stromal cells to enhance differentiation to osteoblasts and to inhibit differentiation to adipocytes *Endocrinology* 1999, *140*, 1630-8.
[41] Coen G Leptin and bone metabolism *J Nephrol* 2004, *17*, 187-9.
[42] Ducy P, *et al.* The osteoblast: a sophisticated fibroblast under central surveillance *Science* 2000, *289*, 1501-4.
[43] Ibaraki K, *et al.* Bone matrix mRNA expression in differentiating fetal bovine osteoblasts *J Bone Miner Res* 1992, *7*, 743-54.
[44] Owen TA, *et al.* Progressive development of the rat osteoblast phenotype in vitro: reciprocal relationships in expression of genes associated with osteoblast proliferation and differentiation during formation of the bone extracellular matrix *J Cell Physiol* 1990, *143*, 420-30.
[45] Boskey AL, *et al.* Osteopontin deficiency increases mineral content and mineral crystallinity in mouse bone *Calcif Tissue Int* 2002, *71*, 145-54.
[46] Ducy P, *et al.* Increased bone formation in osteocalcin-deficient mice *Nature* 1996, *382*, 448-52.
[47] Gundberg CM, *et al.* Osteocalcin: isolation, characterization, and detection *Methods Enzymol* 1984, *107*, 516-44.
[48] Hauschka PV, *et al.* Direct identification of the calcium-binding amino acid, gamma-carboxyglutamate, in mineralized tissue *Proc Natl Acad Sci U S A* 1975, *72*, 3925-9.
[49] Price PA, *et al.* Characterization of a gamma-carboxyglutamic acid-containing protein from bone *Proc Natl Acad Sci U S A* 1976, *73*, 1447-51.
[50] Ferron M, *et al.* Insulin signaling in osteoblasts integrates bone remodeling and energy metabolism *Cell* 2010, *142*, 296-308.

[51] Anderson HC, *et al.* The role of matrix vesicles in growth plate development and biomineralization *Front Biosci* 2005, *10*, 822-37.
[52] Anderson HC Vesicles associated with calcification in the matrix of epiphyseal cartilage *J Cell Biol* 1969, *41*, 59-72.
[53] Anderson HC, *et al.* Pyrophosphate stimulation of calcium uptake into cultured embryonic bones. Fine structure of matrix vesicles and their role in calcification *Dev Biol* 1973, *34*, 211-27.
[54] Arsenault AL, *et al.* Vectorial sequence of mineralization in the turkey leg tendon determined by electron microscopic imaging *Calcif Tissue Int* 1991, *48*, 46-55.
[55] Bernard GW Ultrastructural observations of initial calcification in dentine and enamel *J Ultrastruct Res* 1972, *41*, 1-17.
[56] Reynolds JL, *et al.* Human vascular smooth muscle cells undergo vesicle-mediated calcification in response to changes in extracellular calcium and phosphate concentrations: a potential mechanism for accelerated vascular calcification in ESRD *J Am Soc Nephrol* 2004, *15*, 2857-67.
[57] Cecil RNA, *et al.* Freeze-fracture studies of matrix vesicle calcification in epiphyseal growth plate *Metabolic Bone Disease and Related Research* 1978, *1*, 89-95.
[58] Xiao Z, *et al.* Analysis of the extracellular matrix vesicle proteome in mineralizing osteoblasts *J Cell Physiol* 2007, *210*, 325-35.
[59] Anderson HC Molecular biology of matrix vesicles *Clin Orthop Relat Res* 1995, 266-80.
[60] Boskey AL Noncollagenous matrix proteins and their role in mineralization *Bone Miner* 1989, *6*, 111-23.
[61] Campo RD, *et al.* Changes in cartilage proteoglycans associated with calcification *Calcif Tissue Int* 1986, *39*, 175-84.
[62] Chen NX, *et al.* Annexin-mediated matrix vesicle calcification in vascular smooth muscle cells *J Bone Miner Res* 2008, *23*, 1798-805.
[63] Genge BR, *et al.* Identification of phospholipid-dependent calcium-binding proteins as constituents of matrix vesicles *J Biol Chem* 1989, *264*, 10917-21.
[64] Kirsch T, *et al.* The roles of annexins and types II and X collagen in matrix vesicle-mediated mineralization of growth plate cartilage *J Biol Chem* 2000, *275*, 35577-83.
[65] Fleisch H, *et al.* Effect of pyrophosphate on hydroxyapatite and its implications in calcium homeostasis *Nature* 1966, *212*, 901-3.
[66] Hoebertz A, *et al.* ATP and UTP at low concentrations strongly inhibit bone formation by osteoblasts: a novel role for the P2Y2 receptor in bone remodeling *J Cell Biochem* 2002, *86*, 413-9.
[67] Nahar NN, *et al.* Matrix vesicles are carriers of bone morphogenetic proteins (BMPs), vascular endothelial growth factor (VEGF), and noncollagenous matrix proteins *J Bone Miner Metab* 2008, *26*, 514-9.
[68] Frost HM The skeletal intermediary organization *Metab Bone Dis Relat Res* 1983, *4*, 281-90.
[69] Jee WS, *et al.* Skeletal adaptations during growth *Triangle* 1992, *31*, 77-88.
[70] Demster DW In *Primer on the metabolic bone diseases and disorders of mineral metabolism.*; 6th ed.; Favus MJ, Ed.; The American Society for Bone and Mineral Research: Washington D.C., 2006.
[71] Proff P, *et al.* The molecular mechanism behind bone remodeling: a review *Clin Oral Investig* 2009, *13*, 355-62.
[72] Andersen TL, *et al.* A physical mechanism for coupling bone resorption and formation in adult human bone *Am J Pathol* 2009, *174*, 239-47.
[73] Hauge EM, *et al.* Cancellous bone remodeling occurs in specialized compartments lined by cells expressing osteoblastic markers *J Bone Miner Res* 2001, *16*, 1575-82.
[74] Boyle WJ, *et al.* Osteoclast differentiation and activation *Nature* 2003, *423*, 337-42.
[75] Kostenuik PJ, *et al.* Osteoprotegerin: a physiological and pharmacological inhibitor of bone resorption *Curr Pharm Des* 2001, *7*, 613-35.
[76] Noble BS, *et al.* Mechanical loading: biphasic osteocyte survival and targeting of osteoclasts for bone destruction in rat cortical bone *Am J Physiol Cell Physiol* 2003, *284*, C934-43.

[77] Harada S*, et al.* Control of osteoblast function and regulation of bone mass *Nature* 2003, *423*, 349-55.
[78] Oreffo RO*, et al.* Activation of the bone-derived latent TGF beta complex by isolated osteoclasts *Biochem Biophys Res Commun* 1989, *158*, 817-23.
[79] Matsuo K*, et al.* Osteoclast-osteoblast communication *Arch Biochem Biophys* 2008, *473*, 201-9.
[80] Winkler DG*, et al.* Osteocyte control of bone formation via sclerostin, a novel BMP antagonist *EMBO J* 2003, *22*, 6267-76.
[81] Confavreux CB Bone: from a reservoir of minerals to a regulator of energy metabolism *Kidney Int Suppl* 2011, S14-9.
[82] Ducy P*, et al.* Leptin inhibits bone formation through a hypothalamic relay: a central control of bone mass *Cell* 2000, *100*, 197-207.
[83] Modder UI*, et al.* Relation of serum serotonin levels to bone density and structural parameters in women *J Bone Miner Res* 2010, *25*, 415-22.
[84] Yadav VK*, et al.* Lrp5 controls bone formation by inhibiting serotonin synthesis in the duodenum *Cell* 2008, *135*, 825-37.
[85] Lerner UH Bone remodeling in post-menopausal osteoporosis *J Dent Res* 2006, *85*, 584-95.
[86] Garnero P Bone markers in osteoporosis *Curr Osteoporos Rep* 2009, *7*, 84-90.
[87] Yadav VK*, et al.* Pharmacological inhibition of gut-derived serotonin synthesis is a potential bone anabolic treatment for osteoporosis *Nat Med* 2010, *16*, 308-12.
[88] Seeman E*, et al.* Bone quality--the material and structural basis of bone strength and fragility *N Engl J Med* 2006, *354*, 2250-61.
[89] Landis WJ The strength of a calcified tissue depends in part on the molecular structure and organization of its constituent mineral crystals in their organic matrix *Bone* 1995, *16*, 533-44.
[90] Wiesmann HP*, et al.* Aspects of collagen mineralization in hard tissue formation *Int Rev Cytol* 2005, *242*, 121-56.
[91] Baron R In *Primer on the metabolic bone diseases and disorders of mineral metabolism.*; 6th ed.; Favus MJ, Ed.; The American Society for Bone and Mineral Research: Washington D.C., 2006.
[92] Breslau NA In *Textbook of Endocrine Physiology.* ; Griffin JE and Ojeda SR, Eds.; Oxford University Press: New York, 1996.
[93] Parfitt AM Bone and plasma calcium homeostasis *Bone* 1987, *8 Suppl 1*, S1-8.
[94] Lips P*, et al.* Mean wall thickness of trabecular bone packets in the human iliac crest: changes with age *Calcif Tissue Res* 1978, *26*, 13-7.
[95] Johnell O*, et al.* An estimate of the worldwide prevalence and disability associated with osteoporotic fractures *Osteoporos Int* 2006, *17*, 1726-33.
[96] Leibson CL*, et al.* Mortality, disability, and nursing home use for persons with and without hip fracture: a population-based study *J Am Geriatr Soc* 2002, *50*, 1644-50.
[97] Weitzmann MN*, et al.* Estrogen deficiency and bone loss: an inflammatory tale *J Clin Invest* 2006, *116*, 1186-94.
[98] Sambrook P*, et al.* Osteoporosis *Lancet* 2006, *367*, 2010-8.
[99] Kanis JA*, et al.* Requirements for DXA for the management of osteoporosis in Europe *Osteoporos Int* 2005, *16*, 229-38.
[100] Garnero P*, et al.* Contribution of bone mineral density and bone turnover markers to the estimation of risk of osteoporotic fracture in postmenopausal women *J Musculoskelet Neuronal Interact* 2004, *4*, 50-63.
[101] Chen YG*, et al.* Activin signaling and its role in regulation of cell proliferation, apoptosis, and carcinogenesis *Exp Biol Med (Maywood)* 2006, *231*, 534-44.
[102] Derynck R*, et al.* Smads: transcriptional activators of TGF-beta responses *Cell* 1998, *95*, 737-40.
[103] Kretzschmar M*, et al.* SMADs: mediators and regulators of TGF-beta signaling *Curr Opin Genet Dev* 1998, *8*, 103-11.
[104] Itoh S*, et al.* Signaling of transforming growth factor-beta family members through Smad proteins *Eur J Biochem* 2000, *267*, 6954-67.

[105] Massague J, *et al.* Transcriptional control by the TGF-beta/Smad signaling system *EMBO J* 2000, *19*, 1745-54.
[106] Ling N, *et al.* Isolation and partial characterization of a Mr 32,000 protein with inhibin activity from porcine follicular fluid *Proc Natl Acad Sci U S A* 1985, *82*, 7217-21.
[107] Vale W, *et al.* Purification and characterization of an FSH releasing protein from porcine ovarian follicular fluid *Nature* 1986, *321*, 776-9.
[108] Broxmeyer HE, *et al.* Selective and indirect modulation of human multipotential and erythroid hematopoietic progenitor cell proliferation by recombinant human activin and inhibin *Proc Natl Acad Sci U S A* 1988, *85*, 9052-6.
[109] Gaddy-Kurten D, *et al.* Inhibin suppresses and activin stimulates osteoblastogenesis and osteoclastogenesis in murine bone marrow cultures *Endocrinology* 2002, *143*, 74-83.
[110] Schubert D, *et al.* Activin is a nerve cell survival molecule *Nature* 1990, *344*, 868-70.
[111] Spencer SJ, *et al.* Activin and inhibin in the human adrenal gland. Regulation and differential effects in fetal and adult cells *J Clin Invest* 1992, *90*, 142-9.
[112] Xu J, *et al.* Inhibin antagonizes inhibition of liver cell growth by activin by a dominant-negative mechanism *J Biol Chem* 1995, *270*, 6308-13.
[113] Eijken M, *et al.* The activin A-follistatin system: potent regulator of human extracellular matrix mineralization *FASEB J* 2007, *21*, 2949-60.
[114] Ogawa Y, *et al.* Bovine bone activin enhances bone morphogenetic protein-induced ectopic bone formation *J Biol Chem* 1992, *267*, 14233-7.
[115] Fuller K, *et al.* Activin A is an essential cofactor for osteoclast induction *Biochem Biophys Res Commun* 2000, *268*, 2-7.
[116] Sakai R, *et al.* Activin enhances osteoclast-like cell formation in vitro *Biochem Biophys Res Commun* 1993, *195*, 39-46.
[117] Centrella M, *et al.* Activin-A binding and biochemical effects in osteoblast-enriched cultures from fetal-rat parietal bone *Mol Cell Biol* 1991, *11*, 250-8.
[118] Ikenoue T, *et al.* Inhibitory effects of activin-A on osteoblast differentiation during cultures of fetal rat calvarial cells *J Cell Biochem* 1999, *75*, 206-14.
[119] Pearsall RS, *et al.* A soluble activin type IIA receptor induces bone formation and improves skeletal integrity *Proc Natl Acad Sci U S A* 2008, *105*, 7082-7.
[120] Lotinun S, *et al.* A soluble activin receptor Type IIA fusion protein (ACE-011) increases bone mass via a dual anabolic-antiresorptive effect in Cynomolgus monkeys *Bone* 2010, *46*, 1082-8.
[121] Ruckle J, *et al.* Single-dose, randomized, double-blind, placebo-controlled study of ACE-011 (ActRIIA-IgG1) in postmenopausal women *J Bone Miner Res* 2009, *24*, 744-52.
[122] Deal C Potential new drug targets for osteoporosis *Nat Clin Pract Rheumatol* 2009, *5*, 20-7.
[123] Steitz SA, *et al.* Smooth muscle cell phenotypic transition associated with calcification: upregulation of Cbfa1 and downregulation of smooth muscle lineage markers *Circ Res* 2001, *89*, 1147-54.
[124] Persy V, *et al.* Vascular calcification and bone disease: the calcification paradox *Trends Mol Med* 2009, *15*, 405-16.
[125] Stegemann JP, *et al.* Mechanical, biochemical, and extracellular matrix effects on vascular smooth muscle cell phenotype *J Appl Physiol* 2005, *98*, 2321-7.
[126] Thyberg J Differentiated properties and proliferation of arterial smooth muscle cells in culture *Int Rev Cytol* 1996, *169*, 183-265.
[127] Yamamoto M, *et al.* Type I collagen promotes modulation of cultured rabbit arterial smooth muscle cells from a contractile to a synthetic phenotype *Exp Cell Res* 1993, *204*, 121-9.
[128] Bostrom K, *et al.* Bone morphogenetic protein expression in human atherosclerotic lesions *J Clin Invest* 1993, *91*, 1800-9.
[129] Dhore CR, *et al.* Differential expression of bone matrix regulatory proteins in human atherosclerotic plaques *Arterioscler Thromb Vasc Biol* 2001, *21*, 1998-2003.
[130] Towler DA, *et al.* Diet-induced diabetes activates an osteogenic gene regulatory program in the aortas of low density lipoprotein receptor-deficient mice *J Biol Chem* 1998, *273*, 30427-34.

[131] Schoppet M, *et al.* Localization of osteoprotegerin, tumor necrosis factor-related apoptosis-inducing ligand, and receptor activator of nuclear factor-kappaB ligand in Monckeberg's sclerosis and atherosclerosis *J Clin Endocrinol Metab* 2004, *89*, 4104-12.
[132] Bini A, *et al.* Noncollagenous bone matrix proteins, calcification, and thrombosis in carotid artery atherosclerosis *Arterioscler Thromb Vasc Biol* 1999, *19*, 1852-61.
[133] Douni E, *et al.* A RANKL G278R mutation causing osteopetrosis identifies a functional amino acid essential for trimer assembly in RANKL and TNF *Hum Mol Genet* 2012, *21*, 784-98.
[134] Murshed M, *et al.* Unique coexpression in osteoblasts of broadly expressed genes accounts for the spatial restriction of ECM mineralization to bone *Genes Dev* 2005, *19*, 1093-104.
[135] Shanahan CM, *et al.* Medial localization of mineralization-regulating proteins in association with Monckeberg's sclerosis: evidence for smooth muscle cell-mediated vascular calcification *Circulation* 1999, *100*, 2168-76.
[136] Lomashvili KA, *et al.* Phosphate-induced vascular calcification: role of pyrophosphate and osteopontin *J Am Soc Nephrol* 2004, *15*, 1392-401.
[137] Johnson RC, *et al.* Vascular calcification: pathobiological mechanisms and clinical implications *Circ Res* 2006, *99*, 1044-59.
[138] Bagger YZ, *et al.* Links between cardiovascular disease and osteoporosis in postmenopausal women: serum lipids or atherosclerosis per se? *Osteoporos Int* 2007, *18*, 505-12.
[139] Hyder JA, *et al.* Association between systemic calcified atherosclerosis and bone density *Calcif Tissue Int* 2007, *80*, 301-6.
[140] Schulz E, *et al.* Aortic calcification and the risk of osteoporosis and fractures *J Clin Endocrinol Metab* 2004, *89*, 4246-53.
[141] Tyers M, *et al.* From genomics to proteomics *Nature* 2003, *422*, 193-7.
[142] O'Farrell PH High resolution two-dimensional electrophoresis of proteins *J Biol Chem* 1975, *250*, 4007-21.
[143] Appella E, *et al.* Analysis of the structure of naturally processed peptides bound by class I and class II major histocompatibility complex molecules *EXS* 1995, *73*, 105-19.
[144] Gygi SP, *et al.* Quantitative analysis of complex protein mixtures using isotope-coded affinity tags *Nat Biotechnol* 1999, *17*, 994-9.
[145] Ross PL, *et al.* Multiplexed protein quantitation in Saccharomyces cerevisiae using amine-reactive isobaric tagging reagents *Mol Cell Proteomics* 2004, *3*, 1154-69.
[146] Thompson A, *et al.* Tandem mass tags: a novel quantification strategy for comparative analysis of complex protein mixtures by MS/MS *Anal Chem* 2003, *75*, 1895-904.
[147] Yao X, *et al.* Proteolytic 18O labeling for comparative proteomics: model studies with two serotypes of adenovirus *Anal Chem* 2001, *73*, 2836-42.
[148] Ong SE, *et al.* Stable isotope labeling by amino acids in cell culture, SILAC, as a simple and accurate approach to expression proteomics *Mol Cell Proteomics* 2002, *1*, 376-86.
[149] Wu CC, *et al.* Metabolic labeling of mammalian organisms with stable isotopes for quantitative proteomic analysis *Anal Chem* 2004, *76*, 4951-9.
[150] Mallick P, *et al.* Proteomics: a pragmatic perspective *Nat Biotechnol* 2010, *28*, 695-709.
[151] Ishihama Y, *et al.* Exponentially modified protein abundance index (emPAI) for estimation of absolute protein amount in proteomics by the number of sequenced peptides per protein *Mol Cell Proteomics* 2005, *4*, 1265-72.
[152] Liu H, *et al.* A model for random sampling and estimation of relative protein abundance in shotgun proteomics *Anal Chem* 2004, *76*, 4193-201.
[153] Stasyk T, *et al.* Zooming in: fractionation strategies in proteomics *Proteomics* 2004, *4*, 3704-16.
[154] Foster LJ, *et al.* Differential expression profiling of membrane proteins by quantitative proteomics in a human mesenchymal stem cell line undergoing osteoblast differentiation *Stem Cells* 2005, *23*, 1367-77.
[155] Kratchmarova I, *et al.* Mechanism of divergent growth factor effects in mesenchymal stem cell differentiation *Science* 2005, *308*, 1472-7.

[156] Czupalla C*, et al.* Proteomic analysis of lysosomal acid hydrolases secreted by osteoclasts: implications for lytic enzyme transport and bone metabolism *Mol Cell Proteomics* 2006, *5*, 134-43.
[157] Ha BG*, et al.* Proteomic profile of osteoclast membrane proteins: identification of Na+/H+ exchanger domain containing 2 and its role in osteoclast fusion *Proteomics* 2008, *8*, 2625-39.
[158] Kubota K*, et al.* Proteome analysis of secreted proteins during osteoclast differentiation using two different methods: two-dimensional electrophoresis and isotope-coded affinity tags analysis with two-dimensional chromatography *Proteomics* 2003, *3*, 616-26.

Chapter 2

Proteomic analysis of human osteoblastic cells: relevant proteins and functional categories for differentiation

Rodrigo D.A.M. Alves, Marco Eijken, Sigrid Swagemakers, H. Chiba, Mark K. Titulaer, Peter C. Burgers, Theo M. Luider and Johannes P.T.M. van Leeuwen

Adapted with permission from
Journal of Proteome Research, 2010, 9 (9), pp 4688–4700

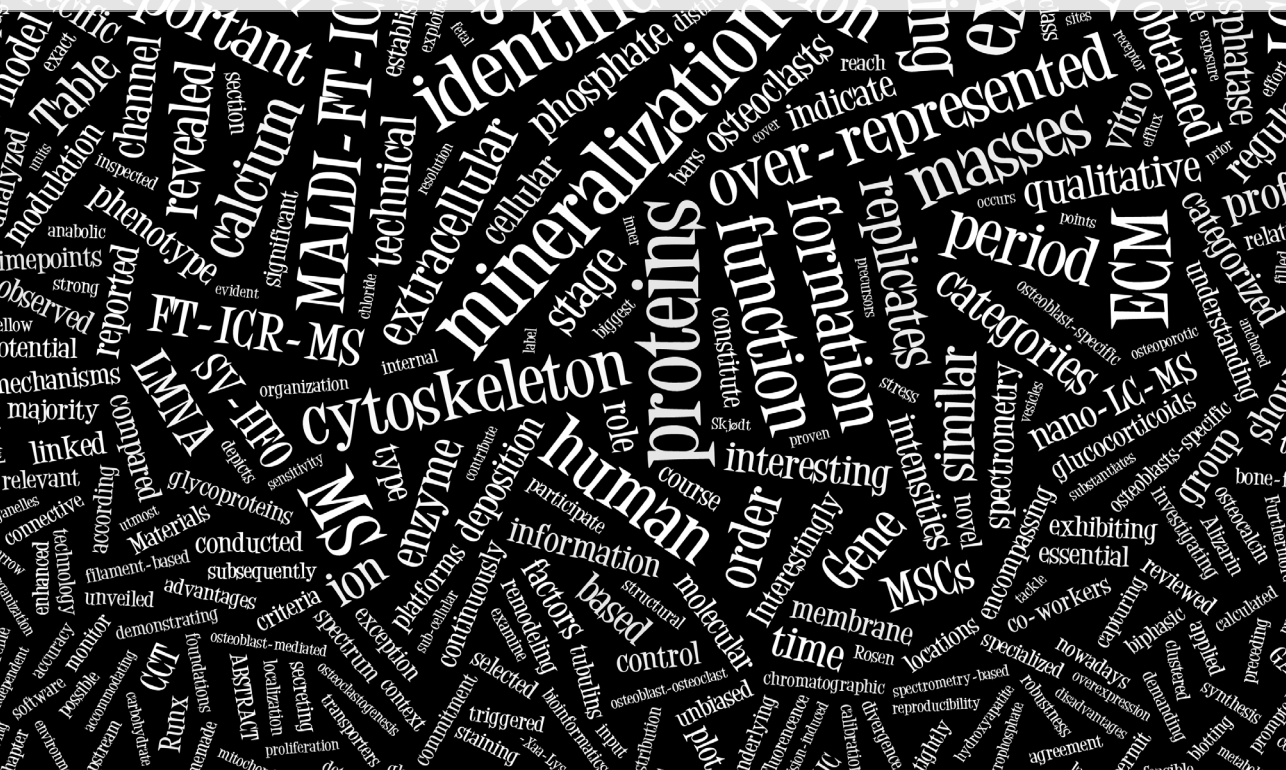

ABSTRACT

Osteoblasts are the bone forming cells, capable of secreting an extracellular matrix with mineralization potential. The exact mechanism by which osteoblasts differentiate and form a mineralized extracellular matrix is presently not fully understood. In order to increase our knowledge about this process, we conducted proteomics analysis in human immortalized pre-osteoblasts (SV-HFO) able to differentiate and mineralize. We identified 381 proteins expressed during the time course of osteoblast differentiation. Gene ontology analysis revealed an over-representation of protein categories established as important players for osteoblast differentiation, bone formation and mineralization such as pyrophosphatases. Proteins involved in antigen presentation, energy metabolism and cytoskeleton re-arrangement constitute other over-represented processes, whose function, albeit interesting is not fully understood in the context of osteoblast differentiation and bone formation. Correlation analysis, based on quantitative data, revealed a biphasic osteoblast differentiation, encompassing a pre-mineralization and a mineralization period. Identified differentially expressed proteins between mineralized and non-mineralized cells include cytoskeleton (e.g. CCT2, PLEC1 and FLNA) and extracellular matrix constituents (FN1, ANXA2 and LGALS1) among others. FT-ICR-MS data obtained for FN1, ANXA2 and LMNA shows a specific regulation of these proteins during the different phases of osteoblast differentiation. Taken together, this study increases our understanding of the proteomics changes that accompany osteoblast differentiation and may permit the discovery of novel modulators of bone formation.

INTRODUCTION

Bone is a highly specialized form of connective tissue. It is very dynamic, being continuously resorbed by osteoclasts and rebuild by osteoblasts. Osteoblasts are the bone-forming cells. They synthesize an extracellular matrix (ECM) and participate in the mineralization of this matrix. While the majority of osteoblasts enter apoptosis, the remainder enters the last stage of osteoblast differentiation becoming osteocytes. The process of osteoblast differentiation from the mesenchymal stem cell (MSC) lineage is tightly regulated and encompasses several steps. Expression of the osteoblasts-specific transcription factors Runx2 and Osterix is essential to drive MSCs towards the osteoblastic lineage[1-3]. After lineage commitment several differentiation steps take place until the formation of mature osteoblasts. These cells are characterized by the expression of the matrix proteins collagen type I, osteocalcin, osteopontin, bone sialoprotein and alkaline phosphatase (ALP), an enzyme which is believed to be involved in bone matrix mineralization[4]. In vitro, human osteoblast differentiation can be triggered by glucocorticoids[5-7], in a process not completely understood. An important step towards understanding osteoblast differentiation is to characterize the osteoblast proteome during differentiation. Over the last years, proteomics technology has made tremendous progress[8-9] and nowadays mass spectrometry (MS)-based proteomics tools can be applied to generate not only qualitative but also quantitative information, to gain a more holistic view of biological systems[8]. Several proteomic studies have been conducted to unravel the mechanisms underlying osteogenesis[10-14]. Yet only a portion of the osteoblast proteome has been unveiled and additional, quantitative proteomic analyses are needed to reach the goal of capturing the full osteoblast proteome.

In this study, we aimed to extend the knowledge about human osteogenesis by investigating the protein expression during the time-course of glucocorticoid-induced osteoblast differentiation and mineralization (differentiating osteoblasts). For this purpose we used the well-characterized pre-osteoblast cell line SV-HFO[15] that develops into mature osteoblasts in a 3-week time period in the presence of glucocorticoids[5]. Two mass spectrometry platforms were used for purposes of identification (nano-LC-MS/MS using an LTQ-Orbitrap) and quantification (MALDI-FT-ICR-MS). Using nano-LC-MS/MS we focused in the identification of proteins expressed by differentiating osteoblast. Moreover, quantitative peptide data was obtained by MALDI-FT-ICR-MS and complemented with specific data-

dependent peptide/protein identification by nano-LC-MS/MS[16].

RESULTS

ALP Activity and Mineralization of Human Pre-osteoblasts

In this study, human pre-osteoblast (SV-HFO) were used, which can be stimulated to differentiate into mature osteoblasts that produce a collagenous ECM that subsequently accumulates mineral. Measuring parameters such as ALP activity and calcium deposition over time can monitor this process. As shown in Figure 1A, differentiating osteoblasts exhibited an increase in ALP activity with a peak around day 10. The ALP increase was followed by a rapid deposition of calcium (Figure 1B). This *in vitro* bone formation model is an excellent model to study protein expression within the different stages of osteoblast differentiation.

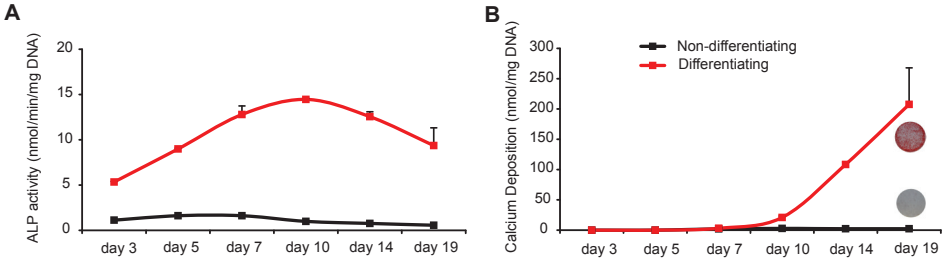

Figure 1. (A) Alkaline phosphatase activity and (B) Calcium deposition in the matrix corrected for cell number (as determined by DNA measurement) in non-differentiating and differentiating human osteoblast cultures. Inserts with Alizarin Red staining at the final timepoint (day 19) are also shown.

Qualitative LC-MS/MS proteome analysis: proteins identified in differentiating human osteoblast cultures

In order to identify as much as possible proteins, we combined chromatographic techniques upstream to detailed MS measurements (nano-LC-MS/MS). We have used the capabilities of this technique to get qualitative insights into the proteins expressed by differentiating osteoblasts combining data from day 5, 10 and 19. This resulted in the successful identification of 381 proteins (Supplementary Table I, Chapter 7). In order to categorize the identified osteoblast proteins we performed gene ontology (GO) annotation over-representation analyses. The proteins were categorized for their annotation related to biological process, molecular function and

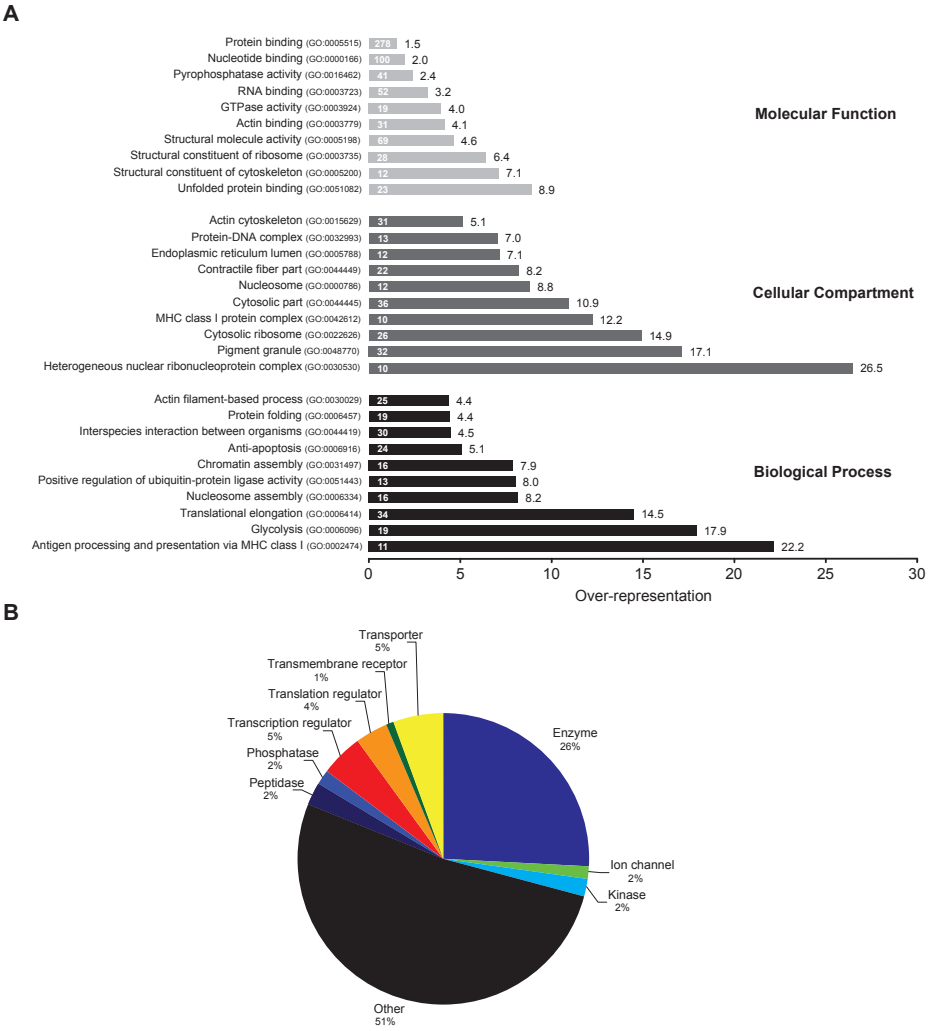

Figure 2. (A) Gene Ontology of the significantly over-represented terms in differentiating osteoblasts (Bonferroni p-value<0.001). Only the 10 highest over-represented terms for biological process, molecular function and cellular compartment categories are shown. Numbers next to the bars indicate over-representation level and numbers embedded in the bars indicate the proteins identified by MS/MS for each category. **(B)** Pie chart representing the functional group distribution of the 381 identified proteins in differentiating osteoblast cultures.

cellular compartment. Figure 2A depicts the significant top GO term categorization by over-representation. Several over-represented terms were related to cytoskeleton

such as structural constituent of the cytoskeleton (GO:0005200), actin cytoskeleton (GO:00015629) and actin filament-based process (GO:0030029). Pyrophosphatase activity (GO:0016462) proteins were over-represented, as well as proteins involved in other distinct processes like energy metabolism (GO:0006096) or antigen processing and presentation (GO:0042612). In addition, the proteins were also categorized in protein families (Figure 2B). Enzymes were the second biggest group of proteins (85 proteins) followed by transporters (18). Phosphatases and ion channels (5 proteins each) were also detected and represent an interesting group of proteins for the process under study, where phosphate and calcium ions represent the foundations for ECM mineralization.

We further inspected for proteins identified and GO annotations that are established players in osteoblast differentiation (Table 1). We have identified 5 proteins linked to skeletal system development, several ECM components including collagens and collagen binding proteins, and proteins that bind to integrins, which are important for ECM-cell signal transduction and osteoblast function (reviewed by Damsky[17]). Other osteoblast-relevant categories included proteins possessing pyrophosphatase activity and calcium ion binding proteins with 41 and 29 proteins, respectively.

Quantitative MALDI-FT-ICR-MS proteome analysis: differentially expressed proteins in mineralization period

Following the qualitative analysis, we used MALDI-FT-ICR-MS to gather quantitative protein expression profiles. A total of 54 individual spectra were obtained corresponding to the day 5, 10 and 19 of differentiating and non-differentiating conditions, analyzed in 3 biological and 3 technical replicates. Data was used as input for homemade software[18] in order to generate a data file containing all information regarding to peptide masses detected and their respective intensities. For each spectrum we obtained 1688-2204 mono-isotopic masses. The exception was one spectrum, a technical replicate of a sample from day 10 non-differentiating condition, that showed only 814 masses and which was excluded from further analysis. Upon performing internal calibration we obtained an average accuracy below 1 ppm in agreement with previous reports using similar equipment[19-20]. We compared all samples according to the criteria mentioned in the Material & Methods section (Selection of Differentially Expressed Peptides part) and identified 422 peptide masses as significantly differentially expressed. Correlation analysis based on measured

Table 1. Gene Ontology terms reporting processes/functions/locations connoted with osteoblast function.

GO category term	Protein	# [a]	Gene [b]	IPI [c]
Skeletal system development (GO:0001501)		5		
	Annexin A2		ANXA2	IPI00418169
	Collagen, type I, alpha 1		COL1A1	IPI00297646
	Glycoprotein NMB		GPNMB	IPI00001592
	Neurofibromin 1		NF1	IPI00220513
	Peroxiredoxin 1		PRDX1	IPI00000874
Extracellular matrix (GO:0031012)		12		
	Collagen, type I, alpha 1		COL1A1	IPI00297646
	Collagen, type VI, alpha 3		COL6A3	IPI00022200
	Fibronectin 1		FN1	IPI00022418
	Galectin 1		LGALS1	IPI00219219
	Superoxide dismutase 1		SOD1	IPI00218733
Calcium ion binding (GO:0005509)		29		
	Annexin A1		ANXA1	IPI00218918
	Calnexin		CANX	IPI00020984
	Myeloid cell leukemia sequence 1		MCL1	IPI00030356
	Protein disulfide isomerase family A, member 4		PDIA4	IPI00009904
	Signal sequence receptor, delta		SSR4	IPI00019385
Pyrophosphatase activity (GO:0016462)		41		
	ATP synthase, H+ transporting, mitochondrial f1 complex, alpha subunit 1		ATP5A1	IPI00440493
	Dynein, axonemal, heavy chain 7		DNAH7	IPI00180384
	Eukaryotic translation elongation factor 1 alpha 1		EEF1A1	IPI00025447
	MDN1, midasin homolog (yeast)		MDN1	IPI00167941
	X-ray repair complementing defective repair in chinese hamster cells 5		XRCC5	IPI00220834
Collagen binding (GO:0005518)		4		
	CD44 molecule		CD44	IPI00297160
	Fibronectin 1		FN1	IPI00022418
	Serpin peptidase inhibitor, clade H , member 1		SERPINH1	IPI00032140
	Thrombospondin 1		THBS1	IPI00296099
Integrin binding (GO:0005178)		5		
	Actinin, alpha 1		ACTN1	IPI00013508
	Actinin, alpha 4		ACTN4	IPI00013808
	Calreticulin		CALR	IPI00020599
	Glycoprotein NMB		GPNMB	IPI00001592
	Thrombospondin 1		THBS1	IPI00296099
Ion channel activity (GO:0005216)		5		
	Voltage-dependent anion channel 1		VDAC1	IPI00216308
	Voltage-dependent anion channel 2		VDAC2	IPI00024145
	Voltage-dependent anion channel 3		VDAC3	IPI00031804
	Transient receptor potential cation channel, subfamily M, member 1		TRPM1	IPI00385124
	Chloride intracellular channel 1		CLIC1	IPI00010896

[a] Number of total proteins in the group. [b] Official gene symbol. [c] IPI accession number.

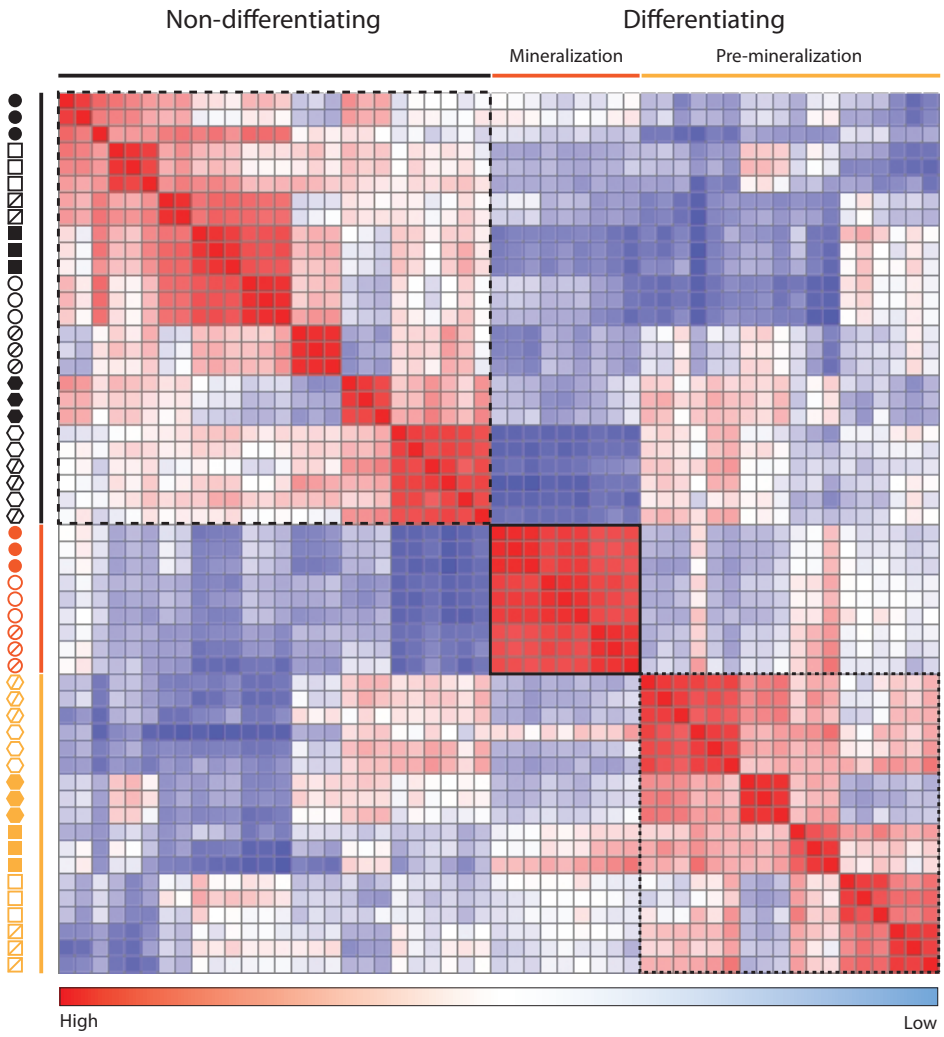

Figure 3. Pearson correlation plot of the 422 significant differentially expressed peptide masses as determined by FT-ICR-MS measurements. All samples, from both differentiating and non-differentiating osteoblasts, are plotted against each other to determine their degree of similarity based on the determined quantitative peptide profile. Lines and geometric shapes: black, non-differentiating condition; yellow and orange, differentiating condition, pre-mineralization and mineralization period respectively. Geometric shapes: circles, day 19; squares, day 10; pentagons, day 5; filled, empty and striped shapes represent the 3 biological replicates, measured each in 3 technical replicates (with exception to a technical replicate from day 10 non-differentiating condition that was excluded from the analysis); Red, high similarity; blue, low similarity.

Table 2. Significantly differentially expressed proteins identified between day 19 mineralized (differentiating condition) vs. day 19 non-mineralized (non-differentiating condition) osteoblasts and between day 19 mineralized vs. day 5 and day 10 pre-mineralization periods.

Protein	Gene Symbol	Peptide sequence	% [b]	IPI [c]	p-value [d]	MH+ Calc. [e]	MH+ FT-ICR [f]	Δ ppm [g]	MH+ Orbitrap [h]	Δ ppm [i]	Δ ppm [j]
Up-regulated at day 19 mineralized versus day 19 non-mineralized osteoblasts											
Tubulin beta-2C chain	TUBB2C	R.LHFFMPGFAPLTSR.G	3.1	IPI00007752.1	0.000358	1620.83557	1620.8359	-0.20	1620.83672	0.71	-0.51
Annexin A2	ANXA2	R.AEDGSVIDYELIDQDAR.D		IPI00455315.3	0.000412	1908.8822	1908.8805	0.89	1908.88066	-0.81	-0.08
Annexin A2	ANXA2	R.RAEDGSVIDYELIDQDAR.D		IPI00455315.3	0.000412	2064.98315	2064.9822	0.46	2064.9727	-5.06	4.60
Annexin A2	ANXA2	K.TDLEKDIISDTSGDFR.K	10.1	IPI00455315.3	0.000574	1811.86572	1811.8646	0.62	1811.86467	-0.58	-0.04
Fibronectin precursor	FN1	K.IAWESPQGQVSR.Y		IPI00022418.1	0.000574	1357.68591	1357.6855	0.30	1357.68474	-0.86	0.56
Fibronectin precursor	FN1	K.HYQINQQWER.T		IPI00022418.1	0.000161	1401.66577	1401.666	-0.16	1401.66667	0.64	-0.48
Fibronectin precursor	FN1	R.WSRPQAPITGYR.I		IPI00022418.1	0.000385	1431.74915	1431.7501	-0.66	1431.75078	1.14	-0.47
Fibronectin precursor	FN1	R.VDVIPVNLPGEHGQR.L	2.1	IPI00022418.1	0.000401	1629.87073	1629.8729	-1.33	1629.87273	1.23	0.10
Heat shock protein HSP 90-alpha 2	HSP90AA1	R.RAPFDLFENR.K		IPI00604607.2	0.000385	1264.64331	1264.6429	0.32	1264.64275	-0.44	0.12
Heat shock protein HSP 90-alpha 2	HSP90AA1	K.SLTNDWEDHLAVK.H	4.3	IPI00604607.2	0.000409	1527.74377	1527.7433	0.31	1527.74272	-0.69	0.38
Heat shock protein HSP 90-beta	HSPA90AB1		1.8	IPI00414676.5							
Lamin-A/C	LMNA	K.LRDLEDSLAR.E		IPI00021405.3	0.000579	1187.63782	1187.6366	1.03	1187.63677	-0.88	-0.14
Lamin-A/C	LMNA	R.NSNLVGAAHEELQQSR.I	3.9	IPI00021405.3	0.000161	1752.8623	1752.8633	-0.57	1752.86271	0.23	0.34
Myosin-9	MYH9	R.LQQELDDLLVDLDHQR.Q	0.8	IPI00019502.2	0.000274	1949.99268	1949.9953	-1.34	1949.99468	1.03	0.32
Peroxiredoxin-6	PRDX6	K.LPFPIIDDR.N	4.0	IPI00220301.4	0.005316	1085.599	1085.5995	-0.46	1085.59868	-0.29	0.76
Polymerase I and transcript release factor	PTRF	K.IIGAVDQIQLTQAQLEER.Q	4.6	IPI00176903.2	0.000412	2025.09753	2025.0996	-1.02	2025.09269	-2.39	3.41
Splicing factor, proline- and glutamine-rich	SFPQ	K.YGEPGEVFINK.G	1.6	IPI00010740.1	0.000321	1252.62085	1252.6204	0.36	1252.62078	-0.06	-0.30
Down-regulated at day 19 mineralized versus day 19 non-mineralized osteoblasts											
Actin, cytoplasmic 1	ACTB	K.AGFAGDDAPR.A		IPI00021439.1	0.000559	976.4483	976.449	-0.72	976.44432	-4.08	4.79
Actin, cytoplasmic 2	ACTG1			IPI00021440.1							
Actin, gamma-enteric smooth muscle	ACTG2			IPI00025416.3							
Actin, aortic smooth muscle	ACTA2			IPI00008603.1							
Actin, alpha skeletal muscle	ACTA1			IPI00021428.1							
Actin, alpha cardiac	ACTC1			IPI00023006.1							
Actin, cytoplasmic 1	ACTB	R.HQGVMVGMGQK.D		IPI00021439.1	0.000792	1171.57104	1171.5708	0.20	1171.57274	1.45	-1.66
Actin, cytoplasmic 2	ACTG1			IPI00021440.1							
Actin, gamma-enteric smooth muscle	ACTG2		5.6	IPI00025416.3							
Actin, aortic smooth muscle	ACTA2		5.6	IPI00008603.1							
Actin, alpha skeletal muscle	ACTA1		5.6	IPI00021428.1							
Actin, alpha cardiac	ACTC1		5.6	IPI00023006.1							
Actin, cytoplasmic 1	ACTB	R.VAPEEHPVLLTEAPLNPK.A	10.4	IPI00021439.1	0.000792	1954.06445	1954.0653	-0.43	1954.06474	0.15	0.29
Actin, cytoplasmic 2	ACTG1		10.4	IPI00021440.1							
Tubulin alpha-1 chain	TUBA4A	K.VGINYQPPTVVPGGDLAK.V	4.3	IPI00007750.1	0.000412	1824.98547	1824.9863	-0.45	1824.98674	0.70	-0.24
T-complex protein 1 subunit beta	CCT2	R.GATQQILDEAER.S	2.2	IPI00297779.6	0.001849	1330.65979	1330.6604	-0.46	1330.66069	0.68	-0.22
DNA-binding protein A	CSDA	K.GAEAANVTGPDGVPVEGSR.Y	5.1	IPI00031801.4	0.005316	1782.86169	1782.8652	-1.97	1782.86467	1.67	0.30
Cysteine and glycine-rich protein 1	CSRP1	K.GFGFGQGAGALVHSE	7.8	IPI00442073.4	0.000358	1433.68079	1433.6808	-0.01	1433.68072	-0.05	0.06
Heterogeneous nuclear ribonucleoprotein R	HNRNPR	R.NLATTVTEEILEK.S	2.1	IPI00012074.3	0.000161	1460.7843	1460.7858	-1.03	1460.78667	1.62	-0.60
Heat shock 70 kDa protein 4	HSPA4	R.AFSDPFVEAEK.S	1.3	IPI00002966.1	0.000875	1239.58923	1239.5878	1.15	1239.58867	-0.45	-0.70
Hypothetical protein	HSPA5	K.NQLTSNPENTVFDAK.R	2.3	IPI00003362.2	0.000574	1677.80786	1677.8083	-0.26	1677.80876	0.54	-0.27
Heat shock cognate 71 kDa protein	HSPA8	R.RFDDAVVQSDMK.H		IPI00003865.1	0.000314	1410.66821	1410.6688	-0.42	1410.66875	0.38	0.04
Heat shock cognate 71 kDa protein	HSPA8	K.NQVAMNPTNTVFDAK.R	5.5	IPI00003865.1	0.000412	1649.79517	1649.7936	0.95	1649.79278	-1.45	0.50
Galectin-1	LGALS1	K.LPDGYEFK.F	6.0	IPI00219219.2	0.005316	968.47235	968.4737	-1.39	968.47472	2.45	-1.05
Myosin-9	MYH9	R.IAEFTTNLTEEEEK.S	0.7	IPI00019502.2	0.000385	1653.7854	1653.7853	0.06	1653.78472	-0.41	0.35
Myosin regulatory light polypeptide 9	MYL9	R.FTDEEVDEMYR.E	6.4	IPI00220278.4	0.000570	1433.58899	1433.5904	-0.98	1433.59075	1.23	-0.24
5'-nucleotidase precursor	NT5E	K.YPFIVTSDDGR.K	1.9	IPI00009456.1	0.000161	1269.61096	1269.6095	1.15	1269.60612	-3.81	2.66
Pyruvate kinase isozymes M1/M2	PKM2	R.VNFAMNVGK.A		IPI00479186.4	0.000385	979.50299	979.5034	-0.42	979.50673	3.82	-3.40
Pyruvate kinase isozymes M1/M2	PKM2	R.TATESFASDPILYR.P		IPI00479186.4	0.000412	1570.77478	1570.7742	0.37	1570.77471	-0.04	-0.32
Pyruvate kinase isozymes R/L	PKM2	R.GDLGIEIPAEK.V	6.4	IPI00479186.4	0.000574	1141.60999	1141.6103	-0.27	1141.61077	0.68	-0.41
Pyruvate kinase isozymes R/L	PKLR		1.9	IPI00027165.3							
Procollagen-lysine,2-oxoglutarate 5-dioxygenase 2 precursor	PLOD2	K.IVGPEENLSQAEAR.N	1.9	IPI00472165.1	0.005316	1512.76526	1512.7649	0.24	1512.7647	-0.37	0.13
40S ribosomal protein S3	RPS3	R.ELAEDGYSGVEVR.V	5.4	IPI00011253.3	0.000385	1423.66992	1423.6697	0.15	1423.66875	-0.82	0.67
Reticulon-4	RTN4	R.GPLPAAPPVAPER.Q	1.1	IPI00021766.4	0.005316	1271.71069	1271.7105	0.15	1271.71074	0.04	-0.19
Vimentin	VIM	R.ETNLDSLPLVDTHSK.R	3.2	IPI00418471.5	0.000385	1668.84387	1668.8458	-1.16	1668.84673	1.71	-0.56

Table 2. Continued

Protein	Gene Symbol	Peptide sequence	% [b]	IPI [c]	p-value [d]	MH+ calc. [e]	MH+ FT-ICR [f]	Δ ppm [g]	MH+ Orbitrap [h]	Δ ppm [i]	Δ ppm [j]
Up-regulated at day 19 mineralized versus day 5 and 10 pre-mineralization period											
Eukaryotic translation initiation factor 3 subunit 1	EIF3J	K.ETFGVNNAVYGIDAMNPSSR.D	7.8	IPI00290461.3	0.001849	2141.99194	2141.9882	1.75	2141.99272	0.36	-2.11
Heat shock protein HSP 90-alpha 2	HSP90AA1	R.RAPFDLFENR.K	1.9	IPI00604607.2	0.000787	1264.64331	1264.6429	0.32	1264.64275	-0.44	0.12
Lamin-A/C	LMNA	K.LRDLEDSLAR.E	1.5	IPI00021405.3	0.000579	1187.63782	1187.6366	1.03	1187.63677	-0.88	-0.14
26S protease regulatory subunit 6A	PSMC3	R.QTYFLPVIGLVDAEK.L	3.4	IPI00018398.4	0.000161	1692.92065	1692.9233	-1.57	1692.92277	1.25	0.31
Splicing factor, proline- and glutamine-rich	SFPQ	K.YGEPGEVFINK.G	1.6	IPI00010740.1	0.000401	1252.62085	1252.6204	0.36	1252.62078	-0.06	-0.30
Hypothetical protein	HSPA5	R.ITPSYVAFTPEGER.L		IPI00003362.2	0.000412	1566.77991	1566.7795	0.26	1566.77874	-0.75	0.49
Hypothetical protein	HSPA5	R.IINEPTAAAIAYGLDKR.E		IPI00003362.2	0.000412	1815.99634	1815.9996	-1.80	1816.00078	2.44	-0.65
Hypothetical protein	HSPA5	K.DNHLLGTFDLTGIPPAPR.G	7.5	IPI00003362.2	0.000412	1934.01306	1934.014	-0.49	1934.01469	0.84	-0.36
Protein disulfide-isomerase precursor	P4HB	K.VDATEESDLAQQYGVR.G	3.2	IPI00010796.1	0.001849	1780.83484	1780.8346	0.13	1780.83477	-0.04	-0.10
Translocon-associated protein delta subunit precursor	SSR4	R.FFDEESYSLLR.K	6.4	IPI00019385.1	0.000452	1405.66345	1405.6612	1.60	1405.66069	-1.96	0.36
Heat shock protein 75 kDa, mitochondrial precursor	TRAP1	R.GVVDSEDIPLNLSR.E	2.0	IPI00030275.5	0.000412	1513.78564	1513.7857	-0.04	1513.78471	-0.61	0.65
Down-regulated at day 19 mineralized versus day 5 and 10 pre-mineralization period											
Actin, cytoplasmic 1	ACTB	R.AVFPSIVGRPR.H		IPI00021439.1	0.000412	1198.70544	1198.7054	0.03	1198.70476	-0.57	0.53
Actin, cytoplasmic 2	ACTG1			IPI00021440.1							
Actin, gamma-enteric smooth muscle	ACTG2			IPI00025416.3							
Actin, aortic smooth muscle	ACTA2			IPI00008603.1							
Actin, alpha skeletal muscle	ACTA1			IPI00021428.1							
Actin, alpha cardiac	ACTC1			IPI00023006.1							
Actin, cytoplasmic 1	ACTB	R.VAPEEHPVLLTEAPLNPK.A		IPI00021439.1	0.000412	1954.06445	1954.0653	-0.43	1954.06474	0.15	0.29
Actin, cytoplasmic 2	ACTG1			IPI00021440.1							
Actin, cytoplasmic 1	ACTB	R.HQGVMVGMGQK.D	10.7	IPI00021439.1	0.000574	1171.57104	1171.5708	0.20	1171.57274	1.45	-1.66
Actin, cytoplasmic 2	ACTG1		10.7	IPI00021440.1							
Actin, gamma-enteric smooth muscle	ACTG2		5.9	IPI00025416.3							
Actin, aortic smooth muscle	ACTA2		5.8	IPI00008603.1							
Actin, alpha skeletal muscle	ACTA1		5.8	IPI00021428.1							
Actin, alpha cardiac	ACTC1		5.8	IPI00023006.1							
Actin, cytoplasmic 1	ACTB	R.SYELPDGQVITIGNER.F		IPI00021439.1	0.000574	1790.89197	1790.8909	0.60	1790.89067	-0.73	0.13
Actin, cytoplasmic 2	ACTG1			IPI00021440.1							
Actin, gamma-enteric smooth muscle	ACTG2		7.2	IPI00025416.3							
Actin, aortic smooth muscle	ACTA2		7.2	IPI00008603.1							
Actin, alpha skeletal muscle	ACTA1		7.2	IPI00021428.1							
Actin, alpha cardiac	ACTC1		7.2	IPI00023006.1							
Actin, cytoplasmic 1	ACTB	N.TVLSGGTTMYPGIADR.M		IPI00021439.1	0.005316	1638.81555	1638.8173	-1.07	1638.8167	0.70	0.37
Actin, cytoplasmic 2	ACTG1			IPI00021440.1							
Actin, cytoplasmic 1	ACTB	Y.VALDFEQEMATAASSSSLEK.S		IPI00021439.1	0.005316	2113.99585	2113.9942	0.78	2113.99272	-1.48	0.70
Actin, cytoplasmic 2	ACTG1			IPI00021440.1							
Actin, cytoplasmic 1	ACTB	K.DLYANTVLSGGTTMYPGIADR.M	22.9	IPI00021439.1	0.000412	2215.07007	2215.0698	0.12	2215.0728	1.23	-1.35
Actin, cytoplasmic 2	ACTG1		22.9	IPI00021440.1							
Annexin A1	ANXA1	R.SEDFGVNEDLADSDAR.A	4.6	IPI00218918.4	0.000744	1739.73547	1739.7338	0.96	1739.73271	-1.59	0.63
Eukaryotic translation initiation factor 4H	EIF4H	R.TVATPLNQVANPNSAIFGGAR.P	8.5	IPI00014263.1	0.005316	2098.104	2098.106	-0.95	2098.11284	4.21	-3.26
Filamin A, alpha	FLNA	R.YAPSEAGLHEMDIR.Y	0.5	IPI00333541.4	0.000314	1588.74243	1588.7406	1.15	1588.74077	-1.04	-0.11
Fibronectin precursor	FN1	K.WLPSSSPVTGYR.V		IPI00022418.1	0.000274	1349.68481	1349.6849	-0.07	1349.68474	-0.05	0.12
Fibronectin precursor	FN1	R.WSRPQAPITGYR.I		IPI00022418.1	0.000574	1431.74915	1431.7501	-0.66	1431.75078	1.14	-0.47
Fibronectin precursor	FN1	R.VDVIPVNLPGEHGQR.L	1.6	IPI00022418.1	0.000792	1629.87073	1629.8729	-1.33	1629.87273	1.23	0.10
Heterogeneous nuclear ribonucleoproteins A2/B1	HNRNPA2B1	R.NMGGPYGGGNYGPGGSGGSGGYGGR.S	7.1	IPI00396378.3	0.000792	2189.90527	2189.9024	1.31	2189.89262	-5.78	4.47
Nucleoside diphosphate kinase B	NME2	R.VMLGETNPADSKPGTIR.G	11.2	IPI00026260.1	0.000412	1785.91638	1785.9185	-1.19	1785.91875	1.33	-0.14
Putative nucleoside diphosphate kinase	NME2P1		12.4	IPI00029091.1							
Nucleoside diphosphate kinase A	NME1		11.2	IPI00012048.1							
Protein disulfide-isomerase A3 precursor	PDIA3	K.MDATANDVPSPYEVR.G	3.0	IPI00025252.1	0.000559	1664.75842	1664.7565	1.15	1664.75676	-1.00	-0.16
Phosphoglycerate mutase 1	PGAM1	R.HGESAWNLENR.F	4.3	IPI00549725.5	0.000412	1312.60291	1312.6024	0.39	1312.60003	-2.19	1.81
Pyruvate kinase 3	PKM2	R.TATESFASDPILYR.P	2.6	IPI00479186.4	0.000412	1570.77478	1570.7742	0.37	1570.77471	-0.04	-0.32
Transketolase	TKT	R.LGQSDPAPLQHQMDIYQK.R	2.9	IPI00643920.2	0.000412	2069.01196	2069.0152	-1.57	2069.01274	0.38	1.19
14-3-3 protein epsilon	YWHAE	K.AASDIAMTELPPTHPIR.L	6.7	IPI00000816.1	0.000412	1819.93713	1819.9379	-0.42	1819.93876	0.90	-0.47
Annexin A2	ANXA2	K.AYTNFDAER.D	2.7	IPI00455315.3	0.000792	1086.48511	1086.485	0.10	1086.48467	-0.40	0.30
Myosin-9	MYH9	K.MQQNIQELEEQLEEEESAR.Q	1.0	IPI00019502.2	0.005316	2333.05615	2333.0549	0.54	2333.054	-0.92	0.39
Vinculin	VCL	K.AVAGNISDPGLQK.S	1.1	IPI00307162.2	0.001849	1269.67969	1269.6821	-1.90	1269.68267	2.35	-0.45

[a] Official gene symbol. [b] Protein sequence coverage. [c] IPI accession number. [d] Differentially expressed peptide level of significance as determined by Wilcoxon test. [e] Calculated peptide mass in the protonated form (MH+). [f] FT-ICR measured peptide mass (MH+). [g] ppm difference between real and FT-ICR measured peptide mass. [h] Orbitrap measured peptide mass (MH+). [i] ppm difference between real and Orbitrap measured peptide mass. [j] ppm difference between FT-ICR and Orbitrap measured peptide mass

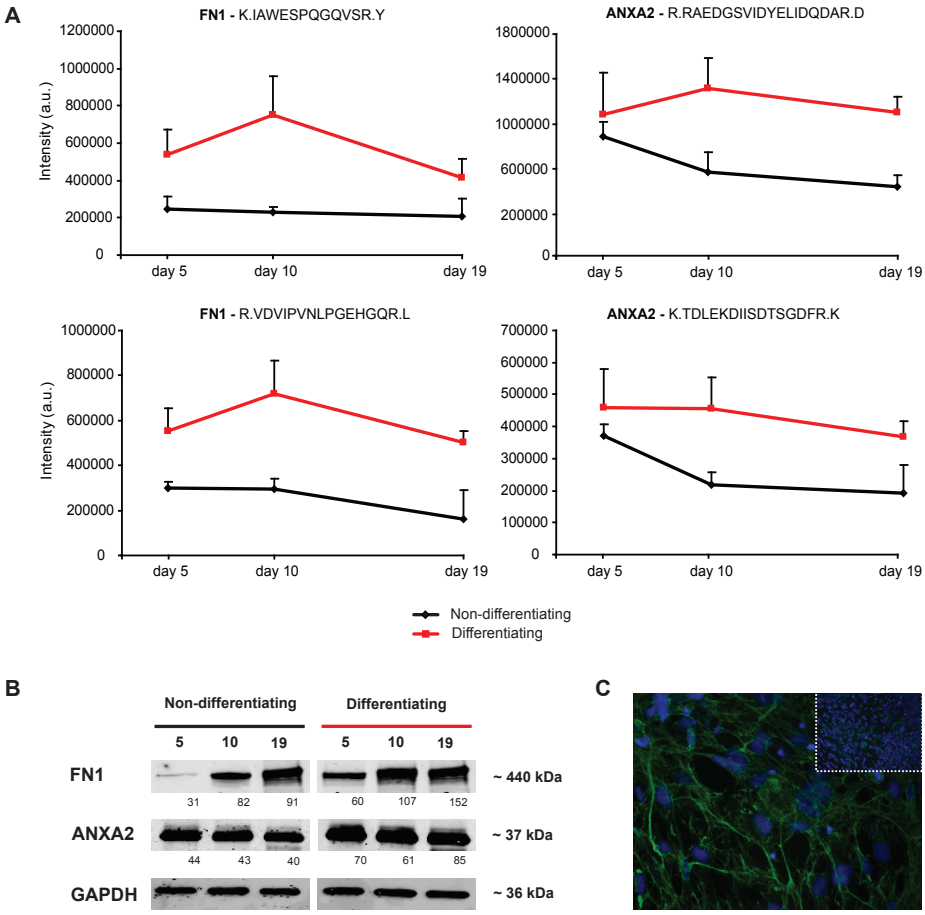

Figure 4. (A) Quantitative FT-ICR-MS profile obtained for FN1 and ANXA2. Two peptides belonging to each of these proteins are shown. **(B)** Immunodetection of FN1, ANXA2 and GAPDH (loading control). Fluorencence detection was done using the LI-COR system. Numbers were calculated using the band intensities and indicate protein expression relative to GAPDH. **(C)** Immunocytochemistry for FN1 in SV-HFO cells from day 19 mineralizing condition. Negative control shown as insert.

intensities of these 422 peptide masses is shown in Figure 3. It is interesting that this unbiased approach delivered a correlation plot with a divergence of the differentiating and non-differentiating conditions. Within the differentiating condition there was also a clear discrepancy between the pre-mineralization and mineralization periods, with a very strong correlation between the samples of the mineralization period (Figure 3). In addition, technical and biological replicates always clustered together

demonstrating the robustness of the MALDI-FT-ICR-MS measurements.

These observations prompted us to examine in more detail the protein expression differences within the differentiating condition, comparing mineralization (day 19) versus the preceding pre-mineralization period (day 5 and day 10). Additionally, we included in these analyses the two extreme phenotypes, i.e. day 19 in differentiating and non-differentiating condition. In total, these comparisons led to an identification of 52 differently expressed proteins (Table 2), according to the criteria to combine MALDI-FT-ICR-MS and LC-MS/MS data mentioned in the Materials and Methods section. Among other proteins, cytoskeleton (actins, tubulins and vimentin), actin binding (CCT2, CSRP1, FLNA, MYH9 and VCL), ECM (FN1, LGALS1) and calcium binding proteins (ANXA2, ANXA1) were identified.

Validation of protein expression and MS-based quantification

We verified that most of the (FT-ICR-MS) quantified peptides, mapping to the same protein, have similar expression patterns (Figure 4A). In order to validate the MS data, we selected two differentially expressed proteins that have been reported to be relevant for bone biology, ANXA2 and FN1. The expression pattern of these proteins was similar for both FT-ICR-MS and western blotting (Figure 4A and 4B). We have also performed immunocytochemistry for FN1. As expected, FN1 immunocytochemistry from mineralized day 19 osteoblasts disclosed a clear extracellular localization of this protein (Figure 4C).

DISCUSSION

In vitro Human osteoblast differentiation models can be an effective model to detect proteins that have pivotal roles in bone formation and potential targets to shift bone remodeling towards the anabolic process. The introduction of mass spectrometry into the proteomics field has made this type of analysis feasible, revealing large set of proteins that can be analyzed using bioinformatics tools to discover protein associations or over-represented biological processes.

In the present work, we aimed to identify and quantify proteins in an effort to gain knowledge about the osteoblast differentiation process and identify novel proteins that may modulate osteoblast mineralization. To this end, we exploited our very well characterized human pre-osteoblast cell model[5, 15] and mass spectrometric analyses to identify proteins against the background of osteoblast differentiation and

in vitro bone formation. Furthermore, we aimed to assess quantitative differences both between differentiated mineralized cultures and their non-differentiated counterparts, as well as between the pre-mineralization and mineralization periods of the differentiated osteoblast culture.

With regard to the protein profile of differentiating osteoblasts, we have identified 381 proteins. GO analysis revealed that cytoskeleton and cytoskeletal related processes were among the highest over-represented terms. This shows the importance of specific cytoskeleton assembly for osteoblast differentiation, also verified by Higuchi and co-workers[21]. It is known that actin filaments (stress fibers) are physically linked to the ECM by integrins[21-23]. These transmembrane glycoproteins can interact with ECM proteins bridging the extracellular with the intracellular compartment. This interaction affects the organization of the cytoskeleton[24], signal transduction and the expression of transcription factors and osteoblast-specific genes in osteoblasts[25-26]. Other identified processes include distinct processes such as glucose metabolism and antigen presentation. New insights linking bone remodeling to energy metabolism control are described in the review by Rosen *et al.*[27]. The fact that these processes were over-represented can be related to the fact that ECM synthesis, maturation and mineralization are highly demanding processes[28], leading to mitochondrial and antioxidant enzyme changes[29].

Interestingly, our data show a high over-representation of proteins belonging to the MHC class I protein complex involved in antigen presentation. Already back in 1989, Skjødt and co-workers[30] reported that osteoblast-like cells function as antigen presenting cells, being able to stimulate peripheral bone marrow cells (PBMCs). Since osteoclasts are derived from PBMC, it is tempting to speculate that over-representation of this type of proteins may be related to the osteoblast effectiveness to stimulate osteoclast differentiation from their precursors or to interact with hematopoietic stem cells in the stem cell niche[31].

Phosphatases and ion channels constitute another group of proteins identified. Some of these proteins have been identified already as important players during osteoblast differentiation. This is the case for the nuclear transmembrane ion channel protein, chloride intracellular channel 1 (CLIC1). Knockdown of CLIC1 suppresses osteoblast differentiation from MSCs whereas protein overexpression increases osteogenic markers such as ALP activity[32]. Other interesting proteins include the voltage-dependent anion channel 1, 2 and 3 (VDAC1, VDAC2 and VDAC3). These membrane proteins play a role in the efflux of metabolites including ATP

and phosphate in the mitochondria[33]. Interestingly, these proteins are recurrently identified in matrix vesicles (MV)[14, 34] the organelles implicated in initiation of mineralization[35-36]. Start of mineral deposition occurs by accommodating the proper environment for crystal growth in the MV. This implicates mobilization of calcium and phosphate to form hydroxyapatite. Phosphate mobilization can be achieved by degradation of pyrophosphate (PPi), a mineralization inhibitor, into free phosphate (Pi). Our data show that enzymes involved in this process were over-represented by more than 2-fold (GO:0016462 pyrophosphatase activity, Figure 2A) supporting its importance for osteoblast-mediated ECM mineralization.

In our quantitative MALDI-FT-ICR-MS approach, we identified 52 differentially expressed proteins between day 19 mineralized and day 19 non-mineralized osteoblasts and between day 19 mineralized and the osteoblast pre-mineralization time points, day 5 and day 10. Some of these proteins will be discussed in more detail. We found that cytoskeleton components (several actins, tubulins and vimentin) and actin binding proteins (CCT2, CSRP1, FLNA, MYH9 and VCL) were differentially expressed in differentiating osteoblasts. This follows the data discussed above and further substantiates a prominent role for cytoskeletal reorganization in osteoblast differentiation. ECM (FN1, LGALS1) and calcium binding (ANXA2, ANXA1) proteins were also identified among differentially expressed proteins. FN1 is an abundant ECM glycoprotein with significantly higher expression, at all timepoints analyzed, in differentiating osteoblasts relative to their non-differentiated counterparts (Figure 4A and 4B). FN1 is required for osteoblast differentiation and mineralization through interaction with the integrin $\alpha 5\beta 1$ FN1 receptor[37]. Besides determining osteoblast cellular fate, FN1 is also required for their survival once osteoblasts are mature[38]. We identified ANXA2 as a protein that was enhanced during stages of pre-mineralization. Other studies showed that osteoblasts over-expressing ANXA2 show enhanced mineralization[39]. ANXA2 is a calcium-dependent phospholipid binding protein located in the ECM and in MV[14, 36] where they are thought to be important for Ca^{2+} uptake[40]. The fact that we observed the highest expression of ANXA2 in the pre-mineralization phase might be associated with increasing ALP activity verified at this stage and the start of Ca^{2+} uptake into the MV. Interestingly, ANXA2 has been shown to be an autocrine factor for osteoclasts, increasing osteoclastogenesis and resorption[41-42]. Here we show that ANXA2 was also expressed and regulated during osteoblast differentiation making it tempting to speculate about implications in the osteoblast-osteoclast crosstalk.

LMNA belongs to the nuclear inner membrane class of proteins. Mutations in this gene display a phenotype compatible with progeria syndrome exhibiting loss of subcutaneous fat, muscular dystrophy and an osteoporotic phenotype[43]. The bone phenotype is thought to be due to a deficit in osteoblast and matrix formation[44-45]. Our data supports the importance of this protein for osteoblast differentiation, with higher expression in differentiating cells. However, while ANXA2 and FN1 levels were higher prior to mineralization, LMNA expression peaked when cells were mature. This difference in expression pattern is probably related to the physiological changes of the osteoblast in its progression towards osteocyte. Thus, these proteins seem to represent hallmarks of the period of osteoblast development, ANXA2 and FN1 of the pre-mineralization and LMNA of the mineralization period.

Also proteins were specifically suppressed in late staged differentiating osteoblasts, including PLOD2, NTE5 and LGALS1. PLOD2 forms hydroxylysine residues in -Xaa-Lys-Gly- sequences in collagens that serve as sites of attachment for carbohydrate units being essential for the stability of the intermolecular collagen cross-links. Mutations in PLOD2 cause Bruck Syndrome in which the bone collagen lacks pyridinolines and the other cross-links based on hydroxylysine aldehydes[46]. NTE5, more often referred as CD73 is a glycosyl phosphatidylinositol (GPI) plasma membrane anchored enzyme[47], regarded as a MSC marker[48-49]. LGALS1 is a ß-galactoside-binding protein that has been implicated in several processes from cell adhesion and migration[50] to proliferation[51] and apoptosis[52]. Human fetal MSCs upon exposure to LGALS1 enter myogenic differentiation[53]. Down-regulation of PLOD2 upon mineralization is perhaps an indication that collagen cross-linking regulation is mostly needed in the pre-mineralization stage, when ECM is actively synthesized. NTE5 and LGALS1 decreased expression might be a sign of cellular maturity towards fully differentiated osteoblasts.

Like any other approach, the use of the MALDI-FT-ICR-MS for label free quantitation has its own advantages and disadvantages. Among the latter is the need to use an independent platform to identify the peptides/proteins profiled, due to the inability to generate good fragmentation data on single charged MALDI ions in FTMS by collision-induced dissociation[54]. On the other hand, MALDI-FT-ICR-MS data does not require extensive data processing and analysis. Other advantages include the high sensitivity and high mass resolution described elsewhere[54-56], and the superior reproducibility of these MS measurements, crucial in quantitative proteomics. Variation of peptide intensity measurements was as low as 15% in

technical replicates and 36% considering biological replicates. For the majority of the different peptides detected that belong to the same protein, the FT-ICR-MS determined expression patterns were similar. Moreover, immunodetection of FN1 and ANXA2 confirmed their up-regulation in differentiated osteoblasts compared to their non-differentiating counterparts.

From the list of proteins generated it is evident that classical osteoblast markers such as RUNX2, ALPL, SPP1, BGLAP and SPARC were not observed. We believe that this was due to the fact that their concentrations were low and beyond the range we could detect. In human cells the range of protein copy numbers is 7-8 orders of magnitude[57] while MS analysis can only cover up to 4-6[58]. To tackle this problem, we believe that the approach here described should be combined with the isolation of sub-cellular and ECM proteomes.

This study aimed to contribute to the knowledge of the osteoblast differentiation program by an unbiased mass spectrometry-based proteomics approach. Qualitative analysis revealed not only proteins expressed by differentiating osteoblasts but also biological processes and molecular functions that drive cells towards bone formation and mineralization. At this level, cytoskeleton, energy metabolism and antigen presentation processes were among the most over-represented categories. Complementation of the analysis with quantitative differences revealed both bone related proteins, with characteristic expression patterns in the course of differentiation (ANXA2, FN1 and LMNA), and other proteins (e.g. LGALS1) not extensively studied in the bone field. The identification of proteins having a proven role in bone function in addition to others with yet unknown bone function strongly supports that the latter are also important for osteoblast differentiation and mineralization. Altogether, our data provides more information in the pursuit of targets for bone formation modulation, which is of utmost importance to develop new therapies for bone related diseases such as osteoporosis.

Supplementary Data

Supplementary data available in Chapter 7.

MATERIALS & METHODS

Cell Culture. Human SV-HFO cells were seeded in a density of $5x10^3$ vital cells/cm^2 and pre-cultured for 1 week in α-MEM (GIBCO, Paisley, UK) supplemented

with 20 mM HEPES, pH 7.5 (Sigma, St. Louis, MO, USA), streptomycin/penicillin, 1.8 mM $CaCl_2$ (Sigma) and 10% heat-inactivated FCS (GIBCO) at 37°C and 5% CO_2 in a humidified atmosphere. During pre-culture cells remained in an undifferentiated stage. At this point cells were seeded in a density of 1 x 10^4 vital cells/cm^2 in the presence of 2% charcoal-treated FCS. For induction of osteoblast differentiation and mineralization the basal medium was freshly supplemented with 10 mM β-glycerophosphate (Sigma) and 100 nM dexamethasone (Sigma). For the non-differentiating condition the culture condition was identical except the presence of dexamethasone. Throughout the remainder of the study, DEX-treated and non-DEX-treated cultures are referred as differentiating and non-differentiating osteoblasts, respectively. The media was replaced every 2-3 days to both non-differentiating and differentiating osteoblasts.

Alkaline Phosphatase. ALP activity was assayed by determining the release of paranitrophenol from paranitrophenylphosphate (20 mM diethanolamine buffer supplemented with 1 mM $MgCl_2$ at pH 9.8) in the SV-HFO lysates for 10 min at 37°C. Adding 0.06 M NaOH stopped the reaction. Adsorption was measured at 405 nm. Results were corrected for the DNA content of the cell lysates.

Mineralization. For quantification of the mineral content cell lysates were incubated overnight in 0.24 M HCl at 4°C. Calcium content was colorimetrically determined with a calcium assay kit (Sigma) according to the manufacturer's instructions. Results were corrected for the DNA content of the cell lysates. For Alizarin Red staining, cell cultures were fixed for 60 min with 70% ethanol on ice. After fixation, cells were washed twice with PBS and stained for 10 min with Alizarin Red solution (saturated Alizarin Red in demineralized water was titrated to pH 4.2 using 0.5% ammonium hydroxide).

Protein Isolation. At day 5, 10 and 19 of culture, non-differentiating and differentiating cells, in three biological replicates (a total of 18 samples), were washed in phosphate-buffered saline (PBS, GIBCO) and lysed directly in a culture dish by adding TRIzol (Invitrogen, Carlsbad, CA, USA). The protein phenol-ethanol phase was stored at -80°C. Proteins were precipitated using methanol/chloroform[59]. To facilitate protein solubilisation and enzymatic cleavage of proteins, pellets were re-suspended in 100 µl of 0.1% (w/v) RapiGest SF (Waters, Milford, MA, USA) in 50 mM ammonium bicarbonate and dissolved by sonification at 70% amplitude and maximum temperature of 18°C (Bransons Ultrasonics, Danbury, CT, USA) until no aggregates were visible. Protein concentration was determined using a BCA

kit (Pierce Biotechnology, Rockford, IL, USA). For digestion, 0.1 mg/ml of trypsin gold, MS grade (Promega, Madison, WI, USA) reconstituted in 50 mM acetic acid was added to each sample, at a 1:50 (w/w) ratio. After overnight incubation at 37ºC, 10% trifluoracetic acid (TFA) was added to the digested protein samples in order to stop the enzymatic reaction and remove Rapigest hydrolytic by-products (final TFA concentration 0.5%, pH < 2). Finally, samples were aliquoted and stored at -80ºC until use for LC-MS/MS and MALDI-FT-ICR-MS.

LC-MS/MS. One microliter of protein sample was injected on to a nanoLC system (Dionex, Amsterdam, The Netherlands) and trapped for 7.5 minutes on a C18 PepMap 100 column (5 mm x 300 μm ID, Dionex, Sunnyvale, CA, USA). Fractionation was performed using a C18 PepMap 100 column (150 mm x 75 μm, 3 μm, 100 Å, Dionex, Sunnyvale, CA, USA) using a 80 minutes gradient running from 0-50% of buffer A (80% ACN, 20% H_2O, 0.1% TFA) in buffer B (100% H_2O, 0.1% TFA), followed by a 23.5 min gradient to 100% B at 250 nL/min (Dionex). A UV detector (214 nm) was used to monitor the separation. The nanoLC was coupled to a LTQ-Orbitrap (Thermo Fisher Scientific, Bremen, Germany). Mass spectrometry data was acquired in both data-independent and dependent mode, the latter to include those peptide masses found to be differentially expressed by MALDI-FT-ICR-MS measurements (see below) for specific sequencing. This pre-selection of data results in an increased chance to identify the peptides of interest than just by default data independent measurements. The mass tolerance of the selected inclusion list was 10 ppm. Fragmentation spectra were searched against the Human International Protein Index (IPI) database v3.18 (June 13, 2006) with SEQUEST using the Bioworks software (Version 3.3, Thermo Electron, San Jose, CA, USA). The mass accuracy for the database was set to 5 ppm for the precursor ions and 1 Da for the fragment ions. Only peptides with a probability less than 0.001 and meeting the SEQUEST HUPO PPP high confidence parameters[60-61] were considered for further analysis. Peptides masses within a mass window of 7 ppm to LC-MS/MS and 2 ppm to the FT-ICR-MS (see section below) measurements were considered as identified. In order to verify isoform specificity and eliminate redundant protein identifications, the peptides were searched against the same IPI Human database using Standalone Blast (Basic Local Alignment Search Tool) software version 2.2.17 with the PAM30 scoring matrix for short aminoacid sequences. Sequence coverage determination was performed using the Protein Coverage Summarizer v1.2.3064 tool, freely available in the website http://omics.pnl.gov/software/ProteinCoverageSummarizer.php.

Bioinformatic Gene Ontology Analysis. Proteins identified in the normal scan mode by LC-MS/MS were analyzed using Ingenuity Pathway Analysis (version 7.60) and DAVID Bioinformatics Resources v6.7 (http://david.abcc.ncifcrf.gov/home.jsp)[62-63] to obtain a comprehensive description of the over-represented biological processes and functional related groups of proteins within our dataset. For DAVID analysis only Bonferroni significant ($p<0.001$) over-represented terms, containing more than 9 proteins, were considered. As background the default *Homo Sapiens* genome was used.

MALDI-FT-ICR-MS. Half microliter of protein sample was mixed with a 2,5-dihydroxy benzoic acid (DHB, Bruker Daltonics, Bremen, Germany) matrix solution (10 mg/ml in 0.1% TFA/water) in a 1:1 (v/v) ratio, spotted onto a 600/384 AnchorChip target plate (Bruker Daltonics) in duplicate and allowed to dry at room temperature. MALDI-FTICR MS measurements were performed in a Bruker Apex-Q equipped with a 9.4 T magnet (Bruker Daltonics). For each measurement scans of 10 shots at 75% laser power were accumulated. Mass spectra were acquired in the mass range of 800-4.000 Da and processed with a Gaussian filter and 2 zero fillings. To ensure good mass accuracy, an external calibration was performed using a Peptide Calibration Standard II (Bruker Daltonics), a mixture that contains Bradykin 1-7, Angiotensin II, Angiotensin I, Substance P, Bombesin, Renin Substrate, ACTH clip 1-17, ACTH clip 18-39 and Somatostatin 28. The 18 samples were measured randomly in triplicate and a total of 54 individual spectra were acquired.

Internal Calibration of FT-ICR-MS data. Raw files obtained from the FT-ICR-MS were used as input for homemade software described elsewhere[18, 64]. Spectra were internally calibrated using 5 omnipresent Actin peptide masses dispersed within the measurement range: 1198.7054, 1515.7491, 1790.8919, 1954.0643, and 2215.0699. After internal calibration the accuracy of the measurements was assessed using 7 peptide masses derived from tubulin, GAPDH and HSPA5: 1143.6351, 1566.7795, 1613.9024, 1701.9072, 1701.9072, 1756.9660, 1824.9863 and 2007.8933. Based on these peptides an average accuracy of less than 1 ppm was obtained. The final matrix contained all masses detected and their respective intensities, in at least 3 independent measurements and with a signal-to-noise (S/N) > 4 to avoid noise peaks.

Normalization of FT-ICR-MS data. Normalization of the measured intensities was achieved multiplying them by a normalization factor. This factor was determined by the ratio of average intensity of all samples to average intensity of the sample to be

normalized. After normalization we inspected the reproducibility for both technical and biological replicates by calculating the coefficient of variance of the 63 peptide masses detected in all samples. For technical replicates the average CV was 11% (range 7-15%) and, for biological replicates the CV was 26% (range 19-36%).

Selection of Differentially Expressed Peptides. Comparison of normalized peptide intensities, including zero values, was performed using a Wilcoxon test[18]. In a first set of analysis, peptide intensities at a specific culture time point (day 5, day 10 or day 19) were compared between non-differentiating and differentiating samples. In a second set of analysis, peptide intensities were compared as a function of time during culture for both non-differentiating and differentiating conditions. Peptide masses with a p-value < 0.001, a p-value < 0.01 and showing an absolute difference (present and absent) between the compared conditions were identified as being differently expressed.

Data Visualization. The geometrical mean of the normalized intensities of all samples was calculated. Values of intensity equal to 0 were regarded as Not a Number (NaN). The level of expression of each peptide mass in every sample was determined relative to this geometric mean and logarithmically transformed (on a base 2 scale). Deviation from the geometrical mean was considered as differential expression, despite possible unaccountable bias introduced by the MALDI ionization process and the analyte interaction with the matrix used. To minimize the latter possibility, we have measured all samples in triplicate, observing acceptable CVs (7-15%) in contrast to other equipments, like the MALDI-TOF, where CVs can be as high as 30%. Similarity between samples, plotted by Pearson's correlation, was done using Omniviz (OmniViz, Maynard, MA, USA, version 5.0).

Immunodetection. Cell culture and protein isolation for western blotting experiments were identical to those described above. Equal amounts of protein per sample were loaded and separated by SDS-PAGE (10% Ready Gel Precast Gels, Bio-Rad, Hercules, CA, USA) and transferred on to a nitrocellulose membrane (Hybond-ECL, Amersham Biosciences, Buckinghamshire, UK). After blocking non-specific signal with 4% fat free milk in Tris-buffered saline (TBS) the membrane was incubated with specific antibodies against fibronectin (mouse monoclonal to FN1; 1:5000, Ab-11, Clone FBN11, NeoMarkers, Cat. MS-1351), annexin A2 (rabbit polyclonal to ANXA2; 1ug/ml, Abcam, Cat. Ab41803) and GAPDH (loading control; mouse monoclonal; 1:20000, Millipore, Cat. MAB374). Membranes were probed with secondary antibodies, goat anti-mouse or goat anti-rabbit IgG,

conjugated with Alexa Fluor 680 (1:5000, Invitrogen, Cat. A21057) or with IRDye 800CW (1:5000, LI-COR, Cat. 926-32211) respectively. Immunoreactive bands were visualized using the LI-COR Infrared Imaging System according to the manufacturers instructions (Odyssey Lincoln, NE, USA). FN1 expression was visualized by immunocytochemistry. Non-differentiating and differentiating treated cells were cultured in similar conditions used for the MS analysis. After fixation in 10% formalin and blocking in PBS/2% BSA cells were incubated with mouse monoclonal FN1 antibody (1:100, Ab-11, Clone FBN11, NeoMarkers, Cat. MS-1351). Next, slides were incubated with secondary antibody, goat anti-mouse IgG conjugated with Alexa Fluor 680 (1:300, Invitrogen, Cat. A21057). Slides were washed 3 times in PBS/0.2% BSA, one time in PBS, one time in 70% ethanol and finally in 100% ethanol. After washing they were mounted in VectaShield containing DAPI (Vector Laboratories, Burlingame, CA, USA). As negative control, cells were not incubated with primary antibody.

REFERENCES

[1] Ducy P, et al. Osf2/Cbfa1: A transcriptional activator of osteoblast differentiation Cell 1997, 89, 747-754.
[2] Komori T, et al. Targeted disruption of Cbfa1 results in a complete lack of bone formation owing to maturational arrest of osteoblasts Cell 1997, 89, 755-764.
[3] Otto F, et al. Cbfa1, a candidate gene for cleidocranial dysplasia syndrome, is essential for osteoblast differentiation and bone development Cell 1997, 89, 765-771.
[4] Aubin JE Regulation of osteoblast formation and function Rev.Endocr.Metab Disord. 2001, 2, 81-94.
[5] Eijken M, et al. The essential role of glucocorticoids for proper human osteoblast differentiation and matrix mineralization Mol.Cell Endocrinol. 2006, 248, 87-93.
[6] Herbertson A, et al. Dexamethasone alters the subpopulation make-up of rat bone marrow stromal cell cultures J.Bone Miner.Res. 1995, 10, 285-294.
[7] Iba K, et al. Glucocorticoids induce mineralization coupled with bone protein expression without influence on growth of a human osteoblastic cell line Cell Struct.Funct. 1995, 20, 319-330.
[8] Patterson SD, et al. Proteomics: the first decade and beyond Nat.Genet. 2003, 33 Suppl, 311-323.
[9] Tyers M, et al. From genomics to proteomics Nature 2003, 422, 193-197.
[10] Foster LJ, et al. Differential expression profiling of membrane proteins by quantitative proteomics in a human mesenchymal stem cell line undergoing osteoblast differentiation Stem Cells 2005, 23, 1367-1377.
[11] Kratchmarova I, et al. Mechanism of divergent growth factor effects in mesenchymal stem cell differentiation Science 2005, 308, 1472-1477.
[12] Salasznyk RM, et al. Comparing the protein expression profiles of human mesenchymal stem cells and human osteoblasts using gene ontologies Stem Cells Dev. 2005, 14, 354-366.
[13] Spreafico A, et al. A proteomic study on human osteoblastic cells proliferation and differentiation Proteomics 2006, 6, 3520-3532.
[14] Xiao Z, et al. Analysis of the extracellular matrix vesicle proteome in mineralizing osteoblasts J. Cell. Physiol. 2007, 210, 325-335.
[15] Chiba H, et al. Establishment and characterization of a simian virus 40-immortalized osteoblastic cell line from normal human bone Jpn.J.Cancer Res. 1993, 84, 290-297.
[16] Stoop MP, et al. The rate of false positive sequence matches of peptides profiled by MALDI MS and identified by MS/MS J. Proteome Res. 2008, 7, 4841-7.
[17] Damsky CH Extracellular matrix-integrin interactions in osteoblast function and tissue remodeling Bone 1999, 25, 95-96.
[18] Titulaer MK, et al. A database application for pre-processing, storage and comparison of mass spectra derived from patients and controls BMC.Bioinformatics. 2006, 7, 403.
[19] Brown SC, et al. Metabolomics applications of FT-ICR mass spectrometry Mass Spectrom.Rev. 2005, 24, 223-231.
[20] Rompp A, et al. Identification of leptomeningeal metastasis-related proteins in cerebrospinal fluid of patients with breast cancer by a combination of MALDI-TOF, MALDI-FTICR and nanoLC-FTICR MS Proteomics. 2007, 7, 474-481.
[21] Higuchi C, et al. Transient dynamic actin cytoskeletal change stimulates the osteoblastic differentiation J. Bone Miner. Metab. 2009, 27, 158-67.
[22] Burridge K, et al. Actin Membrane Interaction in Focal Adhesions Cell Differ Dev 1990, 32, 337-342.
[23] Hynes RO Integrins - Versatility, Modulation, and Signaling in Cell-Adhesion Cell 1992, 69, 11-25.
[24] Siebers MC, et al. Integrins as linker proteins between osteoblasts and bone replacing materials. A critical review Biomaterials 2005, 26, 137-146.

[25] Carvalho RS, et al. Selective adhesion of osteoblastic cells to different integrin ligands induces osteopontin gene expression Matrix Biol. 2003, 22, 241-249.
[26] Cowles EA, et al. Integrin-mediated signaling regulates AP-1 transcription factors and proliferation in osteoblasts J. Biomed. Mater. Res. 2000, 52, 725-737.
[27] Rosen CJ Bone remodeling, energy metabolism, and the molecular clock Cell Metab. 2008, 7, 7-10.
[28] Komarova SV, et al. Bioenergetics and mitochondrial transmembrane potential during differentiation of cultured osteoblasts Am. J. Physiol. Cell Physiol. 2000, 279, C1220-9.
[29] Chen CT, et al. Coordinated changes of mitochondrial biogenesis and antioxidant enzymes during osteogenic differentiation of human mesenchymal stem cells Stem Cells 2008, 26, 960-8.
[30] Skjodt H, et al. Human Osteoblast-Like Cells Expressing Mhc Class-Ii Determinants Stimulate Allogeneic and Autologous Peripheral-Blood Mononuclear-Cells and Function As Antigen-Presenting Cells Immunology 1989, 68, 416-420.
[31] Calvi LM, et al. Osteoblastic cells regulate the haematopoietic stem cell niche Nature 2003, 425, 841-6.
[32] Yang JY, et al. Chloride intracellular channel 1 regulates osteoblast differentiation Bone 2009, 45, 1175-1185.
[33] Rostovtseva T, et al. VDAC channels mediate and gate the flow of ATP: Implications for the regulation of mitochondrial function Biophys. J. 1997, 72, 1954-1962.
[34] Balcerzak M, et al. Proteome analysis of matrix vesicles isolated from femurs of chicken embryo Proteomics 2008, 8, 192-205.
[35] Anderson HC Molecular-Biology of Matrix Vesicles Clin. Orthop. Relat. Res. 1995, 266-280.
[36] Anderson HC, et al. The role of matrix vesicles in growth plate development and biomineralization Front. Biosci. 2005, 10, 822-837.
[37] Moursi AM, et al. Integrin-fibronectin interactions are critical for osteogenesis and osteoblast differentiation J. Dent. Res. 1997, 76, 2261-2261.
[38] Globus RK, et al. Fibronectin is a survival factor for differentiated osteoblasts J. Cell Sci. 1998, 111, 1385-1393.
[39] Gillette JM, et al. The role of annexin 2 in osteoblastic mineralization J. Cell Sci. 2004, 117, 441-449.
[40] Kirsch T, et al. The roles of annexins and types II and X collagen in matrix vesicle-mediated mineralization of growth plate cartilage J. Biol. Chem. 2000, 275, 35577-35583.
[41] Menaa C, et al. Annexin II increases osteoclast formation by stimulating the proliferation of osteoclast precursors in human marrow cultures J Clin Invest 1999, 103, 1605-13.
[42] Takahashi S, et al. Cloning and identification of annexin II as an autocrine/paracrine factor that increases osteoclast formation and bone resorption J. Biol. Chem. 1994, 269, 28696-701.
[43] Mounkes LC, et al. A progeroid syndrome in mice is caused by defects in A-type lamins Nature 2003, 423, 298-301.
[44] Pendas AM, et al. Defective prelamin A processing and muscular and adipocyte alterations in Zmpste24 metalloproteinase-deficient mice Nat. Genet. 2002, 31, 94-99.
[45] Rodrigues GHD, et al. Severe bone changes in a case of Hutchinson-Gilford syndrome Ann. Genet. 2002, 45, 151-155.
[46] Bank RA, et al. Defective collagen crosslinking in bone, but not in ligament or cartilage, in Bruck syndrome: Indications for a bone-specific telopeptide lysyl hydroxylase on chromosome 17 Proc. Natl. Acad. Sci. U. S. A. 1999, 96, 1054-1058.
[47] Naito Y, et al. 5'-Nucleotidase from rat heart Biochemistry 1981, 20, 5188-94.
[48] Buhring HJ, et al. Novel markers for the prospective isolation of human MSC Hematopoietic Stem Cells Vi 2007, 1106, 262-271.
[49] Dominici M, et al. Minimal criteria for defining multipotent mesenchymal stromal cells. The International Society for Cellular Therapy position statement Cytotherapy 2006, 8, 315-317.
[50] Hughes RC Galectins as modulators of cell adhesion Biochimie 2001, 83, 667-676.

[51] Scott K, et al. Galectin-1: A bifunctional regulator of cellular proliferation Glycoconj. J. 2002, 19, 467-477.
[52] Perillo NL, et al. Apoptosis of T-Cells Mediated by Galectin-1 Nature 1995, 378, 736-739.
[53] Chan J, et al. Galectin-1 induces skeletal muscle differentiation in human fetal mesenchymal stem cells and increases muscle regeneration Stem Cells 2006, 24, 1879-1891.
[54] Dekker LJ, et al. FTMS and TOF/TOF mass spectrometry in concert: Identifying peptides with high reliability using matrix prespotted MALDI target plates J. Chromat. B, Analyt. Technol. Biomed. Life Sci. 2007, 847, 62-64.
[55] Schmid AK, et al. Global whole-cell FTICR mass spectrometric proteomics analysis of the heat shock response in the radioresistant bacterium Deinococcus radiodurans J. Proteome Res. 2005, 4, 709-718.
[56] Page JS, et al. FTICR mass spectrometry for qualitative and quantitative bioanalyses Curr. Opin. Biotechnol. 2004, 15, 3-11.
[57] Anderson NL, et al. Proteome and proteomics: New technologies, new concepts, and new words Electrophoresis 1998, 19, 1853-1861.
[58] Rappsilber J, et al. What does it mean to identify a protein in proteomics? Trends Biochem. Sci. 2002, 27, 74-78.
[59] Wessel D, et al. A method for the quantitative recovery of protein in dilute solution in the presence of detergents and lipids Anal.Biochem. 1984, 138, 141-143.
[60] Balgley BM, et al. Comparative evaluation of tandem MS search algorithms using a target-decoy search strategy Mol.Cell Proteomics. 2007, 6, 1599-1608.
[61] Omenn GS, et al. Overview of the HUPO Plasma Proteome Project: results from the pilot phase with 35 collaborating laboratories and multiple analytical groups, generating a core dataset of 3020 proteins and a publicly-available database Proteomics. 2005, 5, 3226-3245.
[62] Dennis G, et al. DAVID: Database for annotation, visualization, and integrated discovery Genome Biol. 2003, 4.
[63] Huang DW, et al. Systematic and integrative analysis of large gene lists using DAVID bioinformatics resources Nat. Protoc. 2009, 4, 44-57.
[64] Titulaer MK, et al. A software application for comparing large numbers of high resolution MALDI-FTICR MS spectra demonstrated by searching candidate biomarkers for glioma blood vessel formation BMC Bioinformatics 2008, 9.

Chapter 3

Activin A suppresses osteoblast mineralization capacity by altering extracellular matrix composition and impairing matrix vesicle production

Rodrigo D.A.M. Alves, Marco Eijken, Karel Bezstarosti, Jeroen A.A. Demmers and Johannes P.T.M. van Leeuwen

Submitted

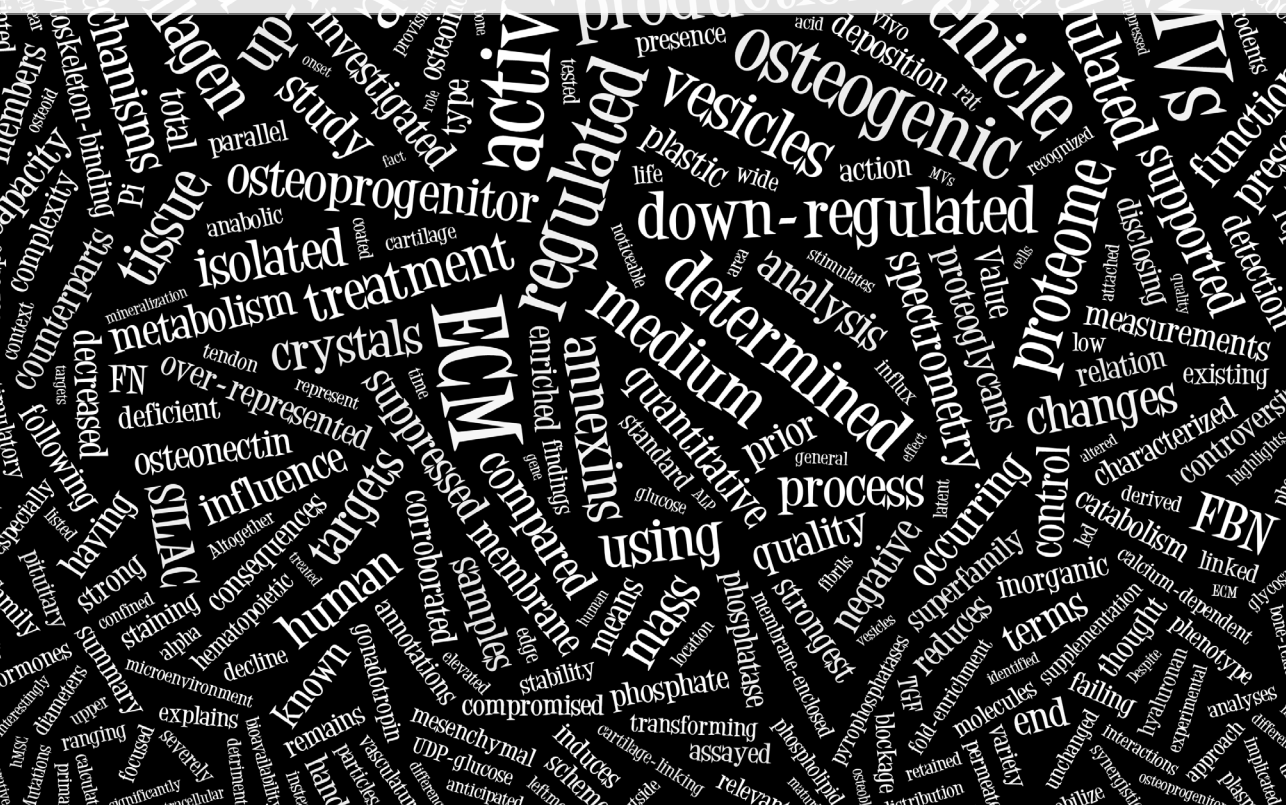

ABSTRACT

During bone formation, osteoblasts deposit an extracellular matrix (ECM) that is mineralized via a process involving production and secretion of highly specialized matrix vesicles (MVs). Activin A, a transforming growth factor-β (TGF-β) superfamily member, was previously shown to have inhibitory effects in human bone formation models through unclear mechanisms. We investigated these mechanisms elicited by activin A during *in vitro* osteogenic differentiation of human mesenchymal stem cells (MSC). Activin A inhibition of ECM mineralization coincided with a strong decline in alkaline phosphatase (ALP) activity in extracellular compartments, ECM and MVs. SILAC-based quantitative proteomics disclosed intricate protein composition alterations in the activin A ECM, including changed expression of collagen XII, osteonectin and several cytoskeleton-binding proteins. Moreover, in activin A osteoblasts MV production was deficient containing very low expression of annexin proteins. ECM enhanced MSC osteogenic development and mineralization. This osteogenic enhancement was significantly decreased when MSC were cultured on ECM produced under activin A treatment. These findings demonstrate that activin A targets the ECM maturation phase of osteoblast differentiation resulting ultimately in the inhibition of mineralization. ECM proteins modulated by activin A are not only determinant for bone mineralization but also possess osteoinductive properties that are relevant for bone tissue regeneration.

INTRODUCTION

The quality of bone tissue is determined by the balanced action of the anabolic bone cells, the osteoblasts, and their catabolic counterparts, the osteoclasts. This process of bone remodeling occurs throughout life and can be influenced by a wide variety of molecules, having ultimately an impact on the quality of bone[1-2]. Activins and inhibins are members of the TGF-β superfamily with predominant antagonistic effects in their classically known target tissues, such as in gonadotropin producing cells in the pituitary and their role in reproduction[3-4]. Other effects have been described in hematopoietic cells[5-6], and in the monocyte/macrophage[7-8] cell lineages. Several consequences of these reproductive hormones, especially those of activin A, are also described in relation to bone metabolism. Activin A is present in bone tissue[9-10] affecting both osteoclasts and osteoblasts. While having a consistent pro-osteoclastogenic effect[7, 11], the activin A impact on osteoblast differentiation is more controversial. In rodents, several reports support a stimulatory effect of activin A on osteoblast differentiation and mineralization[7, 12]. On the other hand, two different studies, using rat and human bone formation models, have demonstrated that activin A treatment has a coherent inhibitory influence on osteogenesis leading to significant reduction of the mineralization capacity[9, 13]. The negative role of activin A in bone formation is also supported by *in vivo* data where blockage of activin signaling resulted in increased bone mass[14-15].

The extracellular compartment is crucial for bone since it determines most of the bone quality properties[16-17], including its strength, stability and integrity. Interestingly, a mature ECM is characterized by the capacity to mineralize even in the absence of further osteoblast activity[9, 18]. This biomineralization process is complex and not fully elucidated but it is thought to be started within MVs[19]. Osteoblasts in bone and other cells in mineralization competent tissues, such as cartilage[20], tendon[21], teeth[22] and calcifying vasculature[23] produce and release from their plasma membrane these vesicles with diameters ranging between 50-200 nm. It is inside these membrane-enclosed particles that first crystals of mineral are formed and grow, before the vesicle membrane is permeated and the mineral crystallization advances into the ECM[24-25]. In this context, proteins that can mobilize calcium and inorganic phosphate (Pi), the backbone of the hydroxyapatite crystals present in bone, are of utmost importance. Pi donor proteins found in MVs include alkaline phosphatase (ALP) and inorganic pyrophosphatases[26] while the annexin family of

proteins is postulated to be crucial for calcium influx into the vesicles[27-29].

In this study we investigated the mechanisms beyond the inhibitory effect of activin A on MSC derived osteoblast differentiation and mineralization. We have previously shown that in human osteoblast cultures activin A influences the expression of many ECM genes altering ECM maturity[9]. Thus, we focused our analysis on extracellular environment changes, namely the ECM and MVs. The characterization of these compartments was done using the state-of-the-art quantitative proteomics tools including SILAC metabolic labeling and mass spectrometry. Furthermore, the importance of ECM composition for osteoblast differentiation was also determined.

RESULTS

Activin A alters the mineralization competence of the ECM

Activin A signaling was previously shown to inhibit mineralization of human osteoblast cultures by altering the ECM maturity[9]. The results from our current study corroborate this data. Activin A treatment resulted in decreased ALP activity followed by impaired mineral deposition in culture (Figure 1A). The maturity of the ECM produced under the activin A stimulus was tested by evaluating whether mineralization could occur in the absence of living cells. To this end, vehicle and activin A treated osteoblast cultures were devitalized just prior to the onset of mineralization (Figure 1B; scheme), withdrawing living cells but keeping the ECM built up to that moment intact[9]. We observed that supplementation of medium to the ECM was enough to induce mineralization of vehicle ECM (Figure 1B). In contrast, ECM synthesized under activin A treatment failed to become mineralized (Figure 1B). To evaluate the extracellular effects of activin A during osteoblast differentiation, we isolated ECM as well as MVs from vehicle and activin A osteoblast cultures.

Activin A significantly reduces ALP activity in ECM and in MVs

ECM and MVs from osteoblast cultures at the onset of mineralization were initially accessed for ALP activity. We observed that ALP activity was significantly reduced in ECM and MVs of activin A treated osteoblasts when compared to their vehicle-treated counterparts (Figure 2). This result supported further the concept that activin A has a significant impact on the osteoblast extracellular milieu. Thus, we set out to analyze and compare the ECM and MVs proteome from vehicle and activin A

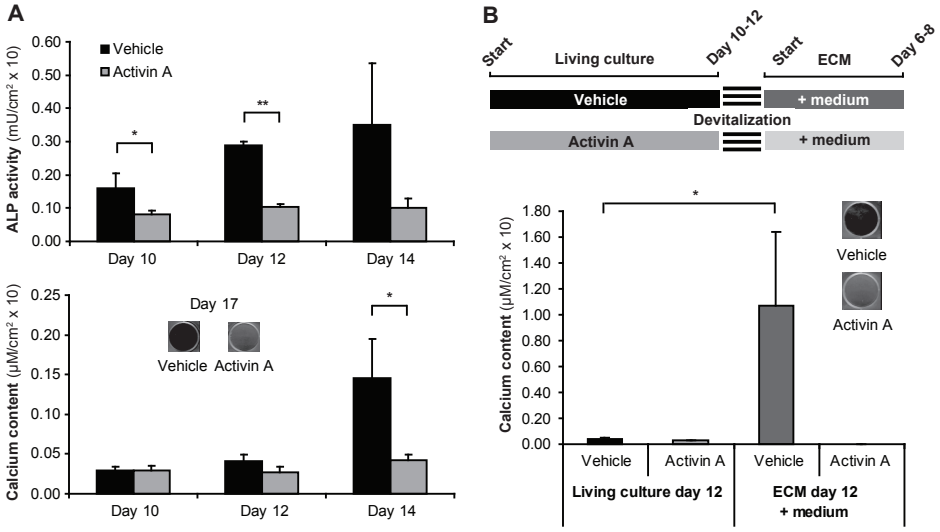

Figure 1. Effect of activin A in osteoblast differentiation and mineralization. MSC were cultured in the presence of osteogenic medium (vehicle) and osteogenic medium containing activin A. **(A)** ALP activity and calcium content in these cultures (n=3). At the end of culture the calcium content was also visualized by Alizarin Red S staining. **(B)** Vehicle and activin A treated cells were cultured until just prior to the onset of mineralization, occurring between days 10-12. At this stage cell cultures were fixed. Devitalized cells were further incubated in osteogenic medium (n=4). At the end of the culture, calcium content was measured and visualized by Alizarin Red S staining. Value means ± SD. * p<0.05; ** p<0.01.

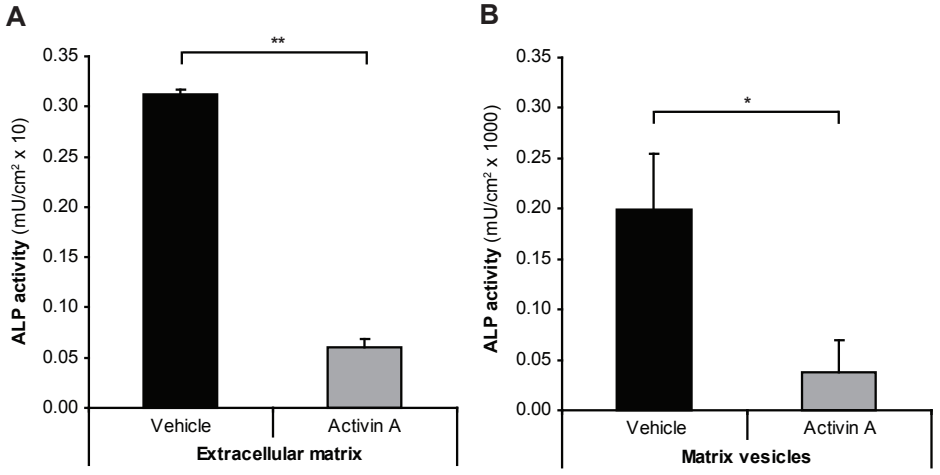

Figure 2. Effect of activin A in ECM and MV ALP activity. **(A)** ECM and **(B)** MVs isolated at the onset of mineralization from vehicle and activin A treated cultures were assayed for ALP activity. Value means ± SD. * p<0.05 ** p<0.01.

treated cultures using a quantitative SILAC-based mass spectrometry approach.

Activin A induces changes in ECM composition and strongly reduces the expression of MVs markers

The analysis of the ECM resulted in the identification of 293 proteins (data not shown). We used Gene Ontology (GO) annotation enrichment analysis to categorize the identified proteins for their cellular localization (Figure 3). The GO term ECM (GO:0044420) was found to be 3.7-fold enriched validating the ECM isolation method. Other over-represented protein groups included proteins associated with membrane structures, like organelle envelope proteins (4.8-fold; GO:0031967) or in close proximity to the membrane, like cell leading edge (4.3-fold; GO:0031252) and cell surface (3.9-fold; GO:0009986) proteins. Interestingly, also vesicle proteins (GO:0031982) were identified to be 4.3-fold over-represented in the ECM samples.

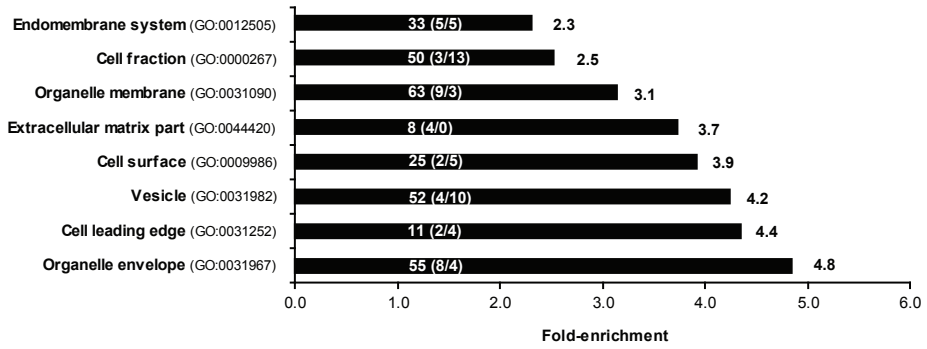

Figure 3. Over-represented cellular compartment annotations for the 293 proteins identified in the ECM. Numbers in front of the bars indicate fold-enrichment level. Numbers within bars indicate proteins identified as belonging to each cellular compartment term and within brackets those that were found to be up-/down-regulated in activin A condition. Only significantly ($p<0.05$) enriched gene ontology terms were considered for analysis.

In quantitative terms mass spectrometry analyses resulted in identification of 104 proteins over 1.5-fold regulated following activin A treatment. More than half of these proteins, 74 proteins, were down-regulated by activin A while only 30 proteins were up-regulated. The 10 strongest up and down-regulated proteins are shown in Table 1. Collagen type XII α1 (COL12A1) was the most up-regulated ECM protein (2.7-fold). Osteonectin (ON), fibronectin 1 (FN1) and fibrillin (FBN) were also up-

regulated by more than 1.9-fold (Table 1). The strongest down-regulated proteins include enzymes participating in carbohydrate catabolism such as UDP-glucose pyrophosphorylase 2 (UGP2; 0.28-fold), phosphoglucomutase 1 (PGM1; 0.30-fold) and phosphogluconate dehydrogenase (PGD; 0.37-fold; Table 1).

Table 1. Proteins regulated by activin A signaling in the ECM. ECM was isolated at the onset of mineralization from SILAC labeled cultures and protein regulation was determined by mass spectrometry measurements. Ratios are averages of reciprocal SILAC experiments. A= Activin A; V=Vehicle. From the 293 proteins identified in the ECM 104 were found to be over 1.5-fold regulated but only the 20 strongest regulated proteins are shown.

#	Protein name	IPI identifier	Gene Symbol	Ratio A/V
	> 1.5-fold UP-regulated by activin A			
1	Collagen alpha-1(XII) chain	IPI00329573	COL12A1	2.66
2	Developmentally-regulated endothelial cell locus 1 protein	IPI00306046	DEL1	2.29
3	CFR-1	IPI00414717	CFR1	2.24
4	Basement-membrane protein 40	IPI00014572	ON	2.20
5	FN1 protein	IPI00845263	FN1	2.11
6	Breast epithelial antigen BA46	IPI00966900	MFGE8	2.07
7	cDNA FLJ58980, highly similar to Sideroflexin-3	IPI00871988	hCG_24661	2.01
8	130 kDa leucine-rich protein	IPI00783271	LRP130	2.00
9	Fibrillin-1	IPI00328113	FBN	1.97
10	CD49 antigen-like family member E	IPI00306604	FNRA	1.93
	> 1.5-fold DOWN-regulated by activin A			
1	cDNA, FLJ95012, highly similar to Homo sapiens UDP-glucose pyrophosphorylase 2	IPI00873223	UGP2	0.28
2	Glucose phosphomutase 1	IPI00219526	PGM1	0.30
3	UDP-glucose 6-dehydrogenase	IPI00031420	UGDH	0.30
4	70 kDa lamin	IPI00021405	LMN1	0.31
5	Collapsin response mediator protein 2	IPI00257508	CRMP2	0.31
6	Cell migration-inducing gene 10 protein	IPI00169383	MIG10	0.34
7	Triosephosphate isomerase	IPI00465028	hCG_25936	0.34
8	Calgizzarin	IPI00013895	MLN70	0.34
9	BPG-dependent PGAM 1	IPI00549725	CDABP0006	0.35
10	6-phosphogluconate dehydrogenase, decarboxylating	IPI00219525	PGD	0.37

Table 2. Proteins regulated by activin A signaling in MVs. MV samples were isolated at the onset of mineralization from SILAC labeled cultures and protein regulation was determined by mass spectrometry measurements. Ratios are averages of reciprocal SILAC experiments. A= Activin A; V=Vehicle. From the 27 proteins identified in MVs 12 were found to be over 1.5-fold regulated.

#	Protein name	IPI identifier	Gene Symbol	Ratio A/V
	> 1.5-fold UP-regulated by activin A			
1	Cartilage-linking protein 1	IPI00023601	CRTL1	1.76
2	Bone proteoglycan II	IPI00012119	DCN	1.51
	> 1.5-fold DOWN-regulated by activin A			
1	Annexin A1	IPI00218918	ANX1	0.11
2	Anchorin CII	IPI00329801	ANX5	0.14
3	35-beta calcimedin	IPI00793199	ANX4	0.15
4	67 kDa calelectrin	IPI00221226	ANX6	0.23
5	Annexin A2	IPI00418169	ANX2	0.24
6	L-lactate dehydrogenase	IPI00947127	LDHA	0.36
7	18 kDa phosphoprotein	IPI00012011	CFL	0.39
8	Alanyl aminopeptidase	IPI00221224	ANPEP	0.46
9	Lung resistance-related protein	IPI00000105	LRP	0.50
10	Cytotactin	IPI00031008	HXB	0.60

In MVs we have identified 27 proteins (data not shown). In total, 12 proteins were ≥1.5-fold regulated by activin A (Table 2). Of those 12, only 2 proteins were increased by activin A, hyaluronan binding protein CRTL1 (1.76-fold) and bone proteoglycan II (DCN; 1.51-fold). Among the 10 down-regulated proteins, 5 were calcium-dependent phospholipid binding proteins known as annexins. Despite markedly down-regulated in MVs (<0.25-fold; Table 2), annexins were unchanged in the ECM. This MV specific modulation and the fact that these proteins are known to be present and functional in MVs[27-29] led us to consider that activin A cultures had severely altered or even compromised MV production.

Activin A treated cells have impaired MV biogenesis at the onset of mineralization

To address the hypothesis that MV production is suppressed in osteoblasts following activin treatment, we isolated and counted MV number in vehicle and activin A treated osteoblast cultures. Number of total MVs and ALP positive MVs (ALP+ MVs) was determined using FACS. The production of MVs, total and ALP+, did not differ between vehicle and activin A conditions before the onset of mineralization (Figure 4A). However, at the onset of mineralization the production of ALP+ MVs in vehicle osteoblasts increased sharply whereas in activin A condition this was significantly suppressed (Figure 4A). At the onset of mineralization, only 8% of the total MVs were ALP+ in the activin A condition compared to the 72% in the vehicle condition (Figure 4A and 4B). In summary, our results indicate a bi-modal effect of activin A by changing the ECM composition and suppressing the provision of the biomineralization initiators, the MVs.

Activin A ECM is capable of signaling to osteoprogenitor cells modulating their mineralization

Next, we investigated further the impact of ECM composition in osteogenesis. For these experiments, vehicle and activin A treated cultures were devitalized just prior to the onset of mineralization similar as shown in Figure 1B. However, this time besides only osteogenic medium we also seeded undifferentiated MSCs in osteogenic medium on top of vehicle and activin A ECMs. In parallel as control cultures, MSC in osteogenic medium were also seeded on plastic in standard culture plates (experimental scheme in Figure 5A). Seeding of MSC onto an existing ECM enhanced and anticipated the mineralization (Figure 5B, vehicle or activin A ECM

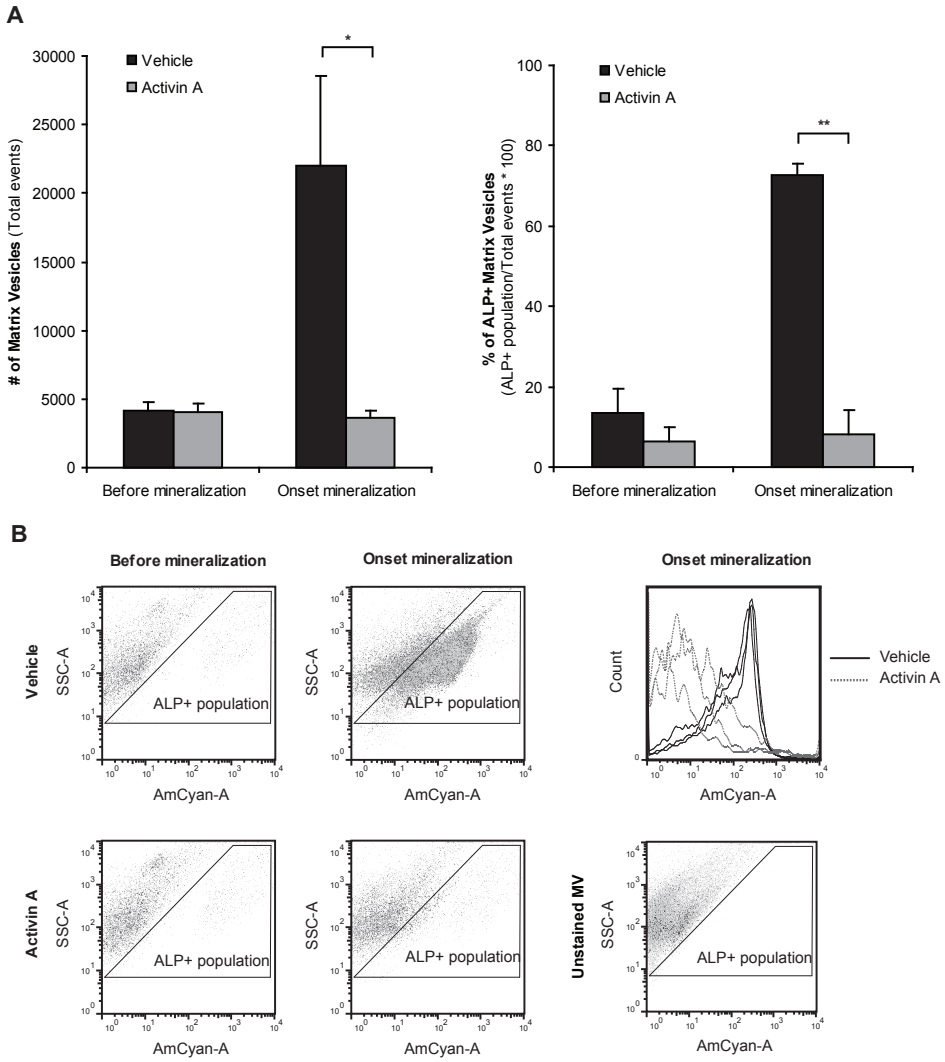

Figure 4. Activin A effect in osteoblast MV production. **(A)** Number of MVs and ALP+ MVs secreted by vehicle and activin A treated cultures before and at the onset of mineralization. **(B)** FACS plots used to calculate the number of MVs in vehicle and activin A samples, before and at the onset of mineralization (4 leftmost panels). The gating was set using ELF97 unstained MV samples (bottom right panel). A histogram with the distribution of the ALP+ MV population before mineralization (n=9) and at the onset of mineralization (n=3) for vehicle and activin A cultures is also shown (upper right panel). * $p<0.05$; ** $p<0.01$.

compared to plastic plates), now occurring already after 6-8 days instead of the 14 days for control cultures on plastic (Figure 1A). Despite significantly less mineralized than MSC on vehicle ECM this was also observed when MSC were seeded on an activin A ECM, which was unable to mineralize in absence of MSC (Figure 5B).

Altogether, these results demonstrate that the osteoblast ECM contains potent signaling clues to osteoprogenitor cells. In this respect, the altered composition of activin A ECM did not represent a complete block for mineralization by osteoprogenitor cells.

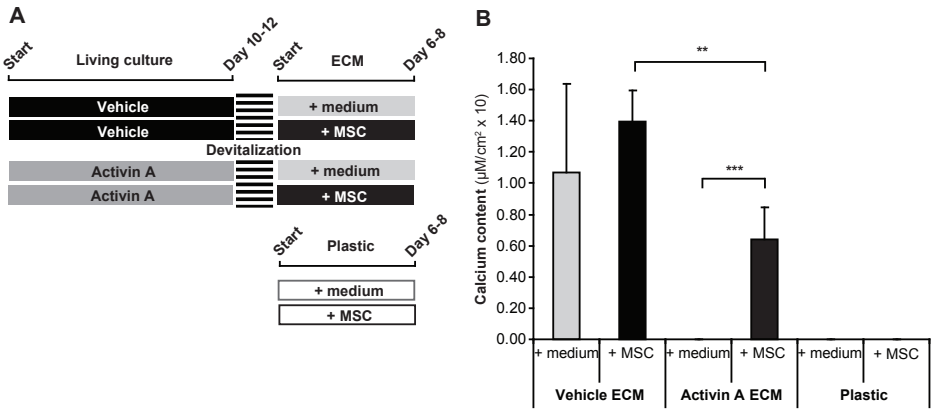

Figure 5. Effect of the ECM in osteoprogenitor cell mineralization. **(A)** Vehicle and activin A treated cultures were devitalized just prior to the onset of mineralization. The remaining ECMs were cultured with osteogenic medium (+ medium) and undifferentiated MSC in osteogenic medium (+ MSC). In parallel, MSCs were also seeded directly on standard plastic cultures plates. **(B)** Calcium content was assayed at the end of culture (n=3). Value means ± SD. **p<0.01; ***p<0.001.

DISCUSSION

This study elucidates the mechanisms underlying activin A inhibition of osteoblast differentiation and mineralization. We demonstrate that activation of activin A signaling during bone formation has detrimental effects on the ECM production and maturation phase[9]. Furthermore, negative effects of activin A are extensible to the mineralization phase by impairing MV production.

Activin A effect on the ECM proteome was predominantly suppressive, with 2-times more down-regulated than up-regulated proteins. Among the latter

we identified collagen XII α1 (COL12A1; IPI00329573), osteonectin (ON; IPI00014572), fibronectin (FN1; IPI00845263) and fibrillin-1 (FBN; IPI00328113). All these proteins have been directly implicated in osteoblast differentiation and bone formation[30-33]. For example, ON deficiency is responsible for compromised osteoblast differentiation and decreased bone formation[30, 34]. Activin A modulation of ON gene expression in osteoblasts[9] and other tissues[35] is consistent with the ON protein regulation we observed despite failing to explain the inhibitory effects of activin A in osteoblast differentiation and mineralization. The complexity of activin A signaling is probably the reason behind these conflicting observations with other proteins overruling ON action during osteoblast differentiation. One of these proteins is FBN. Mutations in the FBN gene are responsible for an increased skeletal size phenotype[36]. FBN is a structural component of the ECM thought to regulate osteoblast maturation with its ability to sequester and control latent TGF-β and BMP bioavailability[33, 37]. Being both TGF-β and BMP potent osteogenic factors[38-39], elevated levels of FBN in the activin A ECM is likely to be determinant for the inhibition of osteoblast differentiation and mineralization observed in activin A.

Linking ECM proteins down-regulated by activin A to bone-related functions was more difficult than for those up-regulated. Many of the proteins inhibited by activin were cytoskeleton-binding proteins (e.g. WDR1, IPI00873622; PLS3, IPI00216694; TPM3, IPI00218319) and proteins involved in carbohydrate metabolism (UGDH, IPI00031420; MIG10, IPI00169383; LDHA, IPI00947127). The detection of proteins that bind to the cytoskeleton is possibly related to the ECM control of cytoskeleton mechanisms[40] recently recognized as important during osteoblast differentiation[41-42]. On the other hand, the detection of glucose metabolism proteins in the ECM is more enigmatic but corroborated in the osteoblast ECM proteome listed by Xiao et al.[43]. Moreover, several other studies indicate the existence of extracellular glycolytic enzymes contained within different types of secreted vesicles[44-45] including MVs[43]. Despite disclosing an extracellular location for these proteins, their function outside the cell remains unknown. Nevertheless, the fact that they are down-regulated by activin A converts them as potential modulators of bone formation.

In general, activin A effect on the ECM proteome was vast with many proteins being targeted. The fact that no single protein was strikingly altered highlights the importance of considering ECM as an integrated compartment. In other words, the function of ECM is determined by the combination of all proteins present

rather than individual proteins. Investigating the functions and interactions of these proteins during osteoblast differentiation is of significance to understand and identify therapeutic targets for bone formation. The more so considering that several proteins we identified have not yet been linked to bone.

Osteoblasts under the influence of activin A secreted significantly less MVs containing an altered protein composition. In contrast to the ECM proteome, the MV proteome comprised more pronounced differences between activin A and vehicle cultures. Proteome analysis showed only two proteins as being more than 1.5-fold up-regulated by activin A in MVs, bone proteoglycan II (DCN; IPI00012119) and cartilage-linking protein 1 (CRTL1; IPI00023601) proteoglycans that bind to type I collagen fibrils[46] and hyaluronic acid[47] respectively. Increased expression of proteoglycans within MVs fit with the negative role of activin A in osteoblast mineralization. The negative charge of their glycosaminoglycan chains is able to compete with phosphate for hydroxyapatite crystallization inhibiting mineral growth[48-49]. DCN, for example is confined to the uncalcified osteoid area being removed from the ECM so calcification can take place[50].

Among the most down-regulated proteins in MVs, we found proteins directly associated with their mineralization competences. Annexin family members (1, 2, 4, 5 and 6) were the most noticeable, proteins usually high abundant in MVs where they act as calcium channels[27-29]. Interestingly, annexins appear to be specifically regulated within MVs since no differences were found in the activin A ECM relative to its vehicle counterpart. MV biogenesis is still controversial[51] but the fact we detected proteins modulated within these vesicles that were not altered in the ECM is coherent with a selective and tightly regulated MV formation process.

Before onset of mineralization, the ECM produced by vehicle osteoblast cultures was mature enough to mineralize independently of further cellular activity. A possible explanation for this is the presence of MVs already attached to the fibrillar collagenous matrix[24], something corroborated by the detection of vesicle proteins in the ECM (Figure 3). These MVs would allow mineral crystals to grow and propagate further to the ECM without additional osteoblast interference. The fact that activin A osteoblasts had impaired MV biogenesis explains the inability of activin A ECM to mineralize.

Osteoblast differentiation is a sequential order of interdependent events[52] thus the MV impairment is likely to be determined by a primary effect on the previous phase of ECM maturation. Furthermore, we believe that this effect on the ECM is unlikely

to be due to a delay in osteoblast differentiation since differentiation marker genes remain unchanged by activin signaling in this bone formation model[9]. Devitalization experiments where ECMs were cultured with osteoprogenitor cells provided more information about maturity of the activin A ECM. Despite less effectively than vehicle, activin A ECM was found capable of enhancing osteoprogenitor cell mineralization, suggesting that activin A ECM still retained, albeit diminished compared to control ECM, capacity to enhance osteoblast differentiation. Because of its inability to support the late stages of mineralization we hypothesize that activin A ECM specifically stimulates the early stages of osteogenesis. Interestingly, collagen and FN1 are two proteins up-regulated in activin A ECM that fit particularly well in this role. Culture plates coated with collagen or FN1 have been shown to enhance osteoblast differentiation[53-54].

In summary, we demonstrated that activin A is a strong modulator of the extracellular microenvironment of osteoblasts by 1) changing the ECM composition and maturity and 2) impairing production of MVs responsible for the start of biomineralization. This supports the concept that osteoblast differentiation is a synergistic process, with disruption of a specific stage (ECM maturation) having consequences for down-stream events (MVs biogenesis) and endpoint phenotype (mineralization). Furthermore, ECMs produced by osteoblasts were found to contain potent osteoinductive properties of particular interest for regenerative medicine. Proteins identified in the ECM to be regulated by activin A constitute potential targets to modulate mineralization and bone tissue quality.

Supplementary Data

Supplementary data available in Chapter 7.

MATERIAL & METHODS

Cell Culture. Human bone marrow-derived Mesenchymal Stem Cells (MSC; PT-2501, Lonza, Walkersville, MD, USA) from two different donors, at passages 4 and 5, were cultured as described previously[9] in 12-well (3.8 cm^2) plates (Greiner bio-one, Frickenhausen, Germany), 75 or 175 cm^2 flasks (Greiner bio-one). The MSC culture medium was freshly supplemented with 100 nM dexamethasone (DEX, Sigma) and 10 mM ß-glycerophosphate (Sigma, St. Louis, MO, USA) for the osteogenic (vehicle) condition. Activin A condition contained an extra supplement

of 25 ng/ml of activin A (R&D Systems, Minneapolis, MN, USA). For quantitative mass spectrometry analysis, MSC were cultured similarly in the presence of SILAC medium: arginine- and lysine-free DMEM/F12-Flex supplemented with 10% dialyzed FCS, 4 mM L-glutamine, penicillin-streptomycin, 4.5 g/L glucose, 20 mM HEPES (Sigma), 1.8 mM $CaCl_2.2H_2O$ (Sigma), pH 7.5. Cells were expanded in both light medium, supplemented with normal L-lysine HCL (12C6,14N2-Lys) and L-arginine (12C6,14N4-Arg), and heavy medium, containing heavy isotopes of the same amino acids (13C6,14N2-Lys and 13C6,15N4-Arg). Complete incorporation of the amino acid isotopes occurred within 3 weeks of cell culture in SILAC medium (Supplementary Figure I, Chapter 7). Vehicle and activin A treated cells were cultured in light and heavy isotope medium reciprocally allowing an optimal differentiation of artifacts and contaminants from biological variation[55]. All SILAC reagents were purchased from Invitrogen (Carlsbad, CA, USA) unless stated otherwise.

Devitalization of cell cultures. Cell devitalization was done as described previously[9] using cells cultured in 12-well plates. Briefly, just prior to the onset of mineralization cell cultures were washed twice in PBS (Gibco BRL, Carlsbad, CA, USA), air dried and frozen at -20°C for at least 24 h. The stage just prior to the onset of mineralization is the period preceding the detection of significant mineral deposition in culture, occurring between day 10-12 or day 15-17, depending on the MSC donor. Next, the devitalized cultures containing an intact ECM synthesized during vehicle (vehicle ECM) or activin A stimulus (activin A ECM) were incubated in osteogenic medium only (+ medium). In another set of experiments, the devitalized cultures were incubated with freshly seeded undifferentiated MSC in osteogenic medium (+MSC) without further addition of activin A. In parallel, as a control for these experiments, MSC in osteogenic medium were seeded on standard plastic plates (plastic). All experiments were followed further until mineralization. At the end of the cultures we performed mineralization assays.

Alkaline Phosphatase activity, protein and mineralization assays. ALP activity and calcium content in cell extracts or isolated MVs were determined as described previously[56]. Briefly, ALP activity was assayed by determining the release of paranitrophenol from paranitrophenylphosphate (20 mM diethanolamine buffer supplemented with 1 mM MgCl2 at pH 9.8) in the cell lysates and in MVs for 10 and 70 min at 37°C respectively. Adsorption was measured at 405 nm. For calcium measurements, cell lysates were incubated overnight in 0.24 M HCl at 4°C. Calcium content was colorimetrically determined with a calcium assay kit (Sigma) according

to the manufacturer's instructions. For mineralization staining, cell cultures were fixed for 60 min with 70% ethanol on ice. After fixation, cells were washed twice with PBS and stained for 10 min with Alizarin Red solution (saturated Alizarin Red in demineralized water was titrated to pH 4.2 using 0.5% ammonium hydroxide). For protein concentration measurements, a BCA kit (Pierce Biotechnology, Rockford, IL, USA) was used following the manufacturers instructions.

Extracellular matrix isolation. To extract proteins from the ECM, vehicle and activin A treated MSC were cultured in 175 cm^2 flasks. After removing the medium, cells were washed three times in PBS and incubated in collagenase/dispase (1mg/ml; Roche, Mannheim, Germany) for 90 min at 37°C. After centrifugation at 500 g for 10 min, to remove cells, the supernatant containing the ECM protein extract was obtained and stored at -80°C until analysis.

Matrix vesicle isolation. MVs were isolated from the medium of 75 or 175 cm^2 culture flasks for subsequent FACS or proteomics analysis respectively, as described previously[57]. Briefly, the culture medium was first centrifuged at 20,000g for 30 min at 4°C, to remove cell debris. The supernatant was collected and further centrifuged at 100,000 g for 60 min at 4°C. After discarding the supernatant, the pellet containing MVs was dissolved in PBS. All ultracentrifugation steps were performed on an Ultracentrifuge L-70 (Beckmann Coulter).

Quantitative mass spectrometry analysis. Protein extracts from SILAC cultures were mixed in a 1:1 ratio of the light (Vehicle or activin A) and heavy (Vehicle or activin A) condition for both the ECM and MVs isolated. The combined light:heavy samples were resolved by one-dimensional SDS-PAGE (NuPAGE 4-12% Bis-Tris Gel, Invitrogen) in duplicate. Protein bands were visualized with Coomassie staining (Bio-safe Coomassie, Bio-Rad, Hercules, CA, USA). SDS-PAGE gel lanes were cut into 2-mm slices using an automatic gel slicer and subjected to in-gel reduction with dithiothreitol, alkylation with iodoacetamide and digestion with trypsin (Promega, sequencing grade), essentially as described by Wilm *et al.*[58]. Nanoflow LC-MS/MS was performed on an 1100 series capillary LC system (Agilent Technologies) coupled to an LTQ-Orbitrap XL mass spectrometer (Thermo) operating in positive mode and equipped with a nanospray source. Peptide mixtures were trapped on a ReproSil C18 reversed phase column (Dr Maisch GmbH; column dimensions 1.5 cm × 100 µm, packed in-house) at a flow rate of 8 µl/min. Peptide separation was performed on ReproSil C18 reversed phase column (Dr Maisch GmbH; column dimensions 15 cm × 50 µm, packed in-house) using a linear gradient from 0 to 80%

B (A = 0.1 % FA; B = 80% (v/v) ACN, 0.1 % FA) in 120 min and at a constant flow rate of 200 nl/min using a splitter. The column eluent was directly sprayed into the ESI source of the mass spectrometer. Mass spectra were acquired in continuum mode; fragmentation of the peptides was performed in data-dependent mode. Data analysis was performed either by using the Mascot search algorithm or the MaxQuant suite. For Mascot searches, peak lists were automatically created from raw data files using the Mascot Distiller software (version 2.2; MatrixScience). The Mascot search algorithm (version 2.2, MatrixScience) was used for searching against the International Protein Index (IPI) database (IPI human release 06/11/2009, version 3.66). The peptide tolerance was typically set to 10 ppm and the fragment ion tolerance to 0.8 Da. A maximum number of 2 missed cleavages by trypsin were allowed and carbamidomethylated cysteine and oxidized methionine were set as fixed and variable modifications, respectively. The Mascot score cut-off value for a positive protein hit was set to 65. Individual peptide MS/MS spectra with Mascot scores below 35 were checked manually and either interpreted as valid identifications or discarded. For quantitative analysis, the mass spectrometric raw data from MaxQuant software suite (version 1.1.1.25) was used[59]. A false discovery rate (FDR) of 0.01 for proteins and peptides and a minimum peptide length of 6 amino acids were required. The mass accuracy of the precursor ions was improved by the time-dependent recalibration algorithm of MaxQuant. The Andromeda search engine was used to search the MS/MS spectra against the IPI human database concatenated with the reversed versions of all sequences. A maximum of two missed cleavages were allowed. The fragment mass tolerance was set to 0.6 Da. Enzyme specificity was set to trypsin. Further modifications were cysteine carbamidomethylation (fixed) as well as protein N-terminal acetylation, methionine oxidation and lysine ubiquitination (variable). Only proteins identified with at least 2 unique peptides and 2 quantification events were considered for analysis. MaxQuant automatically quantified SILAC peptides and proteins. SILAC protein ratios were calculated as the median of all peptide ratios assigned to the protein. In addition a posterior error probability for each MS/MS spectrum below or equal to 0.1 was required. In case the identified peptides of two proteins were the same or the identified peptides of one protein included all peptides of another protein, these proteins were combined by MaxQuant and reported as one protein group. Before statistical analysis, known contaminants and reverse hits were removed.

Flow Cytometry analysis. The number of cell-secreted MVs and ALP+ MVs was determined by flow cytometry as described elsewhere[60]. Briefly, 12.5 µL of freshly isolated MVs were incubated for 20 min in the dark with 12.5 µL ELF-97 staining solution (0.2 M ELF-97 (Invitrogen) in 1.1 M acetic acid, 0.011 M $NaNO_2$, pH 8.0). ELF-97 is a phosphatase substrate, which at pH 8 detects alkaline phosphatase. As negative control, MVs or the ELF-97 staining solution was replaced by PBS. For each of these mixes 125 µl PBS were added. Vesicles were measured in a Becton Dickinson FACS-Canto (BD Bioscience) in the AmCyan-A channel (488nm).

Gene Ontology analysis. Gene Ontology (GO) analyses were obtained using DAVID Bioinformatics Resources 6.7[61-62]. Only significantly ($p<0.05$) enriched terms in comparison to whole genome background (DAVID default) were selected.

Statistical analysis. All experiments were repeated at least three times. Values are mean ± SD and significance was calculated using a Student's t-test.

REFERENCES

[1] Canalis E, et al. Growth factors and the regulation of bone remodeling J Clin Invest 1988, 81, 277-81.

[2] Manolagas SC, et al. Bone marrow, cytokines, and bone remodeling. Emerging insights into the pathophysiology of osteoporosis N Engl J Med 1995, 332, 305-11.

[3] Ling N, et al. Isolation and partial characterization of a Mr 32,000 protein with inhibin activity from porcine follicular fluid Proc Natl Acad Sci U S A 1985, 82, 7217-21.

[4] Vale W, et al. Purification and characterization of an FSH releasing protein from porcine ovarian follicular fluid Nature 1986, 321, 776-9.

[5] Broxmeyer HE, et al. Selective and indirect modulation of human multipotential and erythroid hematopoietic progenitor cell proliferation by recombinant human activin and inhibin Proc Natl Acad Sci U S A 1988, 85, 9052-6.

[6] Lebrun JJ, et al. Activin and inhibin have antagonistic effects on ligand-dependent heteromerization of the type I and type II activin receptors and human erythroid differentiation Mol Cell Biol 1997, 17, 1682-91.

[7] Gaddy-Kurten D, et al. Inhibin suppresses and activin stimulates osteoblastogenesis and osteoclastogenesis in murine bone marrow cultures Endocrinology 2002, 143, 74-83.

[8] Yamada R, et al. Induction of differentiation of the human promyelocytic cell line HL-60 by activin/EDF Biochem Biophys Res Commun 1992, 187, 79-85.

[9] Eijken M, et al. The activin A-follistatin system: potent regulator of human extracellular matrix mineralization FASEB J 2007, 21, 2949-60.

[10] Ogawa Y, et al. Bovine bone activin enhances bone morphogenetic protein-induced ectopic bone formation J Biol Chem 1992, 267, 14233-7.

[11] Fuller K, et al. Activin A is an essential cofactor for osteoclast induction Biochem Biophys Res Commun 2000, 268, 2-7.

[12] Centrella M, et al. Activin-A binding and biochemical effects in osteoblast-enriched cultures from fetal-rat parietal bone Mol Cell Biol 1991, 11, 250-8.

[13] Ikenoue T, et al. Inhibitory effects of activin-A on osteoblast differentiation during cultures of fetal rat calvarial cells J Cell Biochem 1999, 75, 206-14.

[14] Pearsall RS, et al. A soluble activin type IIA receptor induces bone formation and improves skeletal integrity Proc Natl Acad Sci U S A 2008, 105, 7082-7.

[15] Lotinun S, et al. A soluble activin receptor Type IIA fusion protein (ACE-011) increases bone mass via a dual anabolic-antiresorptive effect in Cynomolgus monkeys Bone 2010, 46, 1082-8.

[16] Baum J, et al. Folding of peptide models of collagen and misfolding in disease Curr Opin Struct Biol 1999, 9, 122-8.

[17] Fantner GE, et al. Influence of the degradation of the organic matrix on the microscopic fracture behavior of trabecular bone Bone 2004, 35, 1013-22.

[18] Fratzl-Zelman N, et al. Matrix mineralization in MC3T3-E1 cell cultures initiated by beta-glycerophosphate pulse Bone 1998, 23, 511-20.

[19] Anderson HC, et al. Pyrophosphate stimulation of calcium uptake into cultured embryonic bones. Fine structure of matrix vesicles and their role in calcification Dev Biol 1973, 34, 211-27.

[20] Anderson HC Vesicles associated with calcification in the matrix of epiphyseal cartilage J Cell Biol 1969, 41, 59-72.

[21] Arsenault AL, et al. Vectorial sequence of mineralization in the turkey leg tendon determined by electron microscopic imaging Calcif Tissue Int 1991, 48, 46-55.

[22] Bernard GW Ultrastructural observations of initial calcification in dentine and enamel J Ultrastruct Res 1972, 41, 1-17.

[23] Tanimura A, et al. Matrix vesicles in atherosclerotic calcification Proc Soc Exp Biol Med 1983, 172, 173-7.

[24] Anderson HC, et al. The role of matrix vesicles in growth plate development and biomineralization Front Biosci 2005, 10, 822-37.
[25] Morris DC, et al. Immunolocalization of alkaline phosphatase in osteoblasts and matrix vesicles of human fetal bone Bone Miner 1992, 19, 287-98.
[26] Ali SY, et al. Isolation and characterization of calcifying matrix vesicles from epiphyseal cartilage Proc Natl Acad Sci U S A 1970, 67, 1513-20.
[27] Chen NX, et al. Annexin-mediated matrix vesicle calcification in vascular smooth muscle cells J Bone Miner Res 2008, 23, 1798-805.
[28] Genge BR, et al. Identification of phospholipid-dependent calcium-binding proteins as constituents of matrix vesicles J Biol Chem 1989, 264, 10917-21.
[29] Kirsch T, et al. The roles of annexins and types II and X collagen in matrix vesicle-mediated mineralization of growth plate cartilage J Biol Chem 2000, 275, 35577-83.
[30] Delany AM, et al. Osteonectin-null mutation compromises osteoblast formation, maturation, and survival Endocrinology 2003, 144, 2588-96.
[31] Izu Y, et al. Type XII collagen regulates osteoblast polarity and communication during bone formation J Cell Biol 2011, 193, 1115-30.
[32] Moursi AM, et al. Interactions between integrin receptors and fibronectin are required for calvarial osteoblast differentiation in vitro J Cell Sci 1997, 110 (Pt 18), 2187-96.
[33] Nistala H, et al. Fibrillin-1 and -2 differentially modulate endogenous TGF-beta and BMP bioavailability during bone formation J Cell Biol 2010, 190, 1107-21.
[34] Delany AM, et al. Osteopenia and decreased bone formation in osteonectin-deficient mice J Clin Invest 2000, 105, 915-23.
[35] Damjanovski S, et al. Regulation of SPARC expression during early Xenopus development: evolutionary divergence and conservation of DNA regulatory elements between amphibians and mammals Dev Genes Evol 1998, 207, 453-61.
[36] Green MC, et al. Tight-skin, a new mutation of the mouse causing excessive growth of connective tissue and skeleton Am J Pathol 1976, 82, 493-512.
[37] Chaudhry SS, et al. Fibrillin-1 regulates the bioavailability of TGFbeta1 J Cell Biol 2007, 176, 355-67.
[38] Erlebacher A, et al. Osteoblastic responses to TGF-beta during bone remodeling Mol Biol Cell 1998, 9, 1903-18.
[39] Katagiri T, et al. Bone morphogenetic protein-2 converts the differentiation pathway of C2C12 myoblasts into the osteoblast lineage J Cell Biol 1994, 127, 1755-66.
[40] Wang N, et al. Control of cytoskeletal mechanics by extracellular matrix, cell shape, and mechanical tension Biophys J 1994, 66, 2181-9.
[41] Higuchi C, et al. Transient dynamic actin cytoskeletal change stimulates the osteoblastic differentiation J Bone Miner Metab 2009, 27, 158-67.
[42] Drabek K, et al. GPM6B regulates osteoblast function and induction of mineralization by controlling cytoskeleton and matrix vesicle release J Bone Miner Res 2011, 26, 2045-51.
[43] Xiao Z, et al. Proteomic analysis of extracellular matrix and vesicles J Proteomics 2009, 72, 34-45.
[44] Graner MW, et al. Proteomic and immunologic analyses of brain tumor exosomes FASEB J 2009, 23, 1541-57.
[45] Ikemoto A, et al. Glycolysis and glutamate accumulation into synaptic vesicles. Role of glyceraldehyde phosphate dehydrogenase and 3-phosphoglycerate kinase J Biol Chem 2003, 278, 5929-40.
[46] Svensson L, et al. Decorin-binding sites for collagen type I are mainly located in leucine-rich repeats 4-5 J Biol Chem 1995, 270, 20712-6.
[47] Franzen A, et al. Cartilage proteoglycan aggregate formation. Role of link protein Biochem J 1981, 197, 669-74.
[48] Chen CC, et al. Mechanisms of proteoglycan inhibition of hydroxyapatite growth Calcif Tissue Int 1985, 37, 395-400.

[49] Chen CC, et al. The inhibitory effect of cartilage proteoglycans on hydroxyapatite growth Calcif Tissue Int 1984, 36, 285-90.
[50] Hoshi K, et al. The primary calcification in bones follows removal of decorin and fusion of collagen fibrils J Bone Miner Res 1999, 14, 273-80.
[51] Anderson HC Molecular biology of matrix vesicles Clin Orthop Relat Res 1995, 266-80.
[52] Aubin JE Regulation of osteoblast formation and function Rev Endocr Metab Disord 2001, 2, 81-94.
[53] Thaler R, et al. Extra-cellular matrix suppresses expression of the apoptosis mediator Fas by epigenetic DNA methylation Apoptosis 2010, 15, 728-37.
[54] Kim TI, et al. Fibronectin fragment promotes osteoblast-associated gene expression and biological activity of human osteoblast-like cell Biotechnol Lett 2003, 25, 2007-11.
[55] Wang YK, et al. Inverse 15N-metabolic labeling/mass spectrometry for comparative proteomics and rapid identification of protein markers/targets Rapid Commun Mass Spectrom 2002, 16, 1389-97.
[56] Eijken M, et al. The essential role of glucocorticoids for proper human osteoblast differentiation and matrix mineralization Mol Cell Endocrinol 2006, 248, 87-93.
[57] Johnson K, et al. Matrix vesicle plasma cell membrane glycoprotein-1 regulates mineralization by murine osteoblastic MC3T3 cells Journal of Bone and Mineral Research 1999, 14, 883-92.
[58] Wilm M, et al. Femtomole sequencing of proteins from polyacrylamide gels by nano-electrospray mass spectrometry Nature 1996, 379, 466-9.
[59] Cox J, et al. Andromeda: a peptide search engine integrated into the MaxQuant environment J Proteome Res 2011, 10, 1794-805.
[60] Woeckel VJ, et al. 1Alpha,25-(OH)2D3 acts in the early phase of osteoblast differentiation to enhance mineralization via accelerated production of mature matrix vesicles J Cell Physiol 2010, 225, 593-600.
[61] Dennis G, Jr., et al. DAVID: Database for Annotation, Visualization, and Integrated Discovery Genome Biol 2003, 4, P3.
[62] Hosack DA, et al. Identifying biological themes within lists of genes with EASE Genome Biol 2003, 4, R70.

Chapter 4

Unraveling the human bone microenvironment beyond the classical extracellular matrix proteins: a human bone protein library

Rodrigo D.A.M. Alves, Jeroen A.A. Demmers, Karel Bezstarosti, Bram C.J. van der Eerden, Jan A.N. Verhaar, Marco Eijken and Johannes P.T.M. van Leeuwen

Adapted with permission from Journal of Proteome Research, 2011, 10 (10), pp 4725–4733

ABSTRACT

A characteristic feature of bone, differentiating it from other connective tissues, is the mineralized extracellular matrix (ECM). Mineral accounts for the majority of the bone tissue volume, being the remainder organic material mostly derived from collagen. This and the fact that only a limited number of non-collagenous ECM proteins are described, provides a limited view of the bone tissue composition and bone metabolism, the more so considering the increasing understanding of ECM significance for cellular form and function. For this reason, we set out to analyze and extensively characterize the human bone proteome using large-scale mass spectrometry-based methods. Bone samples of four individuals were analyzed identifying 3038 unique proteins. 1213 of these were present in at least 3 out of 4 bone samples. For quantification purposes we were limited to non-collagenous proteins (NCPs) and we could quantify 1051 NCPs. Most classical bone matrix proteins mentioned in literature were detected but were not among the high abundant ones. Gene ontology analyses identified high abundant groups of proteins with a functional link to mineralization and mineral metabolism such as transporters, pyrophosphatase activity and Ca^{2+}-dependent phospholipid binding proteins. ECM proteins were as well over-represented together with nucleosome and antioxidant activity proteins, which have not been extensively characterized as being important for bone. In conclusion, our data clearly demonstrates that human bone tissue is a reservoir of a wide variety of proteins. In addition to the classical osteoblast-derived ECM, we have identified many proteins from different sources and of unknown function in bone. Thus, this study represents an informative library of bone proteins forming a source for novel bone formation modulators as well as biomarkers for bone diseases such as osteoporosis.

INTRODUCTION

Bone is a specialized form of connective tissue that serves three main functions: support, for muscle attachment and locomotion, protection, for vital organs and bone marrow, and metabolic, regulating the serum mineral balance crucial for life.[1] The specialized properties of bone tissue are a result of the activity of the bone-forming cells, the osteoblasts, which produce an organic extracellular matrix (ECM) with mineralization capacity, the osteocytes and the bone resorbing cells, the osteoclasts.

In terms of content, bone tissue can be grossly divided in inorganic mineral material (mostly hydroxylapatite) and organic material from cells and ECM. The bone mineral represents 80-90% of the volume in compact bones, decreasing to 15-25% in trabecular bones.[1] For the organic part, the ECM is the main contributor, with cells representing only 2-5%[2] of which 95% are fully differentiated osteoblasts, the osteocytes.[3] At the protein level, collagens (mainly type I, COL1A1) represent 90% of the total bone protein content.[1, 4] After collagens, osteocalcin (BGLAP), a specific osteoblast protein, is regarded as the most abundant non-collagenous protein (NCP) found in bone matrix.[5] It comprises 10-20% of the known NCPs in bone[6-8] being detected at concentrations ranging from 0.28 mg/g in human to 2.0-2.5 mg/g in bovine dry bone.[5] We have previously detected BGLAP and several other NCPs in the bone matrix by immunohistochemistry[9]. Other classical NCPs include alkaline phosphatase (ALPL), osteopontin (SPP1), osteonectin (SPARC) and matrix-gla protein (MGP), all playing a role in the mineralization process. Signaling factors such as bone morphogenetic proteins (BMP's), growth factors and cytokines[2] are also present in bone but at lower concentrations. BMP-2 has been isolated from bovine bone with yields of 1 ng/g of bone powder.[10] Altogether, these proteins represent the current picture of bone drawn in literature, with only a few proteins describing a complex tissue. We hypothesized that the bone ECM should contain a broader range of proteins. This is fed by the emerging knowledge that the ECM is not only important to build a strong bone but that ECM composition is crucial for cell shape which can have profound effects in cell behavior.[11-12] Furthermore, the recent findings that a bone ECM protein (BGLAP) can function as a hormone, regulating energy metabolism[13-14] as well as male fertility,[15] provides a renovated interest in mapping the bone ECM proteome. Analogously to BGLAP, other ECM proteins, upon release during osteoclast resorption, might as well exert effects peripherally on different tissues and organs.

In this study we generated a detailed proteome of human trabecular bone by SDS-PAGE combined with nano-LC-MS/MS. Using spectral counting quantitative information provided by the emPAI scores[16] we could classify the proteins for their abundance demonstrating that the bone environment is rich and diverse in protein content, going beyond the classical bone proteins often mentioned in literature. The proteins identified may form a lead to new insights into bone metabolism and are a potential source for new bone turnover markers and ultimately bone disease biomarkers.

RESULTS

Quantification of non-collagenous proteins in bone based on spectral counting

With our in-depth bone proteome analysis we identified in total 3038 unique proteins. 844 proteins were present in all 4 samples and 1213 of them were present in at least 3 out of 4 bone samples (Supplementary Table II, Chapter 7). For the rest of the analyses we decided to focus on those proteins present in at least 3 samples, excluding gender and patient specific proteins, the latter a possible source of protein contamination from co-resected tissue. Next, we quantified the relative abundance of the detected proteins in our human bone samples using spectral counting (emPAI scores,[16] see Material & Methods section for more details). It is important to refer that for several of the identified proteins, the emPAI scores were missing. These include among others, cases where insufficient protein data was acquired or manually assigned protein identifications (for detailed explanation see http://www.matrixscience.com/help/quant_empai_help.html). The identified collagen proteins belong to a group of proteins that we did not quantify either, albeit for different reasons. They require special isolation procedures to be properly digested by trypsin and detected by mass spectrometry.[17] Since we have not followed such a protocol, collagen abundances based on emPAI scores are probably underestimated. For this reason collagens were left out of any quantitative analysis. In total 1051 out of the 1213 identified proteins could be quantified by spectral counting (Supplementary Table II).

The emPAI scores were also used for quality control assessment. Scores attributed in the different bone samples revealed similar distributions, with only a few hits outside the 1-99th percentile (Figure 1A). For coefficient of variance (CV)

calculation and correlation analysis, we selected the 742 proteins with emPAI scores in all 4 bone samples. An average CV of 46% was obtained for the 4 independent biological samples. EmPAI score correlation plots between the 4 bone samples show that proteins high/low abundant in one sample were also high/low abundant in the other samples (Figure 1B).

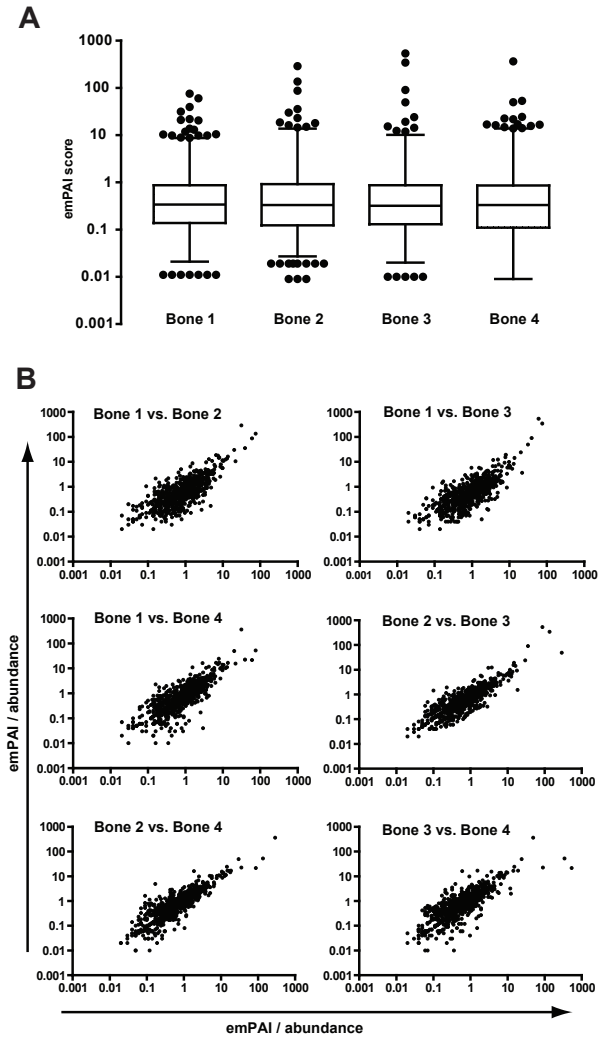

Figure 1. (A) Box and whisker plot with the distribution of all the emPAI scores obtained for the 4 bone samples analyzed. Whiskers represent the 1-99th percentile. **(B)** EmPAI score correlations between the 4 bone samples. Axis showing emPAI scores are in logarithmic scale.

Top abundant proteins versus classical bone proteins

The total of 1051 proteins with an emPAI score in at least 3 out of 4 bone samples were first ranked on basis of there abundance from #1 to #1051. To our surprise, the high abundant proteins were mostly proteins that could not be immediately linked to bone. We found histones (#1 and #11), hemoglobins (#2, #3 and #4) and actins (#7, #14 and #15) among the highest ranked (Figure 2).

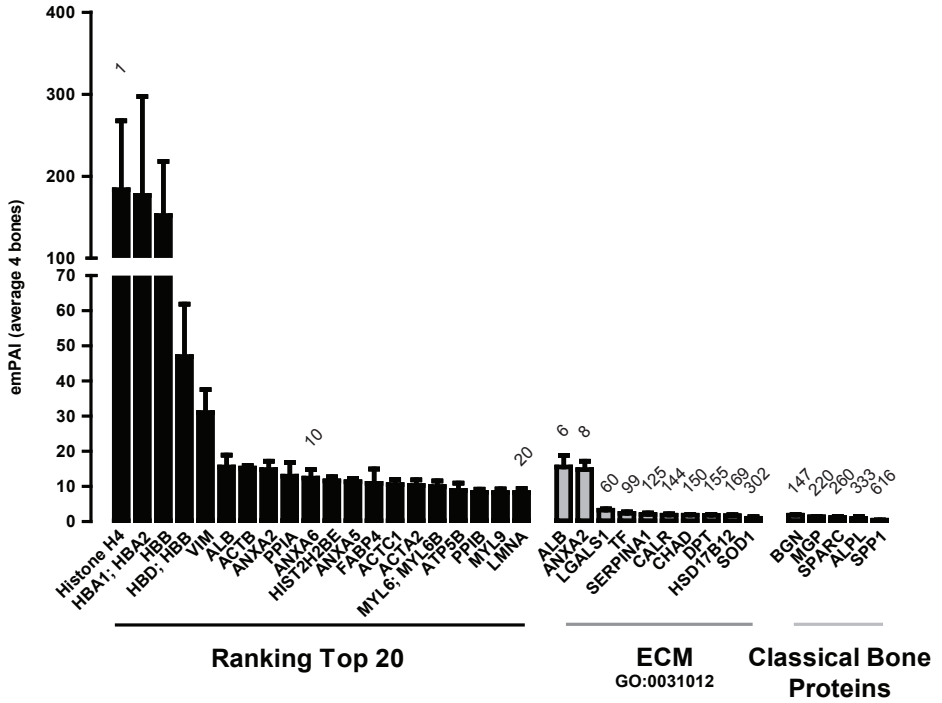

Figure 2. Top 20 most abundant proteins detected in bone tissue, the most abundant ECM proteins in bone and a selection of classical bone proteins. Abundance and ranking of proteins was determined by the average of the emPAI scores (described in Materials and Methods section) obtained for 1051 proteins in at least 3 out of 4 bone samples analyzed. ECM proteins were selected based on Gene Ontology, GO:0031012 extracellular matrix. Classical bone proteins are those described in literature as being expressed in bone tissue. Numbers above the bars indicate the ranking of the proteins. Data is mean ± SEM.

The high expression of Histone H4 in bone was further confirmed using specific antibodies against this protein (Figure 3). Histone H4 could not be detected by Western blot analyses in various bone cell extracts and only faintly in peripheral

blood mononuclear cells (Figure 3). Subsequently, we inspected the ranking list further down for classical bone and GO annotated ECM (GO:0031012) proteins. The most abundant ECM proteins are plotted in Figure 2 together with the 20 overall most abundant ones. The classical bone proteins, biglycan (BGN), matrix-Gla protein (MGP), osteonectin (SPARC), alkaline phosphatase (ALPL) and osteopontin (SPP1) appeared by this order in the ranking as #147, #220, #260, #333 and #616, respectively. Within the category ECM, albumin (ALB) and annexin 2 (ANXA2) were the most abundant proteins. ANXA2 expression in bone can be derived from both osteoblasts and osteoclasts as depicted in Figure 3. Lower in the ECM ranking list, comprising 71 proteins, were galectin-1 (LGALS1, #60), transferring (TF, #99), calreticulin (CALR, #144), chondroadherin (CHAD, #150), estradiol-17-beta-dehydrogenase 12 (HSD17B12, #169), superoxide dismutase 1 (SOD1, #302, Figure 2), decorin (DCN, #307), lumican (LUM, #308) and fibronectin 1 (FN1, #435). Despite the fact that collagens could not be ranked based on emPAI scores, a wide variety of collagen types were detected (type I to XXVIII), including the major bone ECM constituent, COL1A1 (Supplementary Table III, Chapter 7). Other well-known bone related proteins whose expression is reported to be characteristic of the fully differentiated osteoblasts (osteocytes) and osteoclasts were identified (Supplementary Table III). The detected osteocyte related proteins were sclerostin (SOST), matrix extracellular phosphoglycoprotein (MEPE) and phosphate-regulating neutral endopeptidase (PHEX) while carbonic anhydrase 2 (CA2), tartrate-resistant acid phosphatase 5 (ACP5), matrix metalloproteinase-9 (MMP9), cathepsin K (CTSK), V-type proton ATPase 116 kDa subunit (TCIRG1) are known osteoclast functional proteins.

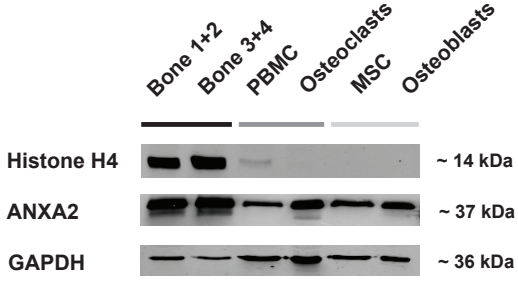

Figure 3. Immunodetection of Histone H4, ANXA2 and GAPDH proteins detected by mass spectrometry in bone tissue. Expression of these proteins was measured in the bone samples as well as in the osteoclast and osteoblast cell lineages differentiated from PBMCs and MSCs respectively.

Over-represented and abundant functionally related proteins

Next we have grouped the identified proteins based on protein families and GO annotations. We have also developed an emPAI-sum score as a measure for the impact of these functionally related protein groups, highlighting important biological mechanisms in the samples analyzed. The results for the emPAI-sum score application to our bone samples is illustrated in Figure 4. As an example, 98 transporter proteins were detected in bone and the sum of their emPAI scores was 247. Within the protein families, following transporters at distance, appear 65 proteins with peptidase activity and an emPAI-sum of 38.1. Besides transcription regulators (28 proteins), kinases (26), transmembrane receptors (23), ion channels (11) we have also detected 3 cytokines (chromosome 19 open reading frame 10; complement component 5; secreted phosphoprotein 1) and 4 growth factors (C-type lectin domain family 11, member A; glia maturation factor, beta; hepatoma-derived growth factor; osteoglycin), with an emPAI-sum of 1.30 and 0.70 respectively (Figure 4A).

Interestingly, among the most abundant protein families was the one annotated with GO term GO:0000786 (i.e. nucleosome) and an emPAI-sum of 212, well above the 71.0 obtained for ECM (GO:0031012) proteins (Figure 4B). We further excluded the hypothesis that the high abundance given by the emPAI scores for nucleosome proteins (including histones) would be a consequence of bias in the protein extraction method, favoring alkaline proteins such as histones (Supplementary Figure II, Chapter 7). Other over-represented terms having high emPAI-sums were pyrophosphatase activity (GO:0016462; emPAI-sum of 180), Ca^{2+}-dependent phospholipid binding (GO:0005544; 49.7), antioxidant activity (GO:0016209; 46.1), integrin (GO:0008305; 3.73) and laminin (GO:0043256; 1.48) complex proteins. The highest abundant proteins within the nucleosome, Ca^{2+}-dependent phospholipid binding and antioxidant activity GO-terms are shown in Figure 4C. Besides being significantly over-represented, these three groups based on these three GO terms also contain many of the most abundant proteins. Histone H4 and Histone H2 were ranked #1 and #2 respectively and the majority of the family members of annexins (ANXA) and antioxidants like peroxiredoxins (PRDX) were also present with high scores.

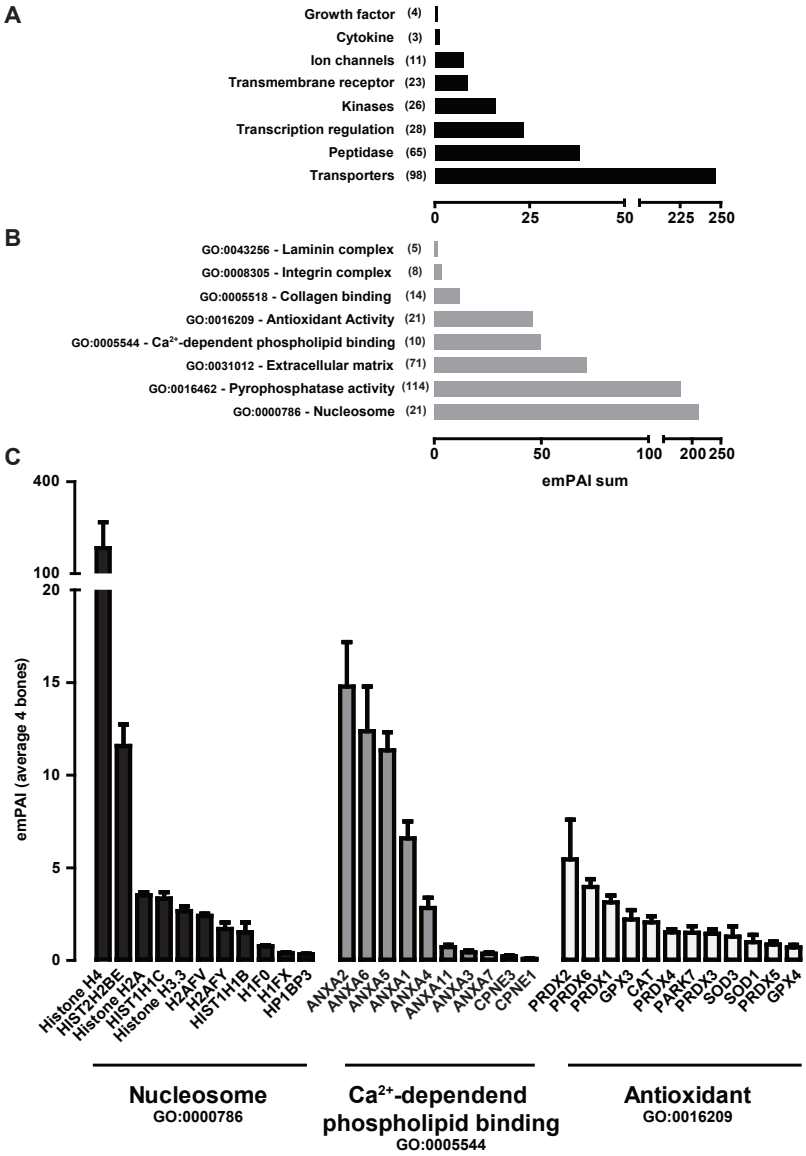

Figure 4. Functional categorization of the 1213 proteins identified in at least 3 out of 4 bones. **(A)** Protein family categorization using Ingenuity and **(B)** significantly ($p<0.01$) over-represented (>2-fold) gene ontology terms highlighted by DAVID. Only protein categories having among the highest emPAI sums are shown (described in Material & methods section). The number of proteins in each category is shown within brackets. **(C)** Detailed overview of the over-represented terms having the highest emPAI score per protein within the term nucleosome (GO:0000786), Ca^{2+}-dependent phospholipid binding (GO:0005544) and antioxidant activity (GO:0016209).

DISCUSSION

Here we report an innovative large scale-proteome study of human bone tissue, where we use spectral counting (emPAI score) to relatively quantify the abundance of the identified proteins. Using this approach we have identified a wide array of proteins expressed in human bone tissue (Supplementary Table II). We detected COL1A1, the most abundant bone protein representing 90% of the protein bone content,[1, 4] among many other collagen types (Supplementary Table III). However, for quantitative analysis, and due the protein isolation method used, the bone proteome, as defined here, is focused on the NCPs, the remaining 10% of the bone protein content.

Data comparison between the (*in vitro*) osteoblast proteome we have previously reported[18] and this bone proteome shows that the majority (over 70%; data not shown) of proteins expressed by osteoblasts are present in the tissue that they produce. More intriguing is the identification of a range of osteoclast proteins in a tissue where the most abundant cell type is the osteocyte and the great majority of proteins are ECM-derived. We hypothesize that these osteoclast proteins are remnants of osteoclast cells that enter apoptosis in the reversal phase of bone remodeling[19] becoming sedimented in the newly formed bone matrix during the subsequent formation phase of the remodeling cycle. Whether these and the other identified bone matrix proteins would serve a further role in bone metabolism is unclear. It is tempting to speculate that these proteins are released during a subsequent resorption cycle and via a process such as transcytosis[20] being transported and if needed being activated by the resorbing osteoclast as reported for TGF-β.[21] This activation mechanism is also valid for BGLAP, as recently demonstrated. Buried in the bone matrix, this protein can simply be activated at the low pH created by osteoclasts during resorption.[14] Upon activation, circulating BGLAP proved to have important endocrine effects, from regulation of energy homeostasis parameters such as insulin sensitivity and glucose tolerance[13-14] to the stimulation of testosterone synthesis favoring male fertility.[15] This data opens up the possibility that other proteins here identified in the bone matrix can also become bioactive having effects in peripheral tissues.

To our surprise, the non-collagenous classical bone proteins often referred in literature (BGN, MGP, SPARC, ALPL, SPP1; complete list in Supplementary Table III) do not appear to be highly abundant. Instead, we identified histone proteins,

hemoglobins, annexins and actin proteins to be highly abundant in bone tissue.

The histone H4 and H2 cluster of proteins were ranked within the top 20 most abundant proteins in bone. The enrichment in histones and other nucleosome proteins is not driven by the protein isolation method (Supplementary Figure II), suggesting that these highly alkaline proteins are indeed enriched in bone. Immunodetection of histone H4 indicates that this protein is not expressed by osteoblasts and osteoclasts and possibly is derived from bone marrow cells or from the circulation. Besides their nuclear localization, histone proteins have recently been reported as extracellular localized, exerting there important biological functions.[22-23] Intriguingly, a circulating histone H4-related osteogenic growth peptide is reported to be a stimulator of osteoblastic activity[24] providing more evidence for a functional role of this protein in bone. We also identified albumin (ALB) as an abundant non-collagenous protein. Despite being a classic plasma protein, this protein is known to bind hydroxylapatite, being accumulated in mineralized bone.[25] Further evidence that circulating proteins maybe sequestered in bone matrix is the observation of hemoglobins (HBA1 and HBB). These are highly expressed by erythrocytes. Not much information is reported regarding hemoglobin expression in bone cells but Jiang and co-workers[26] also report hemoglobin as an abundant protein in bone tissue. We have washed thoroughly the bones in PBS to remove the bone marrow and macroscopically the samples were free of blood contamination. However, we can not exclude that this protein is derived from bone marrow remnants, where erythropoiesis takes place, highlighting the close proximity between these two functionally related organs (reviewed by Del Fattore *et al.*[27]).

The annexin family members are proteins known to be involved in bone metabolism. We have identified ANXA2, ANXA6 and ANXA5 within the top 20 most abundant proteins, and ANXA1, ANXA4, ANXA11, ANXA3 and ANXA7 were also detected. ANXA2, 5 and 6 are reported to be highly concentrated in matrix vesicles, the initiators of mineralization, where they function as calcium channels.[28] ANXA2, the second most abundant ECM protein in our data, is also the most studied annexin in the bone field. It is expressed by osteoblasts enhancing alkaline phosphatase activity[29] and by osteoclasts where it exerts a positive effect, stimulating their formation and activity.[30-31] Within the top 20 of our ranking we found as well various actin proteins (ACTB, ACTC1, ACTA2). In line with this data, high actin expression has been detected in osteoblast lining trabeculae of human bone tissue.[32]

We have previously reported expression of the ECM proteins LGALS1, CALR and SOD1 in cultured differentiating osteoblasts.[18] Here we confirm that these proteins are present in bone and among the most abundant ECM (GO:0031012) proteins. Several other classical bone proteins with ECM localization such as SPP1 and BGN were detected in bone as well, only they were relatively low abundant based on emPAI score. BGLAP (also known as osteocalcin) is widely accepted as the most abundant non-collagenous bone protein.[5] However, we could not detect BGLAP by our method. Mature BGLAP is 49 amino acids long and only 5.8 kDa in size (http://www.uniprot.org/uniprot/P02818), being lost in the SDS-PAGE run, representing a limitation of our method in identifying proteins with small sizes.

We further characterized the bone proteins with respect to their functional relationship. To this end, we took the emPAI score further by calculating an emPAI-sum score for protein families and GO terms identified by bioinformatic tools like Ingenuity and GO analyses. We demonstrate how this emPAI-sum score can be used to quantify the significance of functionally related proteins, facilitating the identification of important biological processes in the samples analyzed.

Using the emPAI-sum score we identified transporters as the most abundant protein family in bone tissue. This family consisted of transporters for sodium/potassium (ATP1B3), calcium (ATP2A2, ATP2B4) and protons (various V-ATPase and ATP synthase subunits). These, together with several identified ion channels (e.g. VDAC1, KCTD12, CLIC1, CLIC4) are probably linked to the specialized bone functions, such as ion mobilization for mineralization and ECM acidification for resorption.[33-34] Most likely, these proteins are cell (e.g. osteoclast) or matrix vesicle remnants sedimented in the bone and/or derived from osteocytes, as it is unlikely that, in contrast to growth factors, these transporters are stored in the bone matrix to serve in later stages of bone metabolism. However, this latter hypothesis can not be excluded. Among the low abundant proteins were cytokines (3 proteins) and growth factors (4 proteins). C19orf10 is a cytokine postulated to play a role in cell proliferation and differentiation. Weiler *et al.*[35] detected this protein in the synovium, in the vicinity of bone tissue, but its exact function remains unknown. One of the growth factors identified was osteoglycin (OGN) an osteoinductive factor stored within the ECM, capable to induce ectopic bone formation and inhibit osteoclast formation.[36] These molecules represent an interesting group of proteins found in bone due to their regulatory functions. Other cytokines and growth factors are known to be present in the bone matrix but their relatively low concentrations

(e.g. 1 ng BMP2/g of bone powder[10]) are likely to be a limitation for their detection with the methodology used.

Over-represented and abundant GO terms include, nucleosome (GO:0000786), pyrophosphatases (GO:0016462), ECM (GO:0031012), Ca^{2+}-dependent phospholipid binding (GO:0005544) and antioxidant activity (GO:0016209) proteins. Less abundantly appear bone related proteins groups, collagen binding (GO:0005518), integrins (GO:0008305) and laminins (GO:0043256). Pyrophosphatase activity proteins are a particularly interesting group of proteins. These proteins can mobilize free phosphate (Pi) from inorganic pyrophosphate (PPi), a mineralization inhibitor.[37] By being enriched in bone tissue, pyrophosphatases may counteract the pyrophosphate inhibitory effect, promoting mineral formation and growth. The over- representation of antioxidant activity proteins, especially the peroxiredoxin family, represents an interesting finding in view of the evidences that reactive oxygen species (ROS) can influence the bone cells, inducing osteoclast activity[38-39] and negatively modulating the osteogenic lineage[40-42]. Interestingly, not only intracellular anti-oxidative mechanisms are present in bone as superoxide dismutase 3 (SOD3), a secreted protein with direct anti-oxidant activity, is found in the ECM bound to heparan sulfate proteoglycan and collagen. Kemp and co-workers[43-44] have demonstrated that SOD3 produced by MSC contributes to the neuroprotective properties of these cells. Since osteoblasts are derived from the MSC lineage it would be interesting to verify whether such protective mechanisms are also present in bone, controlling bone tissue damage. While these mechanisms in bone need further investigation, the detection of 21 abundant antioxidant proteins is a clear sign that this tissue has the protein machinery to control ROS levels, and their influence on osteoblasts and osteoclasts.

Successful application of spectral counting for semi-quantification of proteins after 1D-SDS-PAGE separation have been described elsewhere.[45-46] Fractionation of samples in this manner minimizes the complexity of the total protein/peptide mixture possible deviations from emPAI score/protein abundance linearity, due to random selection for MS/MS events, ion suppression effects or saturation of the MS analyzer/detector.[16] We cannot rule out quantitative variation due to deviations in peptide extraction efficiencies, but overall there is good emPAI reproducibility between the compared biological samples (Figure 1). Also, the total amounts of protein in the different samples are comparable.

In conclusion, this study represents a vast repertoire of proteins and their relative

abundances in human bone tissue. Many of the identified proteins have been already linked to the functional activity of bone, being derived from the classical source, the osteoblast-derived ECM. Additionally, our data indicates other sources for the proteins found in bone, from osteoclast-derived to systemic circulating proteins with affinity for mineral. This is supported by comparative analysis of our bone proteome data and mRNA expression data from trabecular bone biopsies[47] (data publicly available in ArrayExpress, http://www.ebi.ac.uk/arrayexpress/, experiment ID E-MEXP-2219, iliac crest samples), with about 10% of the bone proteins we identified not detected as expressed at mRNA level in the bone tissue. Altogether, this library of proteins identified constitutes the representation of the bone microenvironment and of the osteoblast-ECM-osteoclast interactions. Several proteins remain to be studied in the bone context, being of major interest for the discovery of new bone modulators and a reservoir of potential biomarkers for bone diseases such as osteoporosis. Moreover, the characterization of the bone proteome could help unveil other players involved in the endocrine function of bone, recently highlighted by Ferron *et al*. and Fulzele and colleagues.[13-14]

Supplementary Data

Supplementary data available in Chapter 7.

MATERIAL & METHODS

Bone samples. Cancellous bone was obtained from the proximal femur of patients undergoing total hip replacement surgery for primary osteoarthritis after approval by the local ethical committee (MEC2004-322). Patients with conditions, such as prednisone usage or rheumatoid arthritis, which may affect bone metabolism, were excluded. In this way we were able to collect 4 samples of healthy trabecular femoral bone fragments (2 male and 2 female donors, age range 64-83).

Cell culture. Human bone marrow-derived Mesenchymal Stem Cells (MSC; PT-2501, Lonza, Walkersville, MD, USA) were cultured as described previously[48]. Briefly, for osteogenic differentiation, MSCs were cultured in medium supplemented with 100 nM dexamethasone (DEX, Sigma, St. Louis, MO, USA) and 10 mM ß-glycerophosphate (Sigma). Human Peripheral Blood Mononuclear Cells (PBMCs) were derived from buffy coats (Sanquin, Rotterdam, The Netherlands). After dilution in the same volume of PBS, the cell suspension was added to 15 mL of

Ficoll (Amersham Biosciences, Uppsala, Sweden) and centrifuged for 30 minutes at 1500g at room temperature. The white interface, containing the monocytes, was collected and washed in αMEM (GIBCO, Paisley, UK) containing 15% FCS. Monocytes were seeded at 300.000 cells/cm^2 and cultured in αMEM containing 15% FCS, supplemented with 25 ng/ml human recombinant M-CSF (R&D systems, Minneapolis, MI) and 30 ng/ml human recombinant RANKL (Preprotech, London, United Kingdom) for osteoclast differentiation. Culture media was replaced twice a week. MSC and PBMC cell extracts were collected before induction of differentiation. Cell extracts from differentiated osteoblasts and osteoclasts were obtained from 12 and 21 day cultures respectively.

Protein Isolation. Bone fragments were collected in phosphate-buffered saline (PBS, GIBCO) containing 0.02% sodium azide and a protease-inhibitor cocktail (Complete, EDTA-free, Roche, Mannheim, Germany). Upon collection, the bone tissue was rigorously washed in cold PBS to remove residual blood and cellular debris contamination. To facilitate the extraction of the bone organic constituents, bones were pulverized using a dismembrator (Sartorius, Mikro dismembrator S, Goettingen, Germany) at 2600 rpm for 1 minute. The pulverized bone tissue and the cell extracts were homogenized with TRIzol (1ml/100mg tissue; Invitrogen, Carlsbad, CA, USA) and proteins were isolated following the manufacturer's protocol. Next, proteins were precipitated using methanol/chloroform,[49] re-suspended in 0.1% (w/v) RapiGest SF (Waters, Milford, MA, USA) in 50 mM ammonium bicarbonate and dissolved by sonification (Soniprep 150, Sanyo). Protein concentration was determined using a BCA kit (Pierce Biotechnology, Rockford, IL, USA).

SDS-PAGE. After denaturation, 5 minutes at 95°C, proteins were reduced using 10 mM DTT in 50 mM ammonium bicarbonate for 1 hour at 56°C and alkylated for 1 hour at room in the dark with 10 mM iodoacetamide in 50 mM ammonium bicarbonate. At this point, proteins were freeze-dried and re-suspended in 100 mM triethylammonium bicarbonate buffer (TEAB; Sigma, Switzerland). For each sample, 50 μg of protein were resolved by one-dimensional SDS-PAGE (10% Tris-HCl, Ready Gels, Bio-Rad, Hercules, CA, USA) and visualized with Coomassie staining (Bio-safe Coomassie, Bio-Rad, Hercules, CA, USA).

Mass spectrometry analysis. SDS-PAGE gel lanes were cut into 2-mm slices using an automatic gel slicer and subjected to in-gel digestion with trypsin sequencing grade (Promega, Madison, WI, USA) essentially as described by Wilm *et al.*.[50] Nanoflow LC-MS/MS was performed on an 1100 series capillary LC system

(Agilent Technologies) coupled to an LTQ-Orbitrap mass spectrometer (Thermo) operating in positive mode and equipped with a nanospray source. Peptide mixtures were trapped on a ReproSil C18 reversed phase column (Dr Maisch GmbH; column dimensions 1.5 cm × 100 µm, packed in-house) at a flow rate of 8 µl/min. Peptide separation was performed on ReproSil C18 reversed phase column (Dr Maisch GmbH; column dimensions 15 cm × 50 µm, packed in-house) using a linear gradient from 0 to 80% B (A = 0.1 % FA; B = 80% (v/v) ACN, 0.1 % FA) in 120 min and at a constant flow rate of 200 nl/min using a splitter. The column eluent was directly sprayed into the ESI source of the mass spectrometer. Mass spectra were acquired in continuum mode and fragmentation of the peptides was performed in data-dependent mode. Peak lists were automatically created from raw data files using the Mascot Distiller software (version 2.2; MatrixScience). The Mascot search algorithm (version 2.2, MatrixScience) was used for searching against the International Protein Index (IPI) database (version 3.62; release IPI_human_20090729). The peptide tolerance was typically set to 10 ppm and the fragment ion tolerance to 0.8 Da. A maximum number of 2 missed cleavages by trypsin were allowed and carbamidomethylated cysteine and oxidized methionine were set as fixed and variable modifications, respectively. The Mascot score cut-off value for a positive protein hit was set to 65. Individual peptide MS/MS spectra with Mascot scores below 35 were checked manually and either interpreted as valid identifications or discarded.

Quantitative data analysis using spectral counting. Semi-quantitative data was derived from the exponentially modified protein abundance index (emPAI) score, which is a way of spectral counting. The emPAI score is calculated using the number of detected peptides normalized by the number of theoretically observable ones. Ishihama and colleagues[16] have shown the usefulness of the score by demonstrating that it is roughly proportional to protein abundance. Recently, it has been included by default in the Mascot searches for mass spectrometry-based proteomics. We took advantage of these properties and used the emPAI scores to make a ranking of protein abundance in human bone tissue. Each emPAI score was first normalized by multiplying it with a sample normalization factor (ratio of median emPAI score of all samples to median emPAI score of the sample to be normalized). Next, if a protein had an attributed emPAI score in at least 3 out of the 4 bone samples, it was considered for ranking by calculating the average emPAI score in the 3 or 4 samples.

Bioinformatic Analysis. Ingenuity Pathway Analysis (IPA, version 7.60) and DAVID Bioinformatics Resources v6.7[51-52] were used to obtain a comprehensive description of the functionally related groups of proteins present in our dataset in at least 3 of the bone samples. We first grouped proteins that belong to the same protein family (IPA classification) and that are annotated with the same GO term (DAVID classification). For the latter, only significant ($p<0.01$) 2-fold or higher overrepresented GO terms were considered. Next, we calculated the "grouped abundance" by summing the emPAI scores of the individual proteins that constitute them (emPAI-sum). In this way, a quantitative measurement of these groups of proteins could be also achieved. The Compute pI/MW tool (freely available at: http://expasy.org/tools/pi_tool.html) was used to determine whether the protein isolation method used is biased towards proteins within a specific range of isoelectric point. As a reference the whole IPI proteome database (version 3.62; release IPI_human_20090729) was used. To be able to use this tool, IPI identifiers had to be converted into Swiss-Prot identified, which was achieved using BioMart (http://www.biomart.org).

Western Blotting. Protein isolation for Western blotting experiments was identical to that described above. Equal pooled (Bone 1+2 and 3+4) amounts of protein per sample were loaded, separated by SDS-PAGE and transferred onto a nitrocellulose membrane (Hybond-ECL, Amersham Biosciences, Buckinghamshire, UK). After blocking non-specific signal with 5% BSA in TBS/0.1% Tween-20 the membrane was incubated with antibodies against Annexin A2 (rabbit polyclonal to ANXA2; 1ug/ml, Abcam, Cat. Ab41803), GAPDH (loading control; mouse monoclonal; 1:20000, Millipore, Cat. MAB374) and Histone H4 (rabbit polyclonal to Histone H4 - ChIP Grade; 1:500, Abcam, Cat. Ab7311). Membranes were probed with secondary antibodies, goat anti-mouse or goat anti-rabbit IgG, conjugated with Alexa Fluor 680 (1:5000, Invitrogen, Cat. A21057) or with IRDye 800CW (1:5000, LI-COR, Cat. 926-32211) respectively. Immunoreactive bands were visualized using the LI-COR Infrared Imaging System according to the manufacturers instructions (Odyssey Lincoln, NE, USA).

REFERENCES

[1] Favus MJ, *et al. Primer on the metabolic bone diseases and disorders of mineral metabolism*; 5th ed.; American Society for Bone and Mineral Research: Washington, DC, 2003.

[2] Sommerfeldt DW, *et al.* Biology of bone and how it orchestrates the form and function of the skeleton *Eur Spine J* 2001, *10 Suppl 2*, S86-95.

[3] Franz-Odendaal TA, *et al.* Buried alive: how osteoblasts become osteocytes *Dev Dyn* 2006, *235*, 176-90.

[4] Bilezikian JP, *et al. Principles of bone biology*; Academic Press: San Diego, 1996.

[5] Hauschka PV, *et al.* Osteocalcin and matrix Gla protein: vitamin K-dependent proteins in bone *Physiol Rev* 1989, *69*, 990-1047.

[6] Gundberg CM, *et al.* Osteocalcin: isolation, characterization, and detection *Methods Enzymol* 1984, *107*, 516-44.

[7] Hauschka PV, *et al.* Direct identification of the calcium-binding amino acid, gamma-carboxyglutamate, in mineralized tissue *Proc Natl Acad Sci U S A* 1975, *72*, 3925-9.

[8] Price PA, *et al.* Characterization of a gamma-carboxyglutamic acid-containing protein from bone *Proc Natl Acad Sci U S A* 1976, *73*, 1447-51.

[9] Derkx P, *et al.* Immunolocalization and quantification of noncollagenous bone matrix proteins in methylmethacrylate-embedded adult human bone in combination with histomorphometry *Bone* 1998, *22*, 367-73.

[10] Wozney JM, *et al.* Novel regulators of bone formation: molecular clones and activities *Science* 1988, *242*, 1528-34.

[11] Ingber DE Tensegrity: the architectural basis of cellular mechanotransduction *Annu Rev Physiol* 1997, *59*, 575-99.

[12] Ingber DE Tensegrity II. How structural networks influence cellular information processing networks *J Cell Sci* 2003, *116*, 1397-408.

[13] Fulzele K, *et al.* Insulin receptor signaling in osteoblasts regulates postnatal bone acquisition and body composition *Cell* 2010, *142*, 309-19.

[14] Ferron M, *et al.* Insulin signaling in osteoblasts integrates bone remodeling and energy metabolism *Cell* 2010, *142*, 296-308.

[15] Oury F, *et al.* Endocrine regulation of male fertility by the skeleton *Cell* 2011, *144*, 796-809.

[16] Ishihama Y, *et al.* Exponentially modified protein abundance index (emPAI) for estimation of absolute protein amount in proteomics by the number of sequenced peptides per protein *Mol Cell Proteomics* 2005, *4*, 1265-72.

[17] Zhang G, *et al.* Mass spectrometric analysis of enzymatic digestion of denatured collagen for identification of collagen type *J Chromatogr A* 2006, *1114*, 274-7.

[18] Alves RD, *et al.* Proteomic analysis of human osteoblastic cells: relevant proteins and functional categories for differentiation *J Proteome Res* 2010, *9*, 4688-700.

[19] Hill PA Bone remodeling *Br J Orthod* 1998, *25*, 101-7.

[20] Salo J, *et al.* Removal of osteoclast bone resorption products by transcytosis *Science* 1997, *276*, 270-3.

[21] Oreffo RO, *et al.* Activation of the bone-derived latent TGF beta complex by isolated osteoclasts *Biochem Biophys Res Commun* 1989, *158*, 817-23.

[22] Henriquez JP, *et al.* Extracellular matrix histone H1 binds to perlecan, is present in regenerating skeletal muscle and stimulates myoblast proliferation *J Cell Sci* 2002, *115*, 2041-51.

[23] Xu J, *et al.* Extracellular histones are major mediators of death in sepsis *Nat Med* 2009, *15*, 1318-21.

[24] Bab I, *et al.* Histone H4-related osteogenic growth peptide (OGP): a novel circulating stimulator of osteoblastic activity *EMBO J* 1992, *11*, 1867-73.

[25] Triffitt JT, *et al.* Origin of plasma alpha2HS-glycoprotein and its accumulation in bone *Nature* 1976, *262*, 226-7.

[26] Jiang X, *et al.* Method development of efficient protein extraction in bone tissue for proteome analysis *J Proteome Res* 2007, *6*, 2287-94.
[27] Del Fattore A, *et al.* Bone and bone marrow: the same organ *Arch Biochem Biophys* 2010, *503*, 28-34.
[28] Anderson HC Molecular biology of matrix vesicles *Clin Orthop Relat Res* 1995, 266-80.
[29] Gillette JM, *et al.* The role of annexin 2 in osteoblastic mineralization *J Cell Sci* 2004, *117*, 441-9.
[30] Takahashi S, *et al.* Cloning and identification of annexin II as an autocrine/paracrine factor that increases osteoclast formation and bone resorption *J Biol Chem* 1994, *269*, 28696-701.
[31] Menaa C, *et al.* Annexin II increases osteoclast formation by stimulating the proliferation of osteoclast precursors in human marrow cultures *J Clin Invest* 1999, *103*, 1605-13.
[32] Kinner B, *et al.* Expression of smooth muscle actin in osteoblasts in human bone *J Orthop Res* 2002, *20*, 622-32.
[33] Francis MJ, *et al.* ATPase pumps in osteoclasts and osteoblasts *Int J Biochem Cell Biol* 2002, *34*, 459-76.
[34] Supanchart C, *et al.* Ion channels and transporters in osteoclasts *Arch Biochem Biophys* 2008, *473*, 161-5.
[35] Weiler T, *et al.* The identification and characterization of a novel protein, c19orf10, in the synovium *Arthritis Res Ther* 2007, *9*, R30.
[36] Kukita A, *et al.* Osteoinductive factor inhibits formation of human osteoclast-like cells *Proc Natl Acad Sci U S A* 1990, *87*, 3023-6.
[37] Fleisch H, *et al.* Mechanism of calcification: inhibitory role of pyrophosphate *Nature* 1962, *195*, 911.
[38] Garrett IR, *et al.* Oxygen-derived free radicals stimulate osteoclastic bone resorption in rodent bone in vitro and in vivo *J Clin Invest* 1990, *85*, 632-9.
[39] Koh JM, *et al.* Homocysteine enhances bone resorption by stimulation of osteoclast formation and activity through increased intracellular ROS generation *J Bone Miner Res* 2006, *21*, 1003-11.
[40] Mody N, *et al.* Oxidative stress modulates osteoblastic differentiation of vascular and bone cells *Free Radic Biol Med* 2001, *31*, 509-19.
[41] Bai XC, *et al.* Oxidative stress inhibits osteoblastic differentiation of bone cells by ERK and NF-kappaB *Biochem Biophys Res Commun* 2004, *314*, 197-207.
[42] Bruedigam C, *et al.* A new concept underlying stem cell lineage skewing that explains the detrimental effects of thiazolidinediones on bone *Stem Cells* 2010, *28*, 916-27.
[43] Kemp K, *et al.* Inflammatory cytokine induced regulation of superoxide dismutase 3 expression by human mesenchymal stem cells *Stem Cell Rev* 2010, *6*, 548-59.
[44] Kemp K, *et al.* Mesenchymal stem cell-secreted superoxide dismutase promotes cerebellar neuronal survival *J Neurochem* 2010, *114*, 1569-80.
[45] Mastroleo F, *et al.* Shotgun proteome analysis of Rhodospirillum rubrum S1H: integrating data from gel-free and gel-based peptides fractionation methods *J Proteome Res* 2009, *8*, 2530-41.
[46] Poliakov A, *et al.* Large-scale label-free quantitative proteomics of the pea aphid-Buchnera symbiosis *Mol Cell Proteomics* 2011.
[47] Kalogeropoulos M, *et al.* Zic1 transcription factor in bone: neural developmental protein regulates mechanotransduction in osteocytes *FASEB J* 2010, *24*, 2893-903.
[48] Eijken M, *et al.* The activin A-follistatin system: potent regulator of human extracellular matrix mineralization *FASEB J* 2007, *21*, 2949-60.
[49] Wessel D, *et al.* A method for the quantitative recovery of protein in dilute solution in the presence of detergents and lipids *Anal Biochem* 1984, *138*, 141-3.
[50] Wilm M, *et al.* Femtomole sequencing of proteins from polyacrylamide gels by nano-electrospray mass spectrometry *Nature* 1996, *379*, 466-9.
[51] Dennis G, Jr., *et al.* DAVID: Database for Annotation, Visualization, and Integrated Discovery *Genome Biol* 2003, *4*, P3.
[52] Hosack DA, *et al.* Identifying biological themes within lists of genes with EASE *Genome Biol* 2003, *4*, R70.

Chapter 5

Calcifying vascular cells and osteoblasts: independent cell types exhibiting extracellular matrix and biomineralization-related mimicries

Rodrigo D.A.M. Alves, Marco Eijken, Jeroen van de Peppel and Johannes P.T.M. van Leeuwen

Submitted

ABSTRACT

Ectopic vascular calcifications represent a major clinical problem associated with cardiovascular disease and mortality. However, the mechanisms underlying pathological vascular calcifications are largely unknown hampering the development of therapies to tackle this life threatening medical condition. In order to gain insight into the genes and processes underlying this pathological calcification we performed comparative gene expression profiling. We analyzed the transcriptional profile during VSMC development into calcifying vascular cells (CVCs) and compared this with the transcriptional profile during osteogenic differentiation of human mesenchymal stem cells (MSC). Our data showed that the whole VSMC developed into a unique CVC population based on the expression of the osteogenic and vascular transdifferentiation marker alkaline phosphatase (ALP). Overall the transcriptional program of CVC and osteoblasts did not overlap. We found that CVCs keep a VSMC identity by expressing classical VSMC markers. Bioinformatics gene clustering and correlation analysis disclosed that only a specific set of bone-related mechanisms were similarly regulated in the two cell types. These mechanisms encompassed extracellular matrix (ECM) genes and genes involved in biomineralization. The current data showed that VSMC that develop into CVCs keep their own vascular identity but use a specific set of genes which are also used by osteoblast to initiate matrix calcification. Extracellular matrix genes and genes involved in tissue mineralization constituted the most important common denominators between pathological vascular and physiological bone calcifications. In addition, other genes known to be important for bone formation and mineralization were found be distinctly modulated by CVCs. This observation is interesting since it opens the perspective of tackling undesired vascular calcifications without disturbing physiologic bone formation and *vice versa*.

INTRODUCTION

Vascular calcification in the tunica media of arteries and blood vessels is often observed in the elderly population, in patients with diabetes mellitus and/or chronic kidney disease[1]. Vascular calcifications represent a major clinical problem being in the origin of cardiovascular disease and ultimately mortality[2]. Vascular smooth muscle cells (VSMCs) are contractile cells located at the medial layer of the vessel wall. VSMCs can be triggered to transdifferentiate into calcified vascular cells (CVCs), loosing the phenotypic markers responsible for smooth muscle cell contractility[3-4]. Further physiological alterations of VSMC include entering a synthetic state with abundant production of extracellular matrix (ECM) proteins[1] followed by matrix vesicle-mediated calcification[5-6].

It has been hypothesized that pathological medial calcification is a process analogue to bone mineralization with VSMCs entering an osteoblast-like differentiation program[7]. Atherosclerotic plaques, of medial and valvular origin, express several bone-related ECM proteins, including osteopontin, collagen I, matrix GLA protein, osteonectin and osteocalcin[7-9]. In addition, calcified vascular tissue expresses bone specific transcription factors and bone morphogenetic proteins (BMPs)[10-13]. Despite these similarities with osteoblast differentiation the exact mechanism behind VSMCs transdifferentiation into CVCs remains largely unknown. Some studies have suggested that only a subset of the VSMC pool has osteogenic potential[10, 14]. Pathological vascular calcifications may arise due to loss of mineralization inhibitors, which are continuously expressed in healthy vascular tissue[15]. Mice lacking MGP show spontaneous vascular calcifications[8], a phenotype that is exacerbated when SPP1, another mineralization inhibitor, is deleted[16]. Murshed and colleagues[17] have explored this hypothesis further showing that mineralization can occur in any collagen type I rich tissue that expresses pyrophosphatases such as alkaline phosphatase (ALP). While collagen type I is ubiquitously expressed in the tissues, the co-expression of this ECM protein with ALP is restricted to those that mineralize. ALP is involved in the cleavage of pyrophosphate a potent mineralization inhibitor[18]. This enzyme on its own was shown to be able of inducing calcification in rat models of medial calcification[19]. Normally VSMCs do not express ALP but for unclear reasons they can transdifferentiate into CVCs that show increased ALP activity[6, 20].

In this study we aimed to reveal the processes whereby VSMCs develop into CVCs exhibiting a calcified phenotype. We compared this pathological process to

the physiological mechanism regarded as an analogue process, the differentiation of mesenchymal stem cells into osteoblasts.

Under consideration were three hypotheses, 1) CVCs are osteoblast or osteoblast-like cells transdifferentiating from the VSMC pool, 2) CVCs initiate mineralization using osteoblast-like mechanisms, and 3) CVCs mineralize using mechanisms unrelated to osteoblasts. To address these hypotheses we used genome-wide gene expression analysis during *in vitro* human VSMC development into CVCs and human MSC differentiation into osteoblasts. We investigated these processes in terms of their known specific markers but also in an unbiased general perspective, using bioinformatics tools. Global expression profiles and gene regulation were used to pinpoint the transcriptional program and the identity of a CVC in comparison to the phenotype-resembling osteoblast.

RESULTS

The complete VSMC population develops into an ALP positive population under osteogenic stimuli.

VSMCs and MSCs were cultured in osteogenic medium for 25 days to induce development into CVCs and osteoblast respectively. During this period total ALP activity was measured. As shown in Figure 1A, ALP activity increased in CVCs and osteoblasts cultures compared to their precursor cells with enzymatic activity reaching higher absolute levels in osteoblasts then in their CVC counterparts.

In addition, we measured ALP expression at the individual cell level by flow cytometry. This data (Figure 1B) corroborated the ALP activity measurements. Furthermore it clearly demonstrated that the whole VSMC and MSC population became ALP positive during differentiation towards CVCs and osteoblasts respectively (Figure 1C).

CVCs and osteoblasts have distinct global gene expression profiles.

Next, we performed comparative genome-wide mRNA expression analysis in osteogenic VSMC and MSC cultures to characterize their transcriptional similarities and dissimilarities. Five time-points (day 0, 2, 8, 12 and 25) were analyzed during VSMC development to CVCs and MSC to osteoblasts. The data was normalized and probes/genes expressed in neither VSMC/CVC nor MSC/osteoblasts were excluded from further analysis. The overlap of expressed probes between osteogenic VSMC

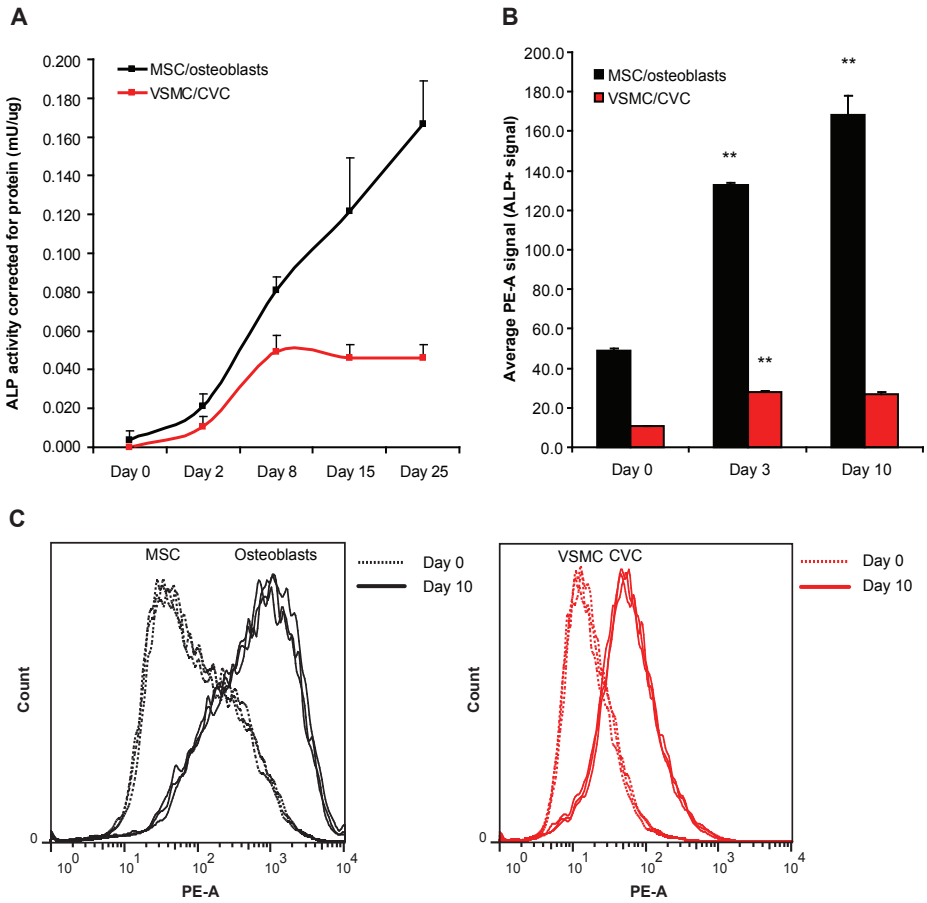

Figure 1. ALP activity and expression during CVC development and osteoblast differentiation. **(A)** ALP activity corrected for protein and **(B)** average ALP+ cell signal measured by FACS at day 0, 3 and 10. **(C)** FACS histogram with the distribution of the ALP+ signal relative to the number of cells (count) at day 0 and 10. Value means ± SD. n=3. ** $p<1x10^{-4}$.

and MSC cultures contained 14733 probes representing 11302 unique genes. These probes/genes were subsequently used for Principle Component Analysis (PCA). PCA allowed simultaneous comparison of multiple time-points in both cell types summarizing the relationship between them. The closer the data points appear in the PCA plot (Figure 2), the more similar their gene expression profiles are. The PCA plot showed that VSMCs and MSCs at the start of culture (day 0) represented two clearly distinct clusters that upon osteogenic stimulation did not converge into an indistinguishable cluster of similarity (Figure 2). In other words, CVCs and

osteoblasts are two distinct cell types in terms of global gene expression.

Several clusters could be identified during CVC and osteoblast development. For both cell types, day 2 represented an intermediate stage after the osteogenic stimuli given to VSMCs and MSCs (day 0; Figure 2). This transient stage is followed by a more stable period, day 8-25, in which gene expression did not change so dramatically (Figure 2).

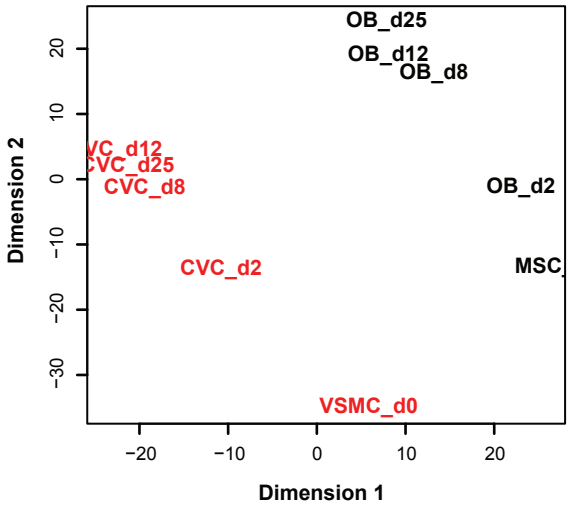

Figure 2. Principal Component Analysis of the global gene expression changes occurring during CVC development and osteoblast differentiation. 14733 probes expressed by both VSMC/CVC and MSC/osteoblasts (OB) at day 0, 2, 8, 12 and 25 were considered for analysis. Distance between samples is directly proportional to gene expression differences. Each time point is represented by the average of 3 biological replicates with exception for day 0 where n=4.

VSMCs maintain their smooth muscle cell identity during CVC development.

In the subsequent analysis we investigated the expression of (vascular) smooth muscle cell marker genes. We selected established VSMC markers described in literature[21], including alpha-actin-2 (ACTA2), caldesmon (CALD1), calponin (CNN1), smooth-muscle myosin (MYH11) and telokin (MYLK) (Figure 3). We verified that CVCs still expressed this panel of marker genes. The expression of many of these genes was even increased compared to their VSMC precursors during osteogenic culture. These data substantiates further that CVCs do not acquire full

osteoblast-like transcriptome but retain the expression of genes responsible for the contractile phenotype of VSMCs.

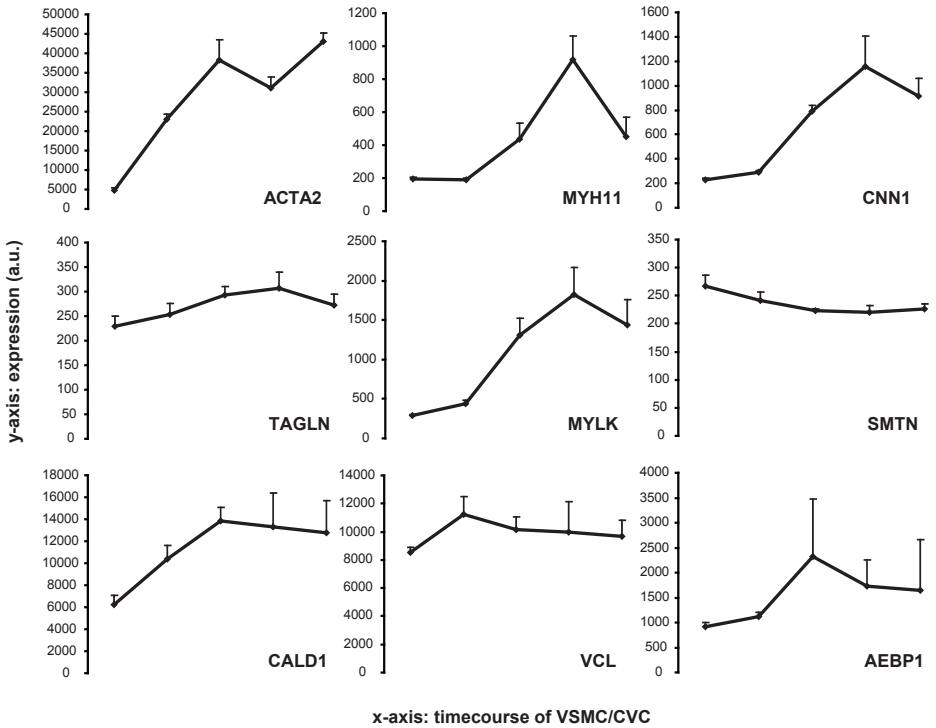

Figure 3. Expression profile of known smooth muscle cell markers during CVC development. Intensity values in arbitrary units are based on data at day 0, 2, 8, 12 and 25. For each time point n=3 with exception for day 0 where n=4. Value means ± SD.

Genes identically regulated by CVCs and osteoblasts are functionally annotated to extracellular region.

To identify whether only specific groups of genes were identically regulated by CVCs and osteoblasts, we have selected differentially expressed genes during VSMC development into CVCs and during MSC differentiation into osteoblasts. Differential expression was calculated for each cell type relative to day 0. Probes/genes were considered differentially expressed when on at least one day during culture their $\log_2$ fold-change compared to day 0 was significantly (q-value<0.001) higher than 0.5 (up-regulation) or lower than -0.5 (down-regulation). During CVC development and osteoblast differentiation 3721 probes and 3114

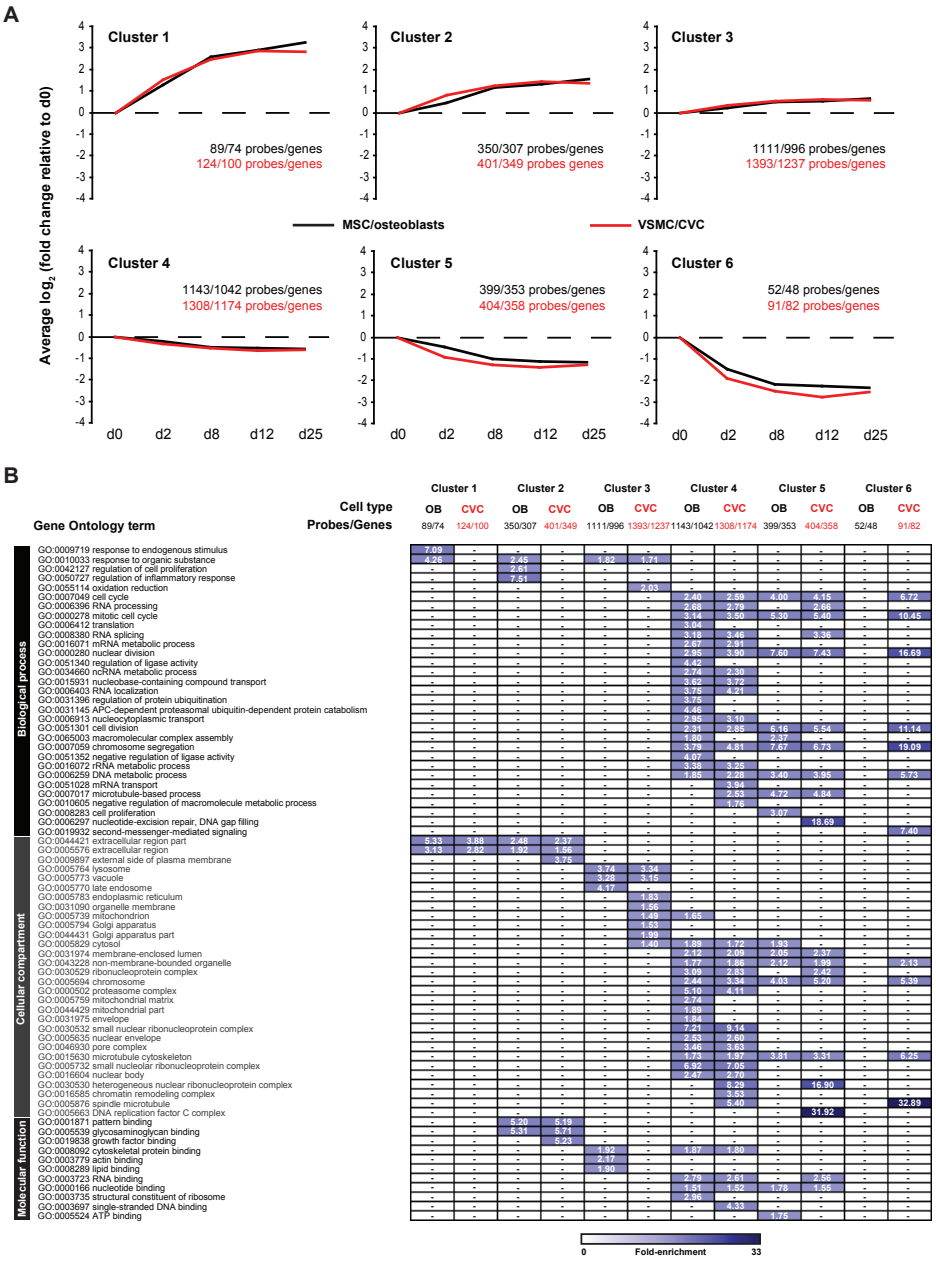

Figure 4. Clustering and respective functional annotation of differentially expressed genes in CVCs and osteoblasts. Differentially expressed genes were grouped using k-means clustering with k=6. **(A)** Clusters of genes with distinct expression profiles for CVCs and osteoblasts. The average of relative gene expression level (log_2 fold change relative to d0) for

all probes within each cluster at the different time points analyzed is shown. **(B)** Functional annotation for each of the 6 clusters in CVCs and osteoblasts. Only significant (Bonferroni p-value<0.05) biological process, cellular compartment and molecular function annotations were considered for analysis. Numbers within grid represent fold-enrichment levels of Gene Ontology (GO)-terms in the distinct clusters. The number of probes/genes comprised in each cluster is also indicated.

probes met this criterion, respectively. Considering the two cell types combined, 4782 probes were found to be differentially expressed (Supplementary Table IV, Chapter 7). Of these 4782 probes, 1638 and 1061 were exclusively differentially expressed in CVCs or in osteoblasts, respectively. Regarding the direction of gene expression regulation, 1968 probes were identically regulated while 150 were oppositely changed during CVC and osteoblast development (Supplementary Table IV).

The temporal and directional expression dynamics of the 4782 differential expressed probes during CVC development and osteoblast differentiation is resumed in Figure 4. K-means clustering separated the differentially expressed probes during CVC development and osteoblast differentiation into clusters sharing common regulation patterns. On basis of Figure of Merit (FOM) analysis we concluded to divide gene expression data in 6 clusters (Figure 4A). This number of clusters was found to provide good predictive power for the k-means algorithm (Supplementary Figure III, Chapter 7) without restricting the cluster size for functional annotation analysis. Functional GO annotation of genes underlying these clusters revealed information about the biological processes, cellular compartments and molecular functions during CVC development and osteoblast differentiation (Figure 4B).

Clusters 1, 2 and 3 contained up-regulated genes while clusters 4, 5 and 6 represented down-regulated genes in both CVCs and osteoblasts (Figure 4A). In clusters 1 and 2 CVCs and osteoblast shared the over-representation of genes linked to extracellular region (GO:0044421 and GO:0005576, Figure 4B). In clusters 3, 4, and 5 several GO-terms were also shared by CVCs and osteoblasts but these were more general GO-terms like cell cycle, RNA processing, chromosome, biological response to organic substance, etc., related to general cell function/metabolism. An exemption was cluster 6 that only showed significant enriched GO terms for CVCs. This fact may be attributed to statistical issues related to the lower number of genes fitting this cluster in osteoblasts. Overall, cluster analyses did not clearly identify sets of bone-related processes or cellular components shared by CVCs and osteoblast. Nevertheless, it was interesting to observe that a common set of extracellular region

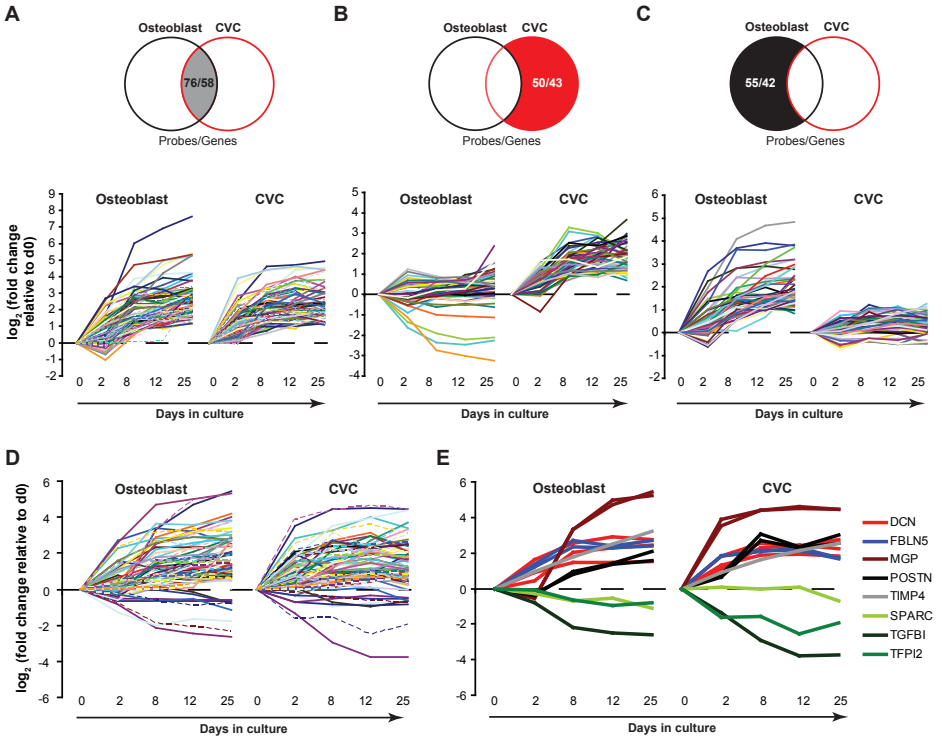

Figure 5. Expression pattern of differentially expressed extracellular region and ECM genes during CVC development and osteoblast differentiation. Temporal expression profile of extracellular region probes/genes present in cluster 1 and 2 (Figure 4) of **(A)** both cell types, **(B)** CVCs only and **(C)** osteoblasts only. **(D)** Expression profile of ECM probes/genes with identical regulation pattern in CVCs and osteoblasts. **(E)** Selection of ECM genes identically regulated in both cell types. Expression is plotted as $\log_2$ fold change relative to d0. Each line plotted represents a probe set. Probe/gene identifiers are provided in Supplementary Table 2 and 3.

genes from cluster 1 and 2 (Figure 4A and 4B) was similarly regulated by both cell types indicating a shared mechanism involving changes in the extracellular environment/matrix.

CVCs express a subset of extracellular matrix genes and genes involved in biomineralization.

Considering the relevance of the extracellular environment for osteoblast differentiation and mineralization, we analysed in greater detail the expression of genes linked to extracellular region present in cluster 1 and 2. Cluster 1 and 2 contained

in total 58 extracellular region genes (equivalent to 76 probes; Supplementary Table V, Chapter 7) overlapping in CVC and osteoblasts (Figure 5A). Expression pattern analyses of the cell type-specific genes from cluster 1 and 2 (43 and 42 for CVCs and osteoblasts respectively; Supplementary Table V) showed clearly distinct expression patterns for CVCs (Figure 5B) and osteoblasts (Figure 5C).

The observation that among the 58 extracellular region genes overlapping in CVCs and osteoblasts was a large subpopulation of ECM genes prompt us to identify differentially expressed ECM genes (GO:0031012) identically modulated in both cell types. From the 126 (160 probes) differentially expressed ECM genes in total 57 (76 probes) were identically modulated in CVCs and osteoblasts (Supplementary Table VI, Chapter 7). The expression pattern of these 57 genes is shown in Figure 5D. A selection from these ECM genes, DCN (decorin), FBLN5 (fibulin 5), MGP (matrix GLA protein), POSTN (periostin), TIMP4 (tissue inhibitor of metalloproteinase 4), SPARC (osteonectin), TGF-βI (transforming growth factor, beta-induced, 68kDa) and TFPI2 (tissue factor pathway inhibitor 2), is also shown in more detail in Figure 5E with some of them are already referenced with respect to bone biology.

In an alternative approach to compare osteoblasts and CVC we performed gene correlation analyses based on a priori selected GO-terms that are relevant for bone formation and mineralization. These GO-terms included among others biomineral tissue development, osteoblast differentiation and regulation of BMP signaling genes (see the full list of GO-terms analyzed in the Material & Methods section). To assess specificity, correlation analyses were also performed for a randomly selected set of expressed genes. Genes involved in biomineral tissue development (25 genes; Supplementary Table VII, Chapter 7) showed the highest correlation between CVCs and osteoblasts (r^2 = 0.31; Figure 6A) with an r^2 much higher than for a similar number of randomly selected expressed genes (r^2 = -0.29; Figure 6E). On the contrary, GO term such as regulation of osteoblast differentiation and BMP signaling failed to correlate CVCs and osteoblasts (Figure 6B and 6C). In Supplementary Figure IV (Chapter 7) the expression pattern of a selection of genes driving the correlation in the GO-term biomineral tissue development and the anti-correlation in the GO-term regulation of BMP signaling is shown. Altogether, our results demonstrate that a specific subset of extracellular genes, including ECM genes, together with genes involved in the regulation of mineralization represent a common denominator between CVCs and osteoblasts.

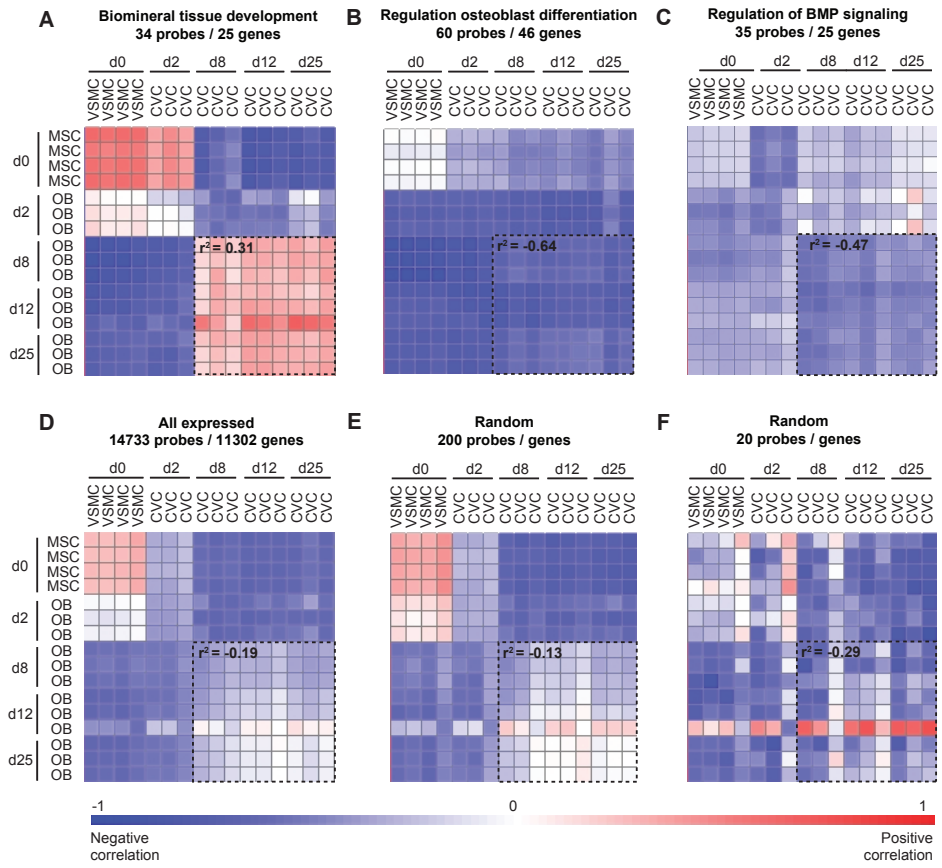

Figure 6. Pearson correlation plot of genes comprised within Gene Ontology (GO)-terms related to bone biology. VSMC/CVC and MSC/osteoblast are plotted against each other to determine their degree of similarity based on **(A)** biomineral tissue development, **(B)** regulation of osteoblast differentiation and **(C)** regulation of BMP signaling genes. As a reference, VSMC/CVC and MSC/osteoblast are also plotted considering **(D)** all expressed genes and **(E-F)** randomly selected genes. Dashed boxes highlight the correlation between CVCs and osteoblasts at day 8-25. Average correlation values (r^2) for this group of samples is shown within the dashed boxes; blue, negative correlation; red, positive correlation.

DISCUSSION

The current comparative global gene expression profiling analyses of osteoblasts and CVC demonstrate that VSMC under and osteogenic stimulus only partially mimic osteoblasts. Despite the fact that CVCs had an overall transcription profile

distinct from osteoblasts, the two cell types regulated identically a subset of ECM and biomineralization genes. These results support the hypothesis that VSMCs require specific osteoblast-related gene modulation and mechanisms to transdifferentiate into CVCs.

The mechanisms responsible for the transformation of a contractile VSMC into a stiff, mineral surrounded cell are still poorly understood. We demonstrated that the whole VSMCs pool has osteogenic potential and becomes ALP positive when exposed to osteogenic stimuli. This contradicts the concept that CVCs are derived from a specific VSMC subpopulation with osteogenic potential, as shown in other vascular calcification models[10, 14]. The relatively homogenous CVC population (based on ALP activity) observed in our study enabled us to use global gene expression profiles.

Genome-wide gene expression analyses in *in vitro* models of pathological and physiological mineralization revealed important characteristics of vascular calcifications. CVC development (and osteoblast differentiation) comprised three major phases. The first phase contained VSMC before being triggered to transdifferentiate (day 0; Figure 2). When VSMC were exposed to an osteogenic stimulus, their transcriptional program was quickly altered entering a transient intermediary stage (day 2; Figure 2) after which transcriptional changes became more subtle (day 8-25; Figure 2). We believe that the intermediary phase represents a commitment period responsible for the transition of VSMC into CVCs. In this respect, the clusters of genes identified to be down-regulated (cluster 4-6; Figure 5) were particularly interesting due to their annotation to GO-terms involved in the regulation of cell cycle, cell division and transcription. We believe that the modulation of genes with such functions is possibly associated to the switch of VSMC from proliferative into transdifferentiating cells[3-4], an effect observed in osteoblasts under the influence of glucocorticoids[22-23].

Regarding the comparative transcription profiling, we identified 57 ECM genes identically regulated by CVCs and osteoblasts. Their common modulation pattern strongly supports their structural and/or regulatory role in both forms of calcification. On the other hand, ECM genes that did not share identical expression in both cell types are likely to be less crucial for mineral deposition. However, ECM gene data is yet difficult to interpret since little is known about the function of most of the proteins encoded by these genes in matrix mineralization. Genes like DCN, MGP and POSTN constitute exceptions, being known for their crucial role during bone formation

and mineralization[8, 24-25]. MGP for example is a potent inhibitor of calcification both in bone and in the vasculature[8]. These genes represent a strong evidence for the implication of the other ECM genes, with yet unknown relationship to matrix mineralization, in vascular calcifications. This evidence is further substantiated by the fact that several ECM genes (e.g. FBLN5, POSTN, TIMP4) are targets of activin A, a potent inhibitor of ECM mineralization[26]. Recently we have identified over 1200 different proteins to be present in bone tissue[27]. It is conceivable that ECM proteins act in concert with each other and that the combination of ECM proteins eventually determine the extent of mineralization. It will be a great challenge to identify and characterize these interactions. The current study demonstrating only a limited overlap in ECM gene expression between osteoblasts and CVC will facilitate this challenge by enabling to focus on the selection of overlapping ECM genes. Additional studies focusing on this subset of genes are essential to prove their involvement in biomineralization and during the atherosclerotic process in particular.

Besides ECM, analysis of genes differentially regulated during physiological and pathological calcifications revealed that CVCs share specific genes related to the GO-term biomineral tissue development. ALPL (alkaline phosphatase), GPNMB (glycoprotein nmb), LEP (leptin), PTN (pleiotrophin) and SRGN (serglycin) were among genes within this GO-term that have been already studied in the context of tissue calcifications. ALPL has been shown to be fundamental for mineralization. This pyrophosphatase inactivates the mineralization inhibitory pyrophosphate[28] facilitating not only bone but also vascular calcifications[17, 19]. Together with ALPL, LEP and GPNMB are genes capable to promote calcifications. LEP is an energy metabolism hormone that enhances mineralization both in bone[29-30] and in vascular tissue[31] while GPNMB, is a glycoprotein implicated in end-stage renal disease (ESRD) a pathological condition associated to ectopic calcifications[32]. Biomineral tissue development genes did not include only genes favouring mineral deposition. SRGN was recently described as an inhibitor of osteoblast mineralization[33]. Despite not described with respect to ectopic mineralizations, the up-regulation of this gene during CVC development might represent a mechanism to protect the vasculature from calcifications similarly to what is described for MGP[15].

Our comparative gene expression profiling constitutes a powerful tool to identify novel targets to control physiological as well as pathological calcifications. Nevertheless, our bioinformatics approach was limited to the identification of genes currently annotated in GO databases as belonging to ECM or involved in

biomineralization. We hypothesize that more ECM and biomineralization genes are involved in both forms of calcification but because they are not yet annotated as such they were missed in our analysis.

Correlation analysis of bone-related genes expressed during VSMC transdifferentiation showed groups of genes negatively correlated between CVCs and osteoblasts, substantiating the uniqueness of the former cell type. For example, genes of the important osteoblast BMP/TGF-β/Activin signaling cascade (e.g. ACVR2A, GREM1, SMAD7) were oppositely regulated by CVCs and osteoblasts. The divergence of these genes in CVCs and osteoblasts supports the concept of cell-specific pathway modulations in both cell types. This is something recently observed in other tissues/cells[34-35] but not yet investigated with respect to medial vascular calcifications and bone. Nevertheless, BMP7 is a gene that appears to corroborate this concept since it is described as promoter of normal osteoblast function[36-37] and capable to prevent atherosclerosis[38-39]. More studies are needed to define the exact role of each of these genes and most importantly their cross-talk to other signaling pathways[40-41], like the Wnt signaling of which we have identified genes distinctly modulated between CVCs and osteoblasts (e.g. SOST and WNT5A).

Altogether, the different analyses support the hypothesis that VSMC transdifferentiate into CVCs keeping their own identity while using mechanisms that osteoblasts use to mineralize. Extracellular (matrix) genes and genes involved in tissue mineralization constituted important common denominators between pathological vascular and physiological bone calcifications. Furthermore, the fact that CVCs regulate genes distinctly from osteoblasts is interesting in the perspective that they might be subject to cell-specific pathway modulation opening the possibility to tackle undesired vascular transdifferentiation and calcification without affecting bone formation and *vice versa*.

Supplementary Data

Supplementary data available in Chapter 7.

MATERIAL & METHODS

Cell Culture. Human bone marrow-derived Mesenchymal Stem Cells (MSCs; PT-2501, Lonza, Walkersville, MD, USA) and Vascular Smooth Muscle Cells (VSMCs; coronary artery smooth muscle cells, CC-2583, Lonza) were

cultured as described previously[21]. Briefly, MSCs and VSMCs were expanded in Mesenchymal Stem Cell Basal Medium (MSCBM, PT-3238, Lonza) supplemented with Mesenchymal Stem Cell Medium SingleQuot Kit (MSCGM, PT-4105, Lonza) and Smooth muscle cell Basal Medium (SmBM, CC-3181, Lonza) supplemented with Smooth muscle Medium-2, SingleQuot Kit (SmGM-2, CC-4149, Lonza) respectively. For induction of MSCs differentiation into osteoblasts (referred also as MSC/osteoblasts) and VSMC development into CVCs (VSMC/CVC), cells were cultured in DMEM medium (GIBCO, Paisley, UK) containing 10% FCS, penicillin/streptomycin, 1.8 mM $CaCl_2$ (Sigma, St. Louis, MO, USA) and 20 mM HEPES (Sigma), pH 7.5. Additionally, this medium was freshly supplemented with 0.1 mM ascorbic acid (Sigma), 10 mM ß-glycerophosphate (Sigma) and 100 nM dexamethasone (DEX, Sigma).

Alkaline Phosphatase and protein concentration. ALP activity was assayed as described elsewhere[42]. Results were corrected for the protein content of the cell lysates. Protein concentration was determined using a BCA kit (Pierce Biotechnology, Rockford, IL, USA) following the manufacturers instructions.

Flow Cytometry analysis of ALP positive cell population. Cells were washed in PBS, trypsinized and fixed in 2% PFA for 10 min at room temperature. Cells were permeabilized in 90% ice-cold methanol and after re-suspension incubated for 10 min in blocking solution (PBS/0.5% BSA). Cells were probed with a primary monoclonal mouse antibody against Alkaline Phosphatase, Tissue Non-Specific (1:100, 1h; ab17973, Abcam). A goat anti-mouse IgG R-Phycoerythrin conjugated antibody (1:50, 30 min; M30004-1, Invitrogen, Camarillo, CA, USA) was used as a secondary antibody. Finally, cells were re-suspended in PBS and the ALP+ population was measured in the PE-A channel (excitation 488 nm) using a Becton Dickinson FACS-Canto (BD Biosciences).

RNA isolation and quantification. Total RNA was isolated using TRIzol (Invitrogen) according to the manufacturer's instructions. An additional step was introduced to remove calcium (derived from ECM). RNA was precipitated by overnight incubation with 4 M LiCl and 50 mM EDTA at –20°C. After precipitation and centrifugation for 30 min at 14,000 rpm and 4°C, the RNA pellet was washed four times with 70% ethanol and dissolved in H_2O. The RNA concentration was determined spectrophotometrically using a NanoDrop ND-2000 (Thermo Scientific, Wilmington, DE, USA) and its quality accessed by RNA 6000 Nano assay on a 21000 Bioanalyzer (Agilent Technologies, Santa Clara, CA, USA), both according

to the manufacturer's instructions.

Illumina gene chip-based expression. Gene-chip based expression was performed essentially as recently described[43] using 3 biological replicates per condition with exception for day 0 cultures for which 4 replicates were used. Briefly, 150 ng of RNA were amplified using the Illumina TotalPrep RNA Amplification kit (Ambion, Austin, TX, USA) as recommended by the manufacturer. Single-stranded cDNA was generated using a T7 oligo(dT) primer and was followed by second-strand cDNA synthesis. cDNA was further transcribed *in vitro* using a T7 RNA polymerase generating biotin-labeled cRNA. After cRNA purification its quality was checked on a Bioanalyzer (Agilent Technologies) and its concentration determined using a NanoDrop (Thermo Scientific). Per array, 750 ng of cRNA were hybridized, washed and detected using the standard Illumina protocol. Slides were scanned on an iScan and analyzed using Genome Studio v2010.1, both from Illumina.

Gene expression data processing. Gene expression data was processed as described elsewhere[43]. Raw gene expression data was background subtracted using Genome Studio and further processed using the Bioconductor R2.10.0 lumi-package[44]. The data was transformed by variance stabilization and quantile normalized. Probes significantly expressed (Illumina detection p-value<0.01) in at least 3 samples from VSMC/CVC and MSC/osteoblasts were considered as expressed and used for subsequent analysis, namely multivariate Principal Component Analysis (PCA). Probes differentially expressed relative to the starting culture condition, i.e. day 0 of culture, were identified using the Bioconductor package 'limma'[45] with adjusted p-values (q-value) to reduce the false discovery rate. Differential expression was considered whenever a probe had a $\log_2$ fold-change > 0.5 (up-regulation) or < -0.5 (down-regulation) relative to day 0 and a q-value <0.001.

Data analysis: clustering, correlation and functional annotations. Differentially expressed probes were analyzed by k-means clustering using Gene Pattern (http://www.broadinstitute.org/cancer/software/genepattern/)[46]. Independent clustering analyses were performed for CVCs and osteoblasts. The predictive power of k-means clustering was computed using FOM analysis in MultiExperiment Viewer v4.7 (http://www.tm4.org/mev/)[47]. The maximum number of clusters and iterations was set to 15 and 50 respectively. From the FOM results we opted for 6 clusters (k=6; Supplementary Figure III) in both cell types. Differentially expressed probes within each of the groups identified by k-means clustering for CVCs and osteoblasts were analyzed using DAVID Bioinformatics Resources 6.7 (http://david.

abcc.ncifcrf.gov/)[48] to obtain a comprehensive description of the over-represented biological processes, cellular compartments and molecular functions. Redundant GO-terms were removed using REViGO (http://revigo.irb.hr/)[49].

In an independent targeted analysis, we matched expressed probes to GO-terms related to bone biology (GO:0031012, ECM; GO:0031214, biomineral tissue development; GO:0030282, bone mineralization; GO:0001503, ossification; GO:0045667, regulation of osteoblast differentiation; GO:0051924, regulation of calcium ion transport; GO:0016462, pyrophosphatase activity; GO:0030510, regulation of BMP signaling pathway). The Illumina probe/gene symbol information underlying each GO-term was retrieved using the Martview query from the BioMart open source tool version 0.7 (http://www.biomart.org). Genes underlying these GO-terms were subsequently used for correlation analysis essentially as described elsewhere[27, 50]. Briefly, we calculated the geometric mean of the intensities for each expressed probe set. The level of expression of each probe set was then determined relative to this geometric mean. The expression values were logarithmically transformed (on a base 2-scale) to impute equal weight to gene-expression levels with similar relative distances to the geometric mean. Deviation from the geometric mean was considered as differential gene expression. Similarities and dissimilarities between VSMC/CVC and MSC/osteoblasts samples were visualized by Pearson's correlation using Omniviz (BioWisdom Inc., version 6.0.1). As a control, similar correlation analysis were performed using randomly selected sets of expressed probes containing similar number of genes as the GO-terms analyzed.

Data availability. The gene expression data here analyzed is publicly available and can be retrieved from the Gene Expression Omnibus (GEO) at the National Center for Biotechnology Information (NCBI) under the accession number GSE37558.

REFERENCES

[1] Hruska KA, *et al.* Bone morphogenetic proteins in vascular calcification *Circ Res* 2005, *97*, 105-14.

[2] Laurent S, *et al.* Aortic stiffness is an independent predictor of all-cause and cardiovascular mortality in hypertensive patients *Hypertension* 2001, *37*, 1236-41.

[3] Steitz SA, *et al.* Smooth muscle cell phenotypic transition associated with calcification: upregulation of Cbfa1 and downregulation of smooth muscle lineage markers *Circ Res* 2001, *89*, 1147-54.

[4] Thyberg J Differentiated properties and proliferation of arterial smooth muscle cells in culture *Int Rev Cytol* 1996, *169*, 183-265.

[5] Chen NX, *et al.* Annexin-mediated matrix vesicle calcification in vascular smooth muscle cells *J Bone Miner Res* 2008, *23*, 1798-805.

[6] Reynolds JL, *et al.* Human vascular smooth muscle cells undergo vesicle-mediated calcification in response to changes in extracellular calcium and phosphate concentrations: a potential mechanism for accelerated vascular calcification in ESRD *J Am Soc Nephrol* 2004, *15*, 2857-67.

[7] Persy V, *et al.* Vascular calcification and bone disease: the calcification paradox *Trends Mol Med* 2009, *15*, 405-16.

[8] Luo G, *et al.* Spontaneous calcification of arteries and cartilage in mice lacking matrix GLA protein *Nature* 1997, *386*, 78-81.

[9] Rekhter MD, *et al.* Type I collagen gene expression in human atherosclerosis. Localization to specific plaque regions *Am J Pathol* 1993, *143*, 1634-48.

[10] Bostrom K, *et al.* Bone morphogenetic protein expression in human atherosclerotic lesions *J Clin Invest* 1993, *91*, 1800-9.

[11] Dhore CR, *et al.* Differential expression of bone matrix regulatory proteins in human atherosclerotic plaques *Arterioscler Thromb Vasc Biol* 2001, *21*, 1998-2003.

[12] Schluesener HJ, *et al.* Immunolocalization of BMP-6, a novel TGF-beta-related cytokine, in normal and atherosclerotic smooth muscle cells *Atherosclerosis* 1995, *113*, 153-6.

[13] Towler DA, *et al.* Diet-induced diabetes activates an osteogenic gene regulatory program in the aortas of low density lipoprotein receptor-deficient mice *J Biol Chem* 1998, *273*, 30427-34.

[14] Watson KE, *et al.* TGF-beta 1 and 25-hydroxycholesterol stimulate osteoblast-like vascular cells to calcify *J Clin Invest* 1994, *93*, 2106-13.

[15] Moe SM, *et al.* Role of calcification inhibitors in the pathogenesis of vascular calcification in chronic kidney disease (CKD) *Kidney Int* 2005, *67*, 2295-304.

[16] Speer MY, *et al.* Inactivation of the osteopontin gene enhances vascular calcification of matrix Gla protein-deficient mice: evidence for osteopontin as an inducible inhibitor of vascular calcification in vivo *J Exp Med* 2002, *196*, 1047-55.

[17] Murshed M, *et al.* Unique coexpression in osteoblasts of broadly expressed genes accounts for the spatial restriction of ECM mineralization to bone *Genes Dev* 2005, *19*, 1093-104.

[18] Fleisch H, *et al.* Effect of pyrophosphate on hydroxyapatite and its implications in calcium homeostasis *Nature* 1966, *212*, 901-3.

[19] Lomashvili KA, *et al.* Phosphate-induced vascular calcification: role of pyrophosphate and osteopontin *J Am Soc Nephrol* 2004, *15*, 1392-401.

[20] Shanahan CM, *et al.* Medial localization of mineralization-regulating proteins in association with Monckeberg's sclerosis: evidence for smooth muscle cell-mediated vascular calcification *Circulation* 1999, *100*, 2168-76.

[21] Owens GK, *et al.* Molecular regulation of vascular smooth muscle cell differentiation in development and disease *Physiol Rev* 2004, *84*, 767-801.

[22] Engelbrecht Y, *et al.* Glucocorticoids induce rapid up-regulation of mitogen-activated protein kinase phosphatase-1 and dephosphorylation of extracellular signal-regulated kinase and impair proliferation in human and mouse osteoblast cell lines *Endocrinology* 2003, *144*, 412-22.

[23] Smith E, *et al.* Glucocorticoids inhibit developmental stage-specific osteoblast cell cycle. Dissociation of cyclin A-cyclin-dependent kinase 2 from E2F4-p130 complexes *J Biol Chem* 2000, *275*, 19992-20001.
[24] Horiuchi K, *et al.* Identification and characterization of a novel protein, periostin, with restricted expression to periosteum and periodontal ligament and increased expression by transforming growth factor beta *J Bone Miner Res* 1999, *14*, 1239-49.
[25] Mochida Y, *et al.* Decorin modulates collagen matrix assembly and mineralization *Matrix Biol* 2009, *28*, 44-52.
[26] Eijken M, *et al.* The activin A-follistatin system: potent regulator of human extracellular matrix mineralization *FASEB J* 2007, *21*, 2949-60.
[27] Alves RD, *et al.* Proteomic analysis of human osteoblastic cells: relevant proteins and functional categories for differentiation *J Proteome Res* 2010, *9*, 4688-700.
[28] Eaton RH, *et al.* Kinetic studies on the orthophosphatase and iorganic pyrophosphatase activities of human alkaline phsophatase *Enzymologia* 1968, *35*, 168-78.
[29] Pasco JA, *et al.* Serum leptin levels are associated with bone mass in nonobese women *J Clin Endocrinol Metab* 2001, *86*, 1884-7.
[30] Reseland JE, *et al.* Leptin is expressed in and secreted from primary cultures of human osteoblasts and promotes bone mineralization *J Bone Miner Res* 2001, *16*, 1426-33.
[31] Parhami F, *et al.* Leptin enhances the calcification of vascular cells: artery wall as a target of leptin *Circ Res* 2001, *88*, 954-60.
[32] Pahl MV, *et al.* Upregulation of monocyte/macrophage HGFIN (Gpnmb/Osteoactivin) expression in end-stage renal disease *Clin J Am Soc Nephrol* 2010, *5*, 56-61.
[33] Theocharis AD, *et al.* Serglycin constitutively secreted by myeloma plasma cells is a potent inhibitor of bone mineralization in vitro *J Biol Chem* 2006, *281*, 35116-28.
[34] Fessing MY, *et al.* BMP signaling induces cell-type-specific changes in gene expression programs of human keratinocytes and fibroblasts *J Invest Dermatol* 2010, *130*, 398-404.
[35] Morikawa M, *et al.* ChIP-seq reveals cell type-specific binding patterns of BMP-specific Smads and a novel binding motif *Nucleic Acids Res* 2011, *39*, 8712-27.
[36] Luo G, *et al.* BMP-7 is an inducer of nephrogenesis, and is also required for eye development and skeletal patterning *Genes Dev* 1995, *9*, 2808-20.
[37] Yeh LC, *et al.* Osteogenic protein-1 (OP-1, BMP-7) induces osteoblastic cell differentiation of the pluripotent mesenchymal cell line C2C12 *J Cell Biochem* 2002, *87*, 292-304.
[38] Davies MR, *et al.* BMP-7 is an efficacious treatment of vascular calcification in a murine model of atherosclerosis and chronic renal failure *J Am Soc Nephrol* 2003, *14*, 1559-67.
[39] Dorai H, *et al.* Bone morphogenetic protein-7 (osteogenic protein-1) inhibits smooth muscle cell proliferation and stimulates the expression of markers that are characteristic of SMC phenotype in vitro *J Cell Physiol* 2000, *184*, 37-45.
[40] Guo X, *et al.* Signaling cross-talk between TGF-beta/BMP and other pathways *Cell Res* 2009, *19*, 71-88.
[41] Nakashima A, *et al.* Cross-talk between Wnt and bone morphogenetic protein 2 (BMP-2) signaling in differentiation pathway of C2C12 myoblasts *J Biol Chem* 2005, *280*, 37660-8.
[42] Eijken M, *et al.* The essential role of glucocorticoids for proper human osteoblast differentiation and matrix mineralization *Mol Cell Endocrinol* 2006, *248*, 87-93.
[43] Drabek K, *et al.* GPM6B regulates osteoblast function and induction of mineralization by controlling cytoskeleton and matrix vesicle release *J Bone Miner Res* 2011, *26*, 2045-51.
[44] Du P, *et al.* lumi: a pipeline for processing Illumina microarray *Bioinformatics* 2008, *24*, 1547-8.
[45] Smyth GK Linear models and empirical bayes methods for assessing differential expression in microarray experiments *Stat Appl Genet Mol Biol* 2004, *3*, Article3.
[46] Reich M, *et al.* GenePattern 2.0 *Nat Genet* 2006, *38*, 500-1.
[47] Yeung KY, *et al.* Validating clustering for gene expression data *Bioinformatics* 2001, *17*, 309-18.

[48] Dennis G, Jr., *et al.* DAVID: Database for Annotation, Visualization, and Integrated Discovery *Genome Biol* 2003, *4*, P3.
[49] Supek F, *et al.* REVIGO summarizes and visualizes long lists of gene ontology terms *PLoS One* 2011, *6*, e21800.
[50] Valk PJ, *et al.* Prognostically useful gene-expression profiles in acute myeloid leukemia *N Engl J Med* 2004, *350*, 1617-28.

Chapter 6

General Discussion

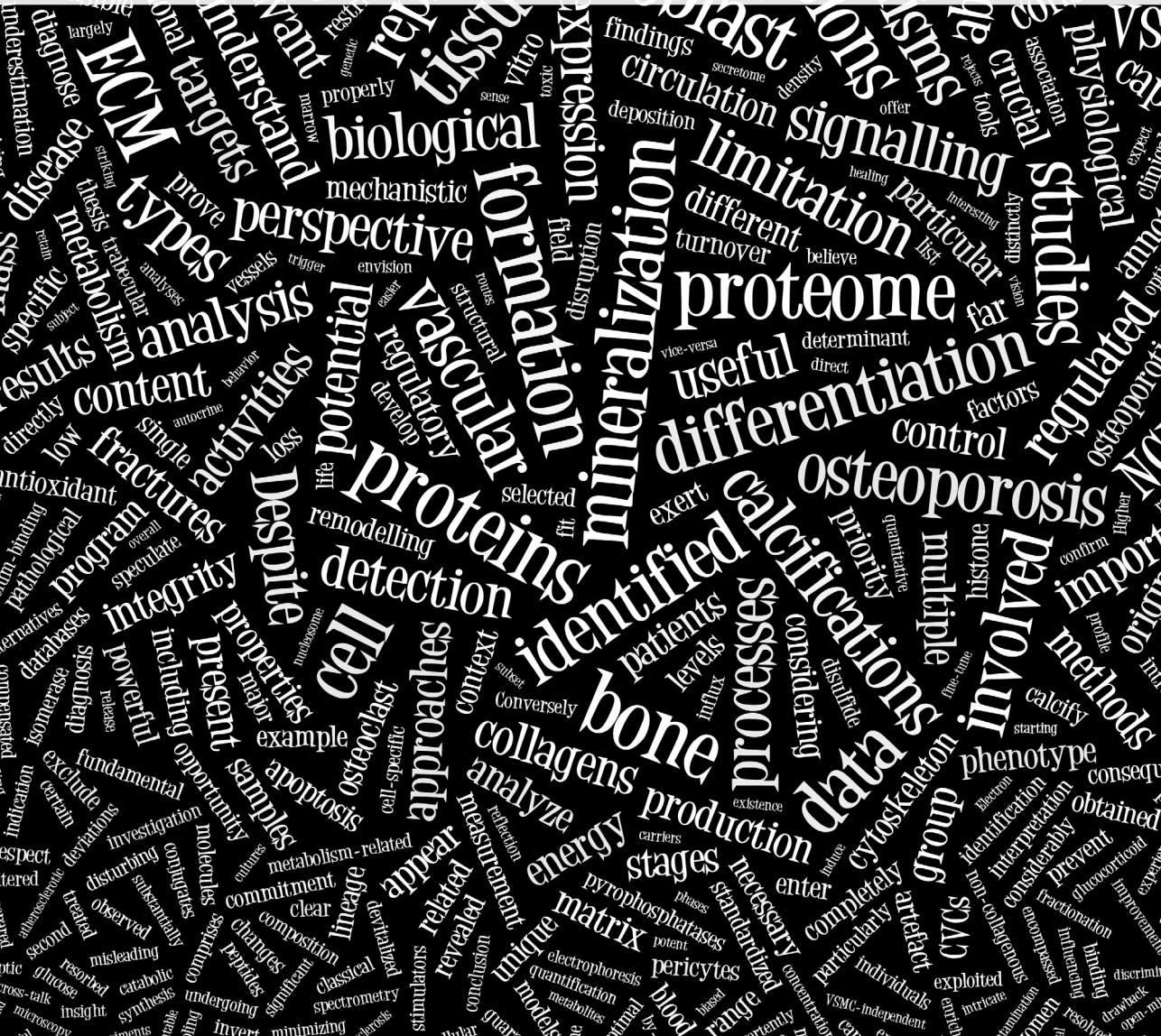

6.1 OSTEOPOROSIS, CHALLENGES AND OPPORTUNITIES

Current therapies in osteoporosis only prevent further degradation of the bone tissue without restoring the bone mass lost before diagnosis of disease. Two major challenges are posed by these facts. The first one is to diagnose osteoporosis at an early stage by optimizing the sensitivity of the diagnostic methods. Although bone mineral density (BMD) is a strong predictor of osteoporosis only about half of the patients are diagnosed with osteoporosis based on their BMD levels[1]. As a result most fractures occur in individuals that do not have low BMD, i.e. not below the 2.5 standard deviations from average peak bone mass of young healthy adults defined by the World Health Organization (WHO) as the diagnosis criteria for osteoporosis[2]. The second challenge is to invert the therapeutic approach in osteoporosis providing alternatives capable of restoring the bone mass lost. Consequently, mechanistic understanding of bone formation is crucial to tackle both of these clinical limitations and to develop (1) therapies promoting bone formation and (2) novel diagnostic biomarkers for osteoporosis.

6.2 BONE FORMATION PROTEOME

In this thesis we have exploited the powerful analytical properties of MS-based proteomics in the context of bone research with particular focus on osteoblasts and the bone formation process. High-throughput proteomics tools were applied for the analysis of osteoblast proteomes during *in vitro* differentiation and mineralization (**Chapter 2 and 3**). In addition, we characterized the protein content of human bone tissue (**Chapter 4**). The overlap between the different datasets, osteoblast differentiation, osteoblast extracellular matrix (ECM) and matrix vesicles (MVs), and bone tissue comprises 88 proteins representing the bone formation proteome (Figure 1).

In our perspective, this type of analysis is crucial to understand the mechanisms behind *in vitro* osteoblast differentiation and their impact on *in vivo* bone formation. The data shown is the first step to identify regulatory targets for bone formation (discussed below in section 6.3 and 6.4). In section 6.5 we also discuss the application of these results in a diagnostic setting to select candidate biomarkers for osteoporosis.

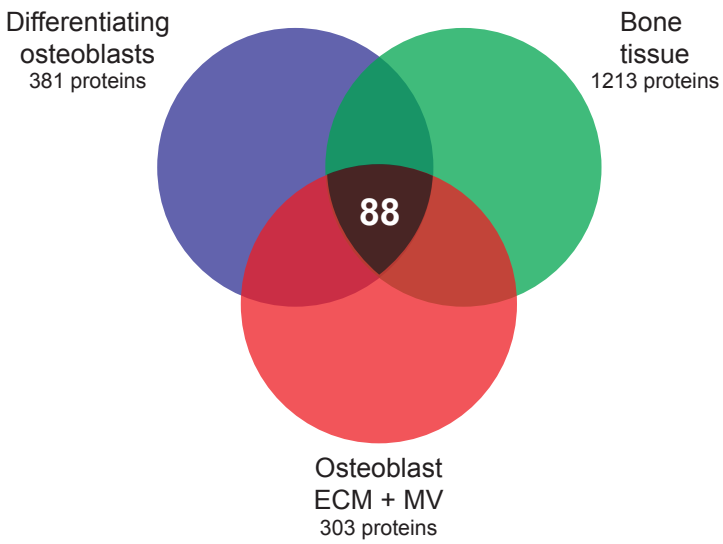

Figure 1. Bone formation proteome. Overlap of proteins expressed in differentiating osteoblasts (381 proteins; Chapter 2), osteoblast ECM+MV (303 proteins; Chapter 3) and bone tissue (1213 proteins; Chapter 4).

6.3 BONE FORMATION PROTEOME: KNOWN OSTEOBLASTS PROTEINS AND MECHANISMS

The bone formation proteome defined by our different studies contains proteins involved in multiple biological processes and molecular functions (Table 1). In physiologic conditions the production of an ECM and the capability to mineralize it is virtually restricted to osteoblasts. The bone formation proteome contained proteins directly related to these unique biological functions of the osteoblasts including ECM proteins and proteins involved in mineralization.

Regarding ECM proteins our methods proved to be limited for the detection of collagens (see further discussion in section 6.6) being restricted to the analysis of the non-collagenous proteins (NCPs). Despite having identified classical bone NCPs, such as SPP1, SPARC, BGN, MGP, FN1, these were far from being high abundant in bone tissue (**Chapter 4, Figure 2**). Moreover, in most cases they were not detectable at all in osteoblast bone formation models (**Chapter 2 and Chapter 3**). This fact is summarized in Table 1, where ECM or ECM-related terms do not appear among the most over-represented in the bone formation proteome depicted in Figure 1.

Table 1. Over-represented biological processes and molecular functions in the bone formation proteome. Bioinformatics analyses of the 88 proteins shown in Figure 1 were done as described in Chapters 2, 3 and 4. Only significant Gene Ontology (GO) terms (Bonferroni p<0.05) are shown.

Molecular Function	# proteins	Fold Enrichment
Protein disulfide isomerase activity (GO:0003756)	4	69.52
Unfolded protein binding (GO:0051082)	10	13.60
Actin binding (GO:0003779)	14	6.72
Cytoskeletal protein binding (GO:0008092)	15	4.66
Calcium ion binding (GO:0005509)	17	2.89
Biological Process	**# proteins**	**Fold Enrichment**
Alcohol catabolic process (GO:0046164)	9	17.89
Regulation of apoptosis (GO:0042981)	21	4.21
Carbohydrate catabolic process (GO:0016052)	9	13.30
Protein folding (GO:0006457)	9	8.19
Actin filament-based process (GO:0030029)	10	6.68
Generation of precursor metabolites and energy (GO:0006091)	11	5.66
Cell redox homeostasis (GO:0045454)	6	15.34

We cannot exclude that ECM proteins might be underestimated due to what is annotated in the databases as ECM proteins. Under certain physiological conditions, proteins within a cell move between different compartments. In bone cells apoptosis (Table 1) could be one condition contributing for intracellular proteins to end up in the extracellular space. Programmed cell death is an integral part of osteoblast differentiation and responsible for controlling the activities of osteoblasts[3-4]. It is possible that after apoptosis many proteins become part of the ECM due to their affinity to other proteins or mineral present there[5-6]. The function of these proteins in bone can be structural, conferring bone tissue with the mechanical properties and quality necessary to exert its functions properly. However, their involvement in regulatory functions would not be surprising considering that apoptosis itself is a mechanism that regulates the bone remodeling balance[7-8].

Mineral deposition during bone formation is dependent on specific proteins that can carry this function. Regarding these, we identified calcium-binding proteins to be among the most over-represented in the bone formation proteome (Table 1). Annexins are a particularly relevant example, being abundant in human bone tissue (**Chapter 4, Figure 4**) and regulated during osteoblast differentiation (**Chapter 2, Table 2**). These proteins are key factors for MV-mediated mineralization, promoting the influx of calcium into these vesicles[9-11] during the last stages of osteoblast

differentiation. Pyrophosphatases and phosphatases represent another class of proteins important for mineralization providing the phosphate that conjugates with calcium for hydroxyapatite formation. Despite not represented in Table 1, many pyrophosphatases were high abundant in the bone tissue (**Chapter 4, Figure 4**).

6.4 BONE FORMATION PROTEOME: NOVEL REGULATORY PROCESSES

Only a small proportion of the bone formation proteome has been studied in the bone field. Conversely, many of the molecular functions and biological processes highlighted in Table 1 can not yet be understood in a functional perspective in bone. In this respect, proteins with disulfide isomerase activity are a good example. Not much is known about the role of this protein family during bone formation but the skeletal phenotype of protein disulfide isomerase A3-defient mice[12] is consistent with an important role of this group of proteins in bone homeostasis.

Cytoskeleton, cytoskeleton binding, antioxidant and energy metabolism-related proteins are important for the integrity of any cell type or tissue in the organisms. The fact that these proteins appear over-represented in differentiating osteoblasts and bone tissue is a clear indication of their specific involvement in bone formation.

Cytoskeletal changes are on the basis of osteoblast lineage commitment[13-14] and the cytoskeleton itself is an intermediary for signals coming from the ECM influencing gene expression and cell behaviour[15-16]. In this context, data from our laboratories identified cytoskeleton organization as a fundamental aspect for MV release during the mineralization period of osteoblast differentiation[17].

The bone formation proteome encompassed several proteins involved in catabolic pathways responsible for the synthesis of energy from carbohydrates (glucose) or alcohol (Table 1). It is tempting to speculate that the detection of these proteins and their enrichment is related to the high metabolic activity of bone. Bone tissue is constantly being broken down and re-built throughout life by processes requiring significant amounts of energy[18]. One consequence of increasing the energy metabolism is the production of toxic by-products, namely reactive oxygen species (ROS)[19]. According to our proteome data, osteoblasts and bone appear to be well prepared to control the levels of ROS. During osteoblast differentiation antioxidant proteins were regulated (**Chapter 2, Table 2**), proteins that were also found in bone tissue as high abundant (**Chapter 4, Figure 4**). Despite highlighting antioxidant proteins as proteins that fit particularly well in a role to preserve bone tissue integrity,

we do not exclude their direct involvement in the regulation of bone formation[20-21] or resorption[22-23].

The findings discussed above illustrate the uniqueness of our proteomics approaches to study bone formation. The main challenge now is data interpretation to decipher the exact role of each protein identified, coupling functionally unknown biological process and molecular functions to known ones in the context of bone formation. Despite the limitations inherent to proteomics analysis (discussed in detail in section 6.6) we revealed new aspects of the bone formation contributing for the mechanistic understanding of this process.

6.5 THE BONE PROTEOME: A SOURCE OF BONE DISEASE BIOMARKERS

The organic part of bone tissue is defined in bone biology textbooks as collagen proteins plus a handful of NCPs[24]. The bone tissue proteome (**Chapter 4**) shows that this definition can be misleading and depreciative for the NCP content of bone. Even though it represents only 10% of total bone protein content, the range of NCPs identified is vast (1213 proteins; **Chapter 4, Figure 4**). Furthermore, osteoblasts were not the unique source of NCPs in trabecular bone. Other cell types and tissues, namely erythrocytes and blood plasma, contribute significantly for the NCP content of this type of bone tissue (**Chapter 4, Figure 2**). We hypothesize that the non-bone derived protein content is a reflection of the intimacy between trabecular bone, surrounding bone marrow and blood vessels[24], thus likely to differ considerably from cortical bone tissue. The functions of these proteins in bone are largely unknown, like for most of the other NCPs identified. However, we envision that they might fit into two functional categories, regulatory proteins involved in the modulation of bone modeling and remodeling and/or structural proteins conferring bone tissue with the mechanical properties necessary to exert its functions properly.

Independent of their origin or function any bone protein identified represents a potential biomarker for bone turnover. In Figure 2 we illustrate the central role of the bone proteome to delineate a strategy for identification of potential biomarkers for bone turnover in osteoporosis. The main assumption of our approach was that bone resorbed and lost should end up invariably in the circulation (Figure 2A). With this in mind, we needed to know (1) which proteins are present in bone that could enter the circulation and (2) which proteins are present in the circulation that could have

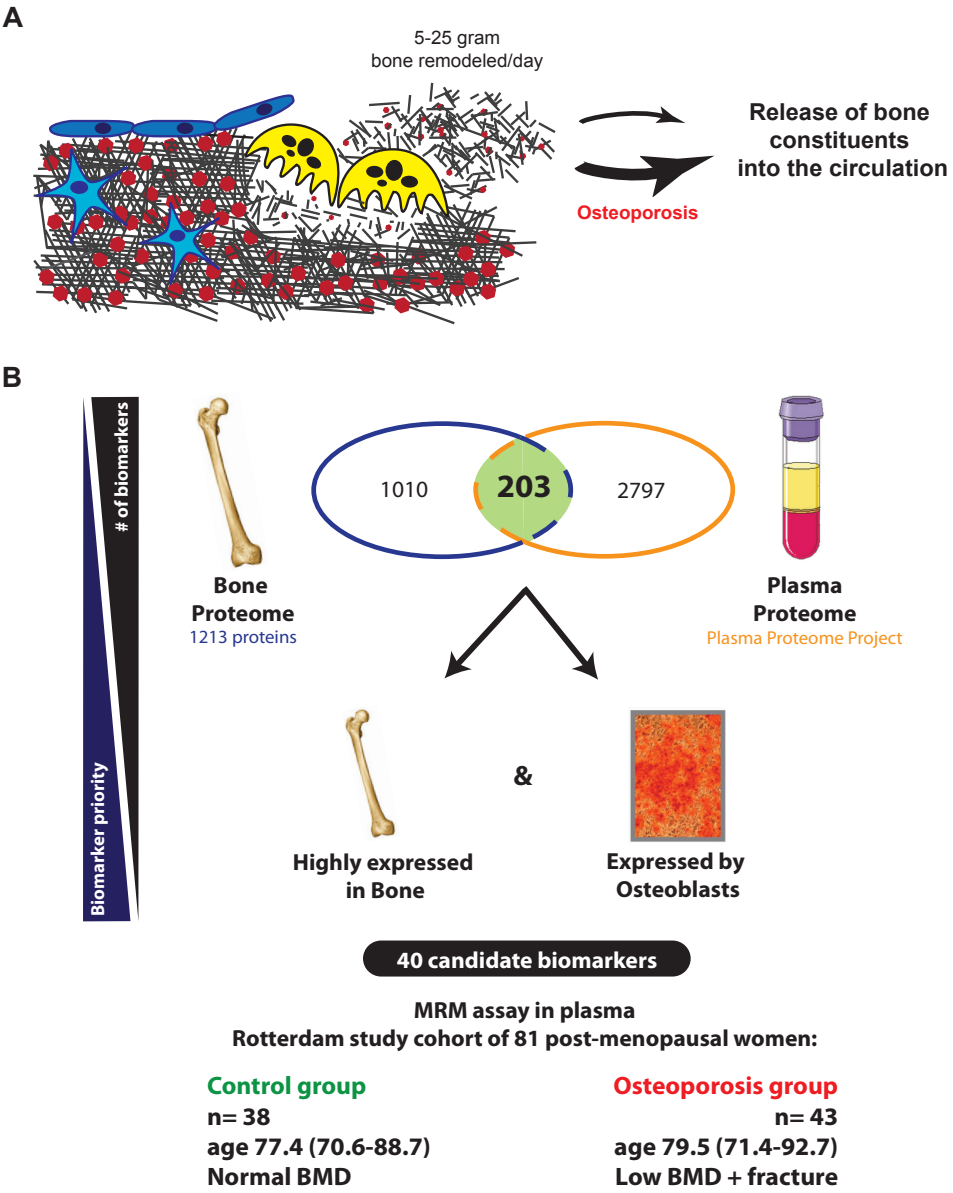

Figure 2. Concept and strategy for identification of potential biomarkers for bone turnover in osteoporosis. **(A)** Bone is continuously being renewed and as a consequence many bone constituents (including proteins) are released into the plasma every day. In osteoporotic conditions the release of bone material into circulation is expected to be significantly enhanced. **(B)** Selection of candidate biomarkers of bone loss based on bone and plasma proteomes.

its origin in bone. For the first part we had the bone proteome data (1213 proteins; **Chapter 4**) and for the latter we used Plasma Proteome Project data containing over 3000 proteins detectable in plasma[25].

The plasma proteome present in bone, i.e. the overlap between bone and plasma, contained 203 proteins. However, screening 203 proteins in plasma with the current methods, mass spectrometry (MS) or ELISA, is not feasible. To reduce further the number of potential biomarkers we established a priority list for these proteins (Figure 2B). Higher priority was given to proteins that had the highest expression in bone and because of that are more likely to be detectable in plasma. In addition, priority was also given to proteins expressed by osteoblast at the transcript level (mRNA array data not shown in this thesis) increasing the likelihood that their origin is the bone tissue. From the priority list we selected 40 proteins to profile in a cohort of plasma samples from post-menopausal women (participants in the Rotterdam Study) with two extreme bone phenotypes, a control group (n=38) having normal BMD without history of fractures and an osteoporotic group (n=43) having low BMD with history of fractures (Figure 2B). Measurement of these proteins in plasma will be done using Multiple Reaction Monitoring (MRM) assays, powerful MS-based assays allowing quantitative measurement of target proteins. With this approach we expect to obtain more insight whether any of these proteins or group of proteins could be useful to diagnose bone loss associated to osteoporosis (see future perspectives in paragraph 6.9). Additionally these proteins might also be useful in the clinic to monitor bone mass loss in patients undergoing long-term glucocorticoid therapy[26-27] and other metabolic bone disorders.

6.6 LIMITATIONS OF THE MS-APPROACHES: ARTEFACT OR BIOLOGY?

MS-based methods to analyze protein expression in biological samples offer the opportunity to identify and quantify an unprecedented number of proteins in single analyses. However, MS approaches in proteomics do have their own limitations and we have directly experienced some of them.

The proteome of biological samples – cells, tissues or body fluids – is extremely complex and cannot be completely resolved by MS-based proteomics approaches yet. However, minimizing this limitation is possible as shown by our studies. Analyzing sub-cellular proteomes of interest, ECM and MVs, with extensive protein fractionation, e.g. gel electrophoresis, revealed to be good solutions enabling the

detection and quantification of 100s (**Chapter 3**) or even 1000s of proteins (**Chapter 4**). Despite the improvement, we recognize that the protein information still missing is determinant to mechanistically understand bone formation. As an example, we were limited in the identification of cytokines and growth factors, signaling molecules whose usual low abundance poses major challenges for detection.

Another limitation of our studies was the underestimation of collagen abundance. Collagens constitute 90% of the total bone protein content[28], something we could not confirm due to the suboptimal cleave of collagens by trypsin. However, we believe that this limitation constituted inadvertently an advantage. The absence of tryptic peptides from high abundant collagens reduced substantially the complexity and dynamic range of peptide concentrations in the samples rendering an easier detection of NCPs.

Interpretation of biological data represents an important aspect to consider while analyzing proteomics data. Protein databases and bioinformatics analysis are helpful to analyze proteomics data but simultaneously biased to what is known so far for the proteins annotated. Many proteins identified in bone tissue (**Chapter 4, Figure 4**) predominantly constituted by ECM and in osteoblast ECM (**Chapter 3, Figure 3**) are not annotated as such. We cannot rule out that these proteins constitute an artefact from intracellular protein contamination. However, it would not be surprising if many of them are truly ECM components containing relevant biological information. This is best illustrated by histone H4 one of the most abundant proteins in bone (**Chapter 4, Figure 2 and 3**). Annotated to the nucleosome complex, histones are also reported to be extracellularly expressed and functional[5, 29-30]. Despite not being able to disclose if histone H4 (and other proteins) expression in bone is an artefact or biology, this result highlights the importance of analyzing proteomics data in an open-minded perspective, considering that for most of the proteins much information is still unknown.

Proteomics analyses (**Chapter 2-4**) were far more challenging than gene expression analysis (**Chapter 5**) due to the lack of standardized analytical methods. However, this drawback is compensated by the fact that protein data is closer to function and phenotype than transcript data, having a greater potential to disclose relevant biological information. This is also the case in the bone field where growing interest in proteomics research might be crucial to understand bone remodeling and to identify biochemical markers of bone disease.

6.7 ACTIVIN SIGNALING IN OSTEOBLAST FATE AND FUNCTION

Activin A is responsible for the inhibition of osteoblast differentiation and mineralization[31-32]. In **Chapter 3** we extended the comprehension about the activin A effects in osteoblast differentiation demonstrating that activin signaling targets ECM maturity (**Figure 2 and Table 1**) disturbing the subsequent mineralization period with impairment of MV secretion (Figure 4).

The activin effect in the ECM composition was relatively mild. If it is true that a broad range of proteins was altered, it is also true that there was no profound disruption of a specific protein or group of proteins (**Chapter 3, Table 1**). Still, the effects on the phenotype were striking supporting the relevance of the ECM compartment as a whole, with small changes to several ECM proteins being possibly more detrimental for osteoblast mineralization than disruption of one single protein at a time. This might represent a protective mechanism to guarantee the stability of bone metabolism and bone tissue in the event of single gene mutations. In this scenario, other proteins with overlapping functions in the ECM are able to compensate for the protein loss without complete disruption of the skeletal integrity needed for life.

The fact that activin A treated osteoblasts had impaired MV biogenesis explains the inability of activin A cultures to mineralize. Being osteoblast differentiation a sequential order of interrelated phases[33], MV impairment is likely to be mediated by the primary negative effect of activin A on ECM maturity. However, devitalization experiments showed that other factors are also involved. The same devitalized activin A ECM that did not become mineralized (**Chapter 3, Figure 1**) was capable to induce MSC osteoprogenitor mineralization (**Chapter 3, Figure 5**) stimulating MV production (preliminary data not shown). Altogether, our data put forward the mechanism that the lack of MV production and mineralization in activin A treated osteoblasts results from the capacity that these cells have to sense altered self-made ECM. This hypothesis is supported by epigenetics and how cells integrate their genetic programs to environmental clues[34]. In osteoblasts, such behavior could prevent them from entering the high energy demanding later stages of differentiation[35], i.e. MV production and mineralization, in the presence of a suboptimal ECM that does not guarantee bone tissue quality.

Studying ECM composition and maturity is of particular relevance for regenerative medicine. Proteins regulated by activin A in the ECM constitute

potential targets to modulate MSC commitment towards the osteogenic lineage holding the perspective to enhance considerably the regeneration of bone tissue from damage.

6.8 PATHOLOGICAL VASCULAR VS. PHYSIOLOGICAL BONE CALCIFICATIONS

In **Chapter 5**, we characterized vascular calcifications comparing them to bone formation and mineralization. Transdifferentiating VSMC did not need to enter an osteogenic-like transcriptional program to develop into CVC (**Chapter 5, Figure 2**) and only a limited number of extracellular (matrix) and biomineralization genes did appear to be important for both CVCs and osteoblasts (**Chapter 5, Figure 5 and 7**).

The data obtained rejects the idea that pathological VSMC derived calcification is overall analogous to osteoblast differentiation and mineralization (reviewed by Persy and D'Haese[36]). We believe that this conflicting data is related to the existence of multiple cells in the vasculature that are able to calcify, namely VSMC[37-38] and pericytes[39-40]. Both cell types are thought to be of MSC origin[41-42] but while VSMC are in a differentiated state, pericytes retain their pluripotency being capable of differentiating into multiple cell lineages, including the osteogenic[43-44]. In this respect, pericytes are closer to MSC than VSMC and better positioned to calcify using similar mechanisms as these osteoprogenitor cells. To make things even more complicated, circulating (osteo)progenitor cells have recently been conjectured to take part in vascular calcifications[45-47]. These cells are mobilized to sites of fracture contributing for fracture healing[48-49] but are also involved in vascular ossifications of end stage aortic valve disease[50]. We speculate that these cells might be increased in the circulation when active resorption takes place perhaps explaining the increased risk for atherosclerosis observed in osteoporotic patients[51].

Altogether our results corroborate the general idea that vascular calcification is a cell mediated process. The fact that CVCs did not completely share the transcriptional program of osteoblasts is interesting in the perspective that they might be subject to cell-specific modulation. Some of the distinctly regulated genes participate in pathways crucial for osteoblast differentiation and mineralization (e.g., BMP signaling, **Chapter 5, Figure 6**) supporting the idea that not all bone mineralization-related genes are necessary to trigger vascular calcifications. This

observation depicts the intricate mechanisms behind mineral deposition in vascular tissues and opens the possibility to target undesired vascular calcifications without disturbing physiologic bone formation and *vice versa*. Despite containing therapeutic potential, this possibility is likely to be far from the *in vivo* situation since in our vision VSMC represent only one of the multiple routes accountable for vascular calcification. More investigation is needed to define the role of VSMC during *in vivo* vascular calcification including possible interactions with the other cell types present in the vessel wall that are capable to mineralize. These studies are likely to unveil intervention targets for pathological calcifications and help to explain their association to osteoporosis.

6.9 FINAL CONCLUSION AND FUTURE PERSPECTIVES

In conclusion, our studies illustrated osteoblast differentiation and bone formation from a proteomics perspective. The protein data obtained form a rich library of targets for researchers in the bone field investigating new modulators of bone formation. Moreover, the data will be a valuable tool to understand molecular mechanisms used by molecular stimulators (e.g. dexamethasone) or inhibitors (e.g. activin A) of osteoblast differentiation and mineralization. Because osteoblasts cross-talk with osteoclasts, many of the proteins identified are also likely to be determinant of osteoclast activities. Despite not being part of our studies, studying the osteoclast proteome remains fundamental to understand bone resorption, coupling between osteoclast and osteoblast activities and thereby the control of bone turnover and metabolism.

The bone tissue proteome data was a strategic complement for the *in vitro* studies constituting a library of potential biomarkers for bone diseases. Forty proteins detected in bone are currently being surveyed in the blood plasma of healthy vs. osteoporotic post-menopausal women. If these proteins can discriminate healthy from osteoporotic patients they could become useful diagnostic markers for osteoporosis with at least similar predictive power as BMD measurements.

Our findings about osteoinductive properties of the osteoblast ECM are of particular interest in regenerative medicine. The proteins of this ECM represent a source of potent signals that control the activity of osteoprogenitor cells modulating their bone formation and mineralization capacity. Identifying which signals are most relevant is now the challenge but the proteins we identified to be modulated

by activin A signaling represent a good starting point. Regarding the inhibitory effect of activin A on mineralization we showed that it was due to impaired MV biogenesis. The role of these vesicles in biomineralization is clear but we hypothesize their functions could go beyond that. MVs could function as carriers of signaling clues (i.e. proteins, microRNAs, hormones and other metabolites) in an autocrine, paracine or even endocrine fashion. Despite the recent findings demonstrating that MVs carry molecules compatible with these signaling functions[52-53] more studies are needed to prove that indeed they exert them. Electron microscopy analysis revealed that osteoblasts secrete a heterogenic population of vesicles (data not shown). This suggests that besides MVs other types of vesicles, e.g. exosomes, should be considered when studying the osteoblast secretome[54].

Regarding our studies on vascular calcification we found that primary VSMC were able to calcify using specific osteoblast mechanisms sharing the expression of extracellular (matrix) genes and genes involved in biomineralization. Additional studies focusing on this subset of genes are essential to prove their involvement in biomineralization and during the atherosclerotic process in particular. But not only the genes commonly regulated by CVCs and osteoblasts deserve attention. Genes distinctly regulated by both cell types have the potential to fine-tune vascular/bone cell physiology in a cell-specific manner. Therefore, tackling VSMC-dependent vascular calcifications without compromising bone mineralization and *vice versa* might be possible. Despite promising, this possibility has to be carefully examined since processes that are relevant for mineralization in one cell type might be irrelevant at all in the other and because vascular calcifications can be originated by other cell types or by VSMC-independent mechanisms.

REFERENCES

[1] Garnero P, *et al.* Contribution of bone mineral density and bone turnover markers to the estimation of risk of osteoporotic fracture in postmenopausal women *J Musculoskelet Neuronal Interact* 2004, *4*, 50-63.

[2] Kanis JA, *et al.* The diagnosis of osteoporosis *J Bone Miner Res* 1994, *9*, 1137-41.

[3] Hock JM, *et al.* Osteoblast apoptosis and bone turnover *J Bone Miner Res* 2001, *16*, 975-84.

[4] Jilka RL, *et al.* Increased bone formation by prevention of osteoblast apoptosis with parathyroid hormone *J Clin Invest* 1999, *104*, 439-46.

[5] Henriquez JP, *et al.* Extracellular matrix histone H1 binds to perlecan, is present in regenerating skeletal muscle and stimulates myoblast proliferation *J Cell Sci* 2002, *115*, 2041-51.

[6] Termine JD, *et al.* Mineral and collagen-binding proteins of fetal calf bone *J Biol Chem* 1981, *256*, 10403-8.

[7] Hughes DE, *et al.* Apoptosis in bone physiology and disease *Mol Pathol* 1997, *50*, 132-7.

[8] Manolagas SC Birth and death of bone cells: basic regulatory mechanisms and implications for the pathogenesis and treatment of osteoporosis *Endocr Rev* 2000, *21*, 115-37.

[9] Arispe N, *et al.* Similarity in calcium channel activity of annexin V and matrix vesicles in planar lipid bilayers *Biophys J* 1996, *71*, 1764-75.

[10] Kirsch T, *et al.* The roles of annexins and types II and X collagen in matrix vesicle-mediated mineralization of growth plate cartilage *J Biol Chem* 2000, *275*, 35577-83.

[11] Anderson HC, *et al.* The role of matrix vesicles in growth plate development and biomineralization *Front Biosci* 2005, *10*, 822-37.

[12] Wang Y, *et al.* Disruption of Pdia3 gene results in bone abnormality and affects 1alpha,25-dihydroxy-vitamin D3-induced rapid activation of PKC *J Steroid Biochem Mol Biol* 2010, *121*, 257-60.

[13] Higuchi C, *et al.* Transient dynamic actin cytoskeletal change stimulates the osteoblastic differentiation *J Bone Miner Metab* 2009, *27*, 158-67.

[14] Oh S, *et al.* Stem cell fate dictated solely by altered nanotube dimension *Proc Natl Acad Sci U S A* 2009, *106*, 2130-5.

[15] Bidwell JP, *et al.* Nuclear matrix proteins and osteoblast gene expression *J Bone Miner Res* 1998, *13*, 155-67.

[16] Lelievre S, *et al.* Extracellular matrix signaling from the cellular membrane skeleton to the nuclear skeleton: a model of gene regulation *Recent Prog Horm Res* 1996, *51*, 417-32.

[17] Drabek K, *et al.* GPM6B regulates osteoblast function and induction of mineralization by controlling cytoskeleton and matrix vesicle release *J Bone Miner Res* 2011, *26*, 2045-51.

[18] Karsenty G, *et al.* The central regulation of bone mass, the first link between bone remodeling and energy metabolism *J Clin Endocrinol Metab* 2010, *95*, 4795-801.

[19] Droge W Free radicals in the physiological control of cell function *Physiol Rev* 2002, *82*, 47-95.

[20] Mody N, *et al.* Oxidative stress modulates osteoblastic differentiation of vascular and bone cells *Free Radic Biol Med* 2001, *31*, 509-19.

[21] Nicolaije C, *et al.* Decreased oxygen tension lowers reactive oxygen species and apoptosis and inhibits osteoblast matrix mineralization through changes in early osteoblast differentiation *J Cell Physiol* 2012, *227*, 1309-18.

[22] Garrett IR, *et al.* Oxygen-derived free radicals stimulate osteoclastic bone resorption in rodent bone in vitro and in vivo *J Clin Invest* 1990, *85*, 632-9.

[23] Koh JM, *et al.* Homocysteine enhances bone resorption by stimulation of osteoclast formation and activity through increased intracellular ROS generation *J Bone Miner Res* 2006, *21*, 1003-11.

[24] Baron R In *Primer on the metabolic bone diseases and disorders of mineral metabolism.*; 6th ed.; Favus MJ, Ed.; The American Society for Bone and Mineral Research: Washington D.C., 2006.

[25] Omenn GS, *et al.* Overview of the HUPO Plasma Proteome Project: results from the pilot phase with 35 collaborating laboratories and multiple analytical groups, generating a core dataset of 3020 proteins and a publicly-available database *Proteomics* 2005, *5*, 3226-45.
[26] Adinoff AD, *et al.* Steroid-induced fractures and bone loss in patients with asthma *N Engl J Med* 1983, *309*, 265-8.
[27] LoCascio V, *et al.* Bone loss in response to long-term glucocorticoid therapy *Bone Miner* 1990, *8*, 39-51.
[28] Bilezikian JP, *et al. Principles of bone biology*; Academic Press: San Diego, 1996.
[29] Bab I, *et al.* Histone H4-related osteogenic growth peptide (OGP): a novel circulating stimulator of osteoblastic activity *EMBO J* 1992, *11*, 1867-73.
[30] Xu J, *et al.* Extracellular histones are major mediators of death in sepsis *Nat Med* 2009, *15*, 1318-21.
[31] Eijken M, *et al.* The activin A-follistatin system: potent regulator of human extracellular matrix mineralization *FASEB J* 2007, *21*, 2949-60.
[32] Pearsall RS, *et al.* A soluble activin type IIA receptor induces bone formation and improves skeletal integrity *Proc Natl Acad Sci U S A* 2008, *105*, 7082-7.
[33] Aubin JE Regulation of osteoblast formation and function *Rev Endocr Metab Disord* 2001, *2*, 81-94.
[34] Jaenisch R, *et al.* Epigenetic regulation of gene expression: how the genome integrates intrinsic and environmental signals *Nat Genet* 2003, *33 Suppl*, 245-54.
[35] Komarova SV, *et al.* Bioenergetics and mitochondrial transmembrane potential during differentiation of cultured osteoblasts *Am J Physiol Cell Physiol* 2000, *279*, C1220-9.
[36] Persy V, *et al.* Vascular calcification and bone disease: the calcification paradox *Trends Mol Med* 2009, *15*, 405-16.
[37] Mori K, *et al.* Dexamethasone enhances In vitro vascular calcification by promoting osteoblastic differentiation of vascular smooth muscle cells *Arterioscler Thromb Vasc Biol* 1999, *19*, 2112-8.
[38] Reynolds JL, *et al.* Human vascular smooth muscle cells undergo vesicle-mediated calcification in response to changes in extracellular calcium and phosphate concentrations: a potential mechanism for accelerated vascular calcification in ESRD *J Am Soc Nephrol* 2004, *15*, 2857-67.
[39] Canfield AE, *et al.* Role of pericytes in vascular calcification: a review *Z Kardiol* 2000, *89 Suppl 2*, 20-7.
[40] Watson KE, *et al.* TGF-beta 1 and 25-hydroxycholesterol stimulate osteoblast-like vascular cells to calcify *J Clin Invest* 1994, *93*, 2106-13.
[41] Tilton RG Capillary pericytes: perspectives and future trends *J Electron Microsc Tech* 1991, *19*, 327-44.
[42] Wissler RW, *et al.* Experimental models of human atherosclerosis *Ann N Y Acad Sci* 1968, *149*, 907-22.
[43] Doherty MJ, *et al.* Vascular pericytes express osteogenic potential in vitro and in vivo *J Bone Miner Res* 1998, *13*, 828-38.
[44] Doherty MJ, *et al.* Gene expression during vascular pericyte differentiation *Crit Rev Eukaryot Gene Expr* 1999, *9*, 1-17.
[45] Pignolo RJ, *et al.* Circulating osteogenic cells: implications for injury, repair, and regeneration *J Bone Miner Res* 2011, *26*, 1685-93.
[46] Roberts N, *et al.* Progenitor cells in vascular disease *J Cell Mol Med* 2005, *9*, 583-91.
[47] Sata M [Circulating progenitors contribute to angiogenesis, vascular repair, and lesion formation] *Rinsho Byori* 2005, *53*, 70-6.
[48] Alm JJ, *et al.* Circulating plastic adherent mesenchymal stem cells in aged hip fracture patients *J Orthop Res* 2010, *28*, 1634-42.
[49] Eghbali-Fatourechi GZ, *et al.* Circulating osteoblast-lineage cells in humans *N Engl J Med* 2005, *352*, 1959-66.
[50] Egan KP, *et al.* Role for circulating osteogenic precursor cells in aortic valvular disease *Arterioscler Thromb Vasc Biol* 2011, *31*, 2965-71.

[51] Hyder JA*, et al.* Association between systemic calcified atherosclerosis and bone density *Calcif Tissue Int* 2007, *80*, 301-6.
[52] Mitton E*, et al.* Articular cartilage vesicles contain RNA *Biochem Biophys Res Commun* 2009, *388*, 533-8.
[53] Nahar NN*, et al.* Matrix vesicles are carriers of bone morphogenetic proteins (BMPs), vascular endothelial growth factor (VEGF), and noncollagenous matrix proteins *J Bone Miner Metab* 2008, *26*, 514-9.
[54] Chiellini C*, et al.* Characterization of human mesenchymal stem cell secretome at early steps of adipocyte and osteoblast differentiation *BMC Mol Biol* 2008, *9*, 26.

Chapter 7

SUMMARY

Bone is a very complex tissue where multiple cells interact. Osteoblasts are the cells responsible for bone formation being directly involved in controlling both bone mass and bone tissue quality. Understanding how these cells differentiate and mineralize is critical to promote healing of the bone after fractures and recovery of the bone mass lost in bone diseases such osteoporosis. In order to develop novel bone anabolic drugs more knowledge about bone formation is needed. Moreover, understanding what is expressed and/or present in bone tissue might reveal biomarkers useful in the clinic to diagnose pathological levels of bone loss. In this thesis we investigated bone formation using in vitro osteoblast differentiation models. The osteoblast response to inhibitors and stimulators of differentiation and mineralization was measured and the constitution of bone tissue was also evaluated using state-of-the-art mass spectrometry-based proteomics tools. In addition, the VSMC-based model of atherosclerosis was put in the context of bone mineralization assessing comparative gene expression profiling and identification of common denominators.

In vitro human osteoblast differentiation is stimulated by glucocorticoids, followed by a sequential order of tight-regulated events including extracellular matrix (ECM) production and mineralization. In **chapter 2** we measured protein changes at different time points of osteoblast differentiation and mineralization, comparing them to their non-differentiated counterparts. We identified 381 proteins to be expressed during osteoblast differentiation. Of these 381 proteins, 52 were differentially expressed between differentiating and non-differentiating osteoblasts. The expression of these 52 proteins demonstrated that the osteoblast differentiation process is essentially a biphasic process comprising pre-mineralization and mineralization periods. The proteins identified are diverse ranging from bone-related extracellular matrix (e.g., LGALS1 and FN1) and calcium ion binding (e.g., ANXAs and CANX) to cytoskeleton (e.g., PLEC1 and FLNA) and nuclear proteins (e.g., LMNA). Several of these have already an established function during osteoblast differentiation but many others remain to be studied in the context of bone formation.

Osteoblast-induced matrix mineralization is known to be strongly inhibited by activins. Despite the clear changes induced by activin A signaling in the osteoblast mineralization phenotype, little is known about its mechanism of action. In **chapter 3** we confirmed that activin A targets the ECM protein production of

osteoblasts and modifies the ECM composition. Furthermore, we demonstrated that these changes have significant consequences for the onset of mineralization by impairing matrix vesicle (MV) production. Besides containing significantly lower ALP activity, the MVs secreted by osteoblast cultures treated with activin A were defective in annexin expression and enriched in proteoglycans, proteins involved in calcium transport and in the inhibition of mineral growth respectively. This study elucidated the mechanisms by which activin A inhibits osteoblast mineralization. Furthermore, it also highlighted the osteoinductive properties of osteoblast ECMs for osteoprogenitor cells. Mesenchymal Stem Cells (MSC) cultured on top of a pre-existing osteoblast-derived ECM quickly exhibited characteristics of mineralizing osteoblasts. Intriguing and requiring further research was the observation that an ECM produced under activin A treatment also exhibited osteoinductive properties to new MSC despite not being able to become mineralized itself.

ECM proteins are major constituents of bone tissue. Proteomics is well positioned to unravel the bone protein composition, a tissue that besides collagens and a handful of non-collagenous proteins (NCP) is poorly characterized. In **chapter 4** we characterized the non-collagenous content of bone identifying and quantifying over 1000 proteins. Surprisingly, classical bone NCPs did not rank as high abundant proteins in bone tissue. Together with known ECM proteins we identified nucleosome, pyrophosphatase activity, Ca^{2+}-dependent phospholipid binding and antioxidant activity proteins to be highly enriched in bone. Interestingly, comparative analyses with osteoblast gene expression profiling analyses showed that the origin of these proteins could not solely be attributed to the bone forming osteoblasts. Potentially also osteoclasts and other cell types appear to contribute significantly to the bone protein composition. This data broadens our knowledge about bone opening possibilities to understand how bone cells integrate their activities together with their environment. Given the fact that the majority of proteins have a yet unknown function in bone we hypothesize that our data might contain novel modulators of bone formation. Furthermore, the proteins identified are interesting in the perspective of finding biomarkers of bone disease.

In pathological circumstances, mineralization can occur in tissues other than bone being vascular calcifications arguably the most relevant and devastating example of ectopic calcification. VSMC transdifferentiation into CVC has been hypothesized to share similar mechanisms with differentiating osteoblasts but so far results are contradictory. **Chapter 5** addressed this issue by comparing gene expression during

CVC and osteoblast development. Globally, these processes did not resemble each other and CVC did not down-regulate expression of VSMC markers. However, some very specific mimicry was found between CVC and osteoblasts. A subset of extracellular (matrix) genes and genes involved in biomineralization were identically regulated by the two cell types suggesting that they represent the most important subset of genes/proteins controlling both forms of mineralization. In addition, other genes relevant for bone formation were oppositely regulated by CVCs and osteoblasts, representing potential routes to modulate vascular and bone mineralization independently. Further research is needed to elucidate the exact implications (if any) of the two gene subsets in vascular calcifications. Altogether we disclosed molecular mechanisms involved in vascular calcifications and possible routes to invert this process. Care should be taken while extrapolating data to the in vivo situation mainly due to the fact that VSMC represent only one of the cell types in the vasculature that are able to start calcifications.

In conclusion, in this thesis we have addressed bone formation in a proteomics perspective. The studies presented laid the foundations for the search of biomarkers for bone formation in blood plasma (see **chapter 6** for more details). We have currently a shortlist of proteins whose levels in the circulation might be altered whenever bone mass loss is increased during primary and secondary osteoporosis. Specific mass spectrometry-based assays are being conducted to compare the concentrations of these proteins in plasma of healthy vs. osteoporotic individuals. In addition, the data generated has great potential to guide research towards the identification of novel therapies for osteoporosis that enable the modulation of bone formation. In this respect, the transcriptomics data obtained comparing vascular calcifications to bone mineralization can be useful to evaluate new modulators of bone formation and their possible implication for ectopic vascular calcifications.

SAMENVATTING

Bot is een complex weefsel waarin verschillende cellen met elkaar interacteren. Osteoblast cellen zijn verantwoordelijk voor nieuwe botaanmaak en zijn direct betrokken bij de regulatie van de botmassa en de kwaliteit van het bot. Het begrijpen hoe botcellen zich ontwikkelen en hoe ze het bot verkalken is essentieel om botheling te stimuleren na een botbreuk of om een lage botmassa in botziektes zoals osteoporose te herstellen. Om nieuwe bot anabole geneesmiddelen te ontwikkelen is er meer kennis nodig over het botvormingsproces. Tevens zal het achterhalen van wat voor eiwitten er aanwezig zijn en welke er gemaakt worden in bot helpen bij het vinden van biomerkers die als diagnose voor botverlies kunnen worden gebruikt. In dit proefschrift is het botvormingsproces onderzocht door gebruik te maken van in vitro osteoblast differentiatie modellen. Hoe osteoblasten reageren op remmers en stimulatoren van osteoblast ontwikkeling en mineralisatie is gemeten door gebruik te maken van "state of the art" massa spectometrie-gebaseerde proteomics methodes. Bovendien is een vasculaire gladde spiercel-gebaseerd model voor atherosclerose (aderverkalking) in de context geplaatst van de verkalking in het bot, waarbij de gedeelde noemers zijn geïdentificeerd door gebruik te maken van genexpressie profilering.

Humane *in vitro* osteoblast differentiatie wordt gestimuleerd door glucocorticoïden gevolgd door opeenvolgende en strak gereguleerde processen waaronder extracellulaire matrix (ECM) productie en mineralisatie. In **hoofdstuk 2** hebben we expressie niveaus van eiwitten gemeten op verschillende tijdstippen tijdens het osteoblast differentiatie proces en vergeleken met niet-differentiërende kweken. We hebben 381 verschillende eiwitten gedetecteerd tijdens het osteoblast differentiatie proces. In totaal kwamen 52 van deze eiwitten verschillend tot expressie tussen differentiërende en niet-differentiërende kweken. Bovendien liet de eiwit expressiedata zien dat osteoblast differentiatie in essentie een bifasisch proces is bestaande uit een pre-mineralisatie en mineralisatie periode. De gevonden eiwitten lopen uiteen van bot-gerelateerde extracellulaire matrix (zoals b.v. LGALS1 en FN1) en calcium ion bindende eiwitten (zoals b.v. ANXAs en CANX) tot cytoskelet (zoals b.v. PLEC1 en FLNA) en nucleaire eiwitten (zoals b.v. LMNA). Een deel van de gevonden eiwitten had reeds een bekende functie in het osteoblast differentiatie proces. De meeste andere eiwitten daarentegen moeten nog bestudeerd worden in relatie tot osteoblast differentiatie.

Activines staan bekend als factoren die het osteoblast-geïnduceerde matrix mineralisatie proces sterk remmen. Ondanks de sterke effecten van activines op het fenotype van de osteoblasten is er nog weinig bekend over het mechanisme hoe deze eiwitten de mineralisatie remmen. In **hoofdstuk 3** hebben we bevestigd dat activine A de productie van ECM eiwitten door osteoblasten reguleert samen met de compositie van de ECM. Bovendien hebben we aangetoond dat dit gevolgen heeft voor de start van de mineralisatie door een verstoorde productie van matrixblaasjes. Tevens hadden matrixblaasjes afkomstig van activin A-behandelde osteoblast kweken een lagere alkalische fosfatase activiteit en waren ze deficiënt voor annexine en verrijkt in proteoglycanen die het mineralisatie proces kunnen remmen. Naast het ontrafelen hoe activine het mineralisatie proces remt, was dit deel van de studie ook belangrijk doordat aangetoond was dat de door osteoblast geproduceerde ECM osteo-inductieve eigenschappen heeft voor osteoblast voorlopercellen. Mesenchymale stamcellen (MSC) die bovenop een door osteoblast geproduceerde ECM waren gekweekt, namen zeer snel osteoblast eigenschappen aan. Een interessante bevinding die nog meer onderzoek vereist, was de observatie dat een ECM geproduceerd door activine-behandelde osteoblasten ook osteo-inductieve eigenschappen heeft ondanks het feit dat deze ECM zelf niet in staat is om te mineraliseren.

ECM eiwitten zijn een belangrijk bestanddeel van botweefsel. Naast collageen eiwitten en een beperkt aantal niet-collagene eiwitten is de ECM van botweefsel slecht gekarakteriseerd. Proteomics is een krachtige methode om de samenstelling van de ECM van bot te ontrafelen. In **hoofdstuk 4** hebben we meer dan 1000 niet-collagene eiwitten in bot geïdentificeerd en gekwantificeerd. Verbazingwekkend was dat de klassieke niet-collagene eiwitten niet de eiwitten waren die het meest voorkwamen in het botweefsel. Naast bekende ECM eiwitten hebben we eiwitten betrokken bij de samenstelling van de nucleosoom, pyropfosfaat activiteit, Ca2+-afhankelijke phospholipide binding en antioxidant activiteit geïdentificeerd als sterk verrijkt in bot. Interessant genoeg toonde genexpressie vergelijking tussen humaan botweefsel en humane osteoblasten aan dat de eiwitsamenstelling van de ECM niet geheel afkomstig is van de osteoblast. Waarschijnlijk dragen osteoclasten en andere celtypen ook bij aan de samenstelling van het botweefsel. Deze data verbreden onze kennis die gebruikt kan worden om te begrijpen hoe botcellen interacteren met hun omgeving. Gegeven het feit dat de meeste door ons geïdentificeerde eiwitten nog geen bekende functie hebben in bot, is onze hypothese dat deze data een aantal nieuwe modulatoren van botvorming kunnen bevatten. In het perspectief van het

vinden van nieuwe biomerkers voor botaandoeningen zijn de door ons gevonden eiwitten ook interessant.

In pathologische condities kunnen andere weefsels naast bot ook mineraliseren met vasculaire verkalking als voorbeeld van een belangrijke en ernstige vorm van ectopische verkalking. Vasculaire gladde spiercel transdifferentiatie naar een verkalkende vasculaire cel is verondersteld via een gelijkwaardig mechanisme te verlopen als de differentiatie van een osteoblast maar tot op heden zijn de resultaten in de literatuur verdeeld. In **hoofdstuk 5** hebben we dit probleem onderzocht door genexpressieprofielen te vergelijken van verkalkende vasculaire cellen en osteoblasten. Globaal gezien waren de processen tussen de twee celtypen verschillend en alle vasculaire merkers kwamen nog tot expressie in de mineraliserende vasculaire cellen. Echter, enkele zeer specifieke processen waren identiek tussen de twee celtypen. Een deel van de extracellulaire (matrix) genen en genen betrokken in het biomineralisatie proces waren identiek gereguleerd. Dit suggereert dat deze eiwitten/genen erg belangrijk zijn in beide vormen van mineralisatie. Tevens waren er relevante genen met betrekking tot botvorming die juist tegengesteld gereguleerd waren. Deze genen kunnen eventueel gebruikt worden om vasculaire en botmineralisatie apart te moduleren. Meer onderzoek is nodig om de implicaties van de twee groepen van genen te achterhalen. Samengevat hebben we belangrijke moleculaire mechanismes gevonden en mogelijk routes om het proces van aderverkalking te keren. Voorzichtigheid dient in acht te worden genomen om deze data te extrapoleren naar de in vivo situatie, zeker omdat vasculaire gladde spiercellen maar 1 van de celtypes zijn, die het verkalking proces kunnen initiëren in het vasculaire milieu.

Concluderend hebben we in dit proefschrift door middel van proteomics technieken het botvormingsproces bestudeerd. De beschreven studies hebben de basis gelegd voor de zoektocht naar nieuwe biomerkers van botvorming in het bloed (zie **hoofdstuk 6** voor meer detail). We hebben een lijst van target eiwitten geïdentificeerd wiens spiegels in bloedplasma zouden kunnen veranderen in situaties van botverlies zoals in primaire of secundaire osteoporose. Specifieke massaspectrofotometrie-gebaseerde analyses worden momenteel uitgevoerd om de bloedplasma spiegels van deze eiwitten te meten in gezonde personen en personen met osteoporose. Tevens hebben de data veel potentie om nieuw onderzoek te starten naar nieuwe therapieën om botvorming te stimuleren. In verband hiermee kan de transcriptoom data, waarbij we de vasculaire mineralisatie en mineralisatie in bot hebben vergeleken, gebruikt worden om nieuwe modulatoren voor botvorming te evalueren of ze implicaties kunnen hebben voor ectopische verkalkingen.

ABBREVIATION INDEX

(c)DNA	(complementary) Deoxyribonucleic acid
(m/c)RNA	(messenger/complementary) Ribonucleic acid
12C6,14N2-Lys	L-lysine
12C6,14N4-Arg	L-arginine
13C6,14N2-Lys	Carbon labeled L-lysine
13C6,15N4-Arg	Carbon/nitrogen labeled L-arginine
ACN	Acetronitrile
ACP5	Tartrate-resistant acid phosphatase 5
ACTA2	Actin, aortic smooth muscle
ACTB	Actin, cytoplasmic 1
ACTC1	Actin, alpha cardiac muscle 1
ACTH	Adrenocorticotropic hormone
ACVR(2A/2B)	Activin A receptor (type IIA or type IIB)
ALB	Albumin
ALP(L)	Alkaline phosphatase
α-MEM	Alpha-minimum essential medium
ANXA(1-7,11)	Annexin (A1, 2, 3, 4, 5, 6, 7 or 11)
ATP1B3	Sodium/potassium-transporting ATPase subunit beta-3
ATP2A2	Sarcoplasmic/endoplasmic reticulum calcium ATPase 2
ATP2B4	Plasma membrane calcium-transporting ATPase 4
BCA	Bicinchoninic acid
BGLAP	Osteocalcin
BGN	Biglycan
BMD	Bone mineral density
BMP(2/7)	Bone morphogenetic protein (2 or 7)
BMUs	Basic multicellular units
BSA	Bovine serum albumin
C19orf10	Chromosome 19 open reading frame 10
CA2	Carbonic anhydrase 2
CALD1	Caldesmon
CALR	Calreticulin
CCT2	T-complex protein 1 subunit beta
CHAD	Chondroadherin
CLIC(1/4)	Chloride intracellular channel (1 or 4)
CNN1	Calponin
COL12A1	Collagen, type XII α1
COL1A1	Collagen type I α1
CRTL1	Hyaluronan binding protein
CSRP1	Cysteine and glycine-rich protein 1
CTSK	Cathepsin K
CV	Coefficient of variance

CVC(s)	Calcifying vascular cell(s)
Da	Dalton
DAPI	4',6-diamidino-2-phenylindole
DAVID	Database for Annotation, Visualization and Integrated Discovery
DCN	Bone proteoglycan II; decorin
DEX	Dexamethasone
DHB	2,5-dihydroxy benzoic acid
DLX5	Distal-less homeobox-5
DMEM	Dulbecco's modified eagle medium
DMP-1	Dentin matrix protein-1
ECM	Extracellular matrix
EDTA	Ethylenediaminetetraacetic acid
ELISA	Enzyme-linked immunoabsorbent assay
emPAI	Exponentially modified protein abundance index
ESRD	End-stage renal disease
FA	Formic acid
FACS	Fluorescence-activated cell sorting
FBLN5	Fibulin 5
FBN	Fibrillin-1
FCS	Fetal calf serum
FDR	False discovery rate
FGF23	Fibroblast growth factor 23
FLNA	Filamin A
FN1	Fibronectin 1
FOM	Figure of merit
FSH	Follicule stimulating hormone
FT-ICR-MS	Fourier transform ion cyclotron resonance mass spectrometry
GAPDH	Glyceraldehyde-3-phosphate dehydrogenase
GEO	Gene Expression Omnibus
GO	Gene Ontology
GPNMB	Glycoprotein nmb
GREM1	Gremlin-1
HBA1	Hemoglobin subunit alpha
HBB	Hemoglobin subunit beta
HSD17B12	Estradiol-17-beta-dehydrogenase 12
HSPA5	Heat shock 70kDa protein 5
HUPO PPP	Human Proteome Organisation Plasma Proteome Project
IBSP	Bone sialoprotein
IPA	Ingenuity Pathway Analysis
IPI	International Protein Index
KCTD12	BTB/POZ domain-containing protein KCTD12
LC	Liquid chromatography
LDHA	L-lactate dehydrogenase
LEP	Leptin

LGALS1	Galectin 1
LiCl	Lithium chloride
LMNA	Lamin-A
LTQ-Orbitrap	Linear trap quadrupole-Orbitrap
LUM	Lumican
MALDI	Matrix-assisted laser desorption/ionization
M-CSF	Macrophage colony-stimulating factor
MEPE	Matrix extracellular phosphoglycoprotein
MGP	Matrix-gla protein
MIG10	Cell migration-inducing gene 10 protein
MMP9	Matrix metalloproteinase-9
MRM	Multiple reaction monitoring
MS	Mass spectrometry
MS/MS	Tandem mass spectrometry
MSC(s)	Mesenchymal stem cell(s)
MSX2	Msh homeobox homologue-2
MV(s)	Matrix vesicle(s)
MYH11	Smooth-muscle myosin
MYH9	Myosin-9
MYLK	Telokin
NaN	Not a number
NCBI	National Center for Biotechnology Information
NCP(s)	Non-collagenous protein(s)
NTE5/CD73	5'-nucleotidase precursor
OGN	Osteoglycin
ON/SPARC	Osteonectin
OPG	Osteoprotegerin
OPN	Osteopontin
PBMCs	Peripheral bone marrow cells
PBS	Phosphate-buffered saline
PCA	Principle component analysis
PFA	Paraformaldehyde
PGD	Phosphogluconate dehydrogenase
PGM1	Phosphoglucomutase 1
PHEX	Phosphate-regulating neutral endopeptidase
Pi	Free phosphate
pI/MW	Isoelectric point/molecular weight
PLEC1	Plectin 1
PLOD2	Procollagen-lysine,2-oxoglutarate 5-dioxygenase 2 precursor
PLS3	Plastin-3
POSTN	Periostin
PPi	Pyrophosphate
ppm	Parts-per-million
PRDX	Peroxiredoxin

PTH	Parathyroid hormone
PTN	Pleiotrophin
RANKL	Receptor activator of NF-kB ligand
ROS	Reactive oxygen species
RUNX2	Runt-related transcription factor 2
S/N	Signal-to-noise
SDS-PAGE	Sodium dodecyl sulfate polyacrylamide gel electrophoresis
SILAC	Stable isotope labeling of amino acids in cell culture
SMAD7	SMAD family member 7
SOD(1/3)	Superoxide dismutase (1 or 3)
SOST	Sclerostin
SP7	Osterix
SPP1	Osteopontin
SRGN	Serglycin
SV-HFO	Simian virus 40 immortalized human fetal osteoblasts
T	Tesla
TBS	Tris-buffered saline
TCIRG1	V-type proton ATPase 116 kDa subunit
TF	Transferrin
TFA	Trifluoracetic acid
TFPI2	Tissue factor pathway inhibitor 2
TGF-βI	Transforming growth factor, beta-induced, 68kDa
TGF-β	Transforming growth factor beta
TIMP4	Tissue inhibitor of metalloproteinase 4
TOF	Time of flight mass spectrometry
TPM3	Gamma-tropomyosin
UGDH	UDP-glucose 6-dehydrogenase
UGP2	UDP-glucose pyrophosphorylase 2
VCL	Vinculin
VDAC(1-3)	Voltage-dependent anion channel (1, 2 or 3)
VEGF	Vascular endothelial growth factor
VSMC(s)	Vascular smooth muscle cell(s)
WDR1	WD repeat domain 1
WHO	World Health Organization
WNT5A	Wingless-type MMTV integration site family, member 5A

SUPPLEMENTARY DATA

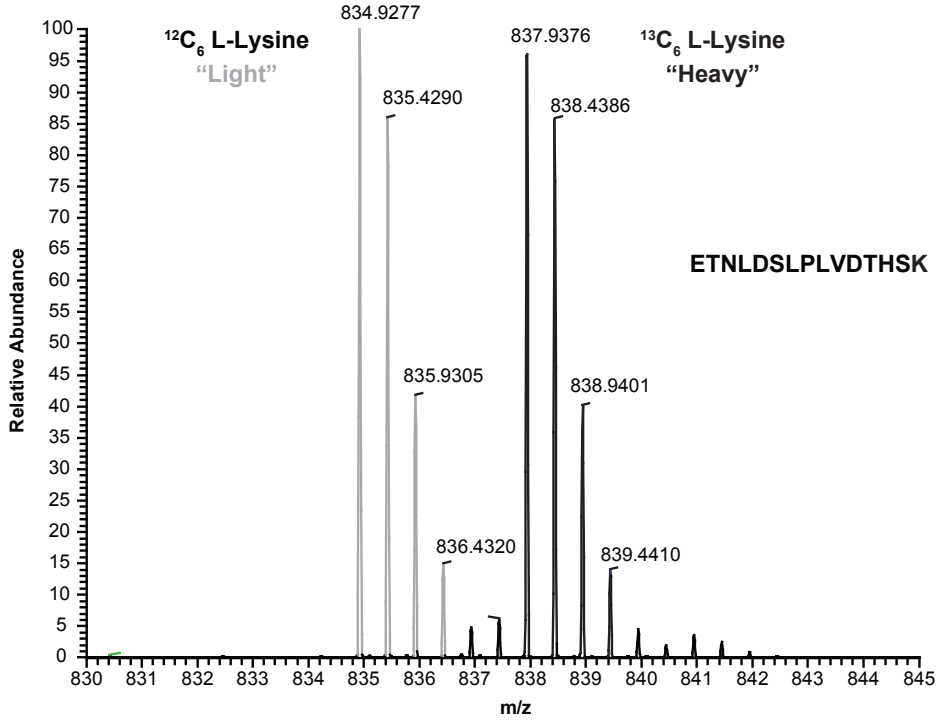

Supplementary Figure I. Metabolic label incorporation. SILAC peak pairs for a double charged tryptic peptide from vimentin in a 1:1 mix of light and heavy samples. The mass difference between the light and heavy peptide is 6 Da.

Supplementary Figure II. Isoelectric point (pI) distribution frequency for the bone proteome (1049 proteins), IPI database proteome (17290) and nucleosome proteins (GO:0000786; 69). Available online at http://pubs.acs.org/doi/suppl/10.1021/pr200522n, filename pr200522n_si_003.pdf.

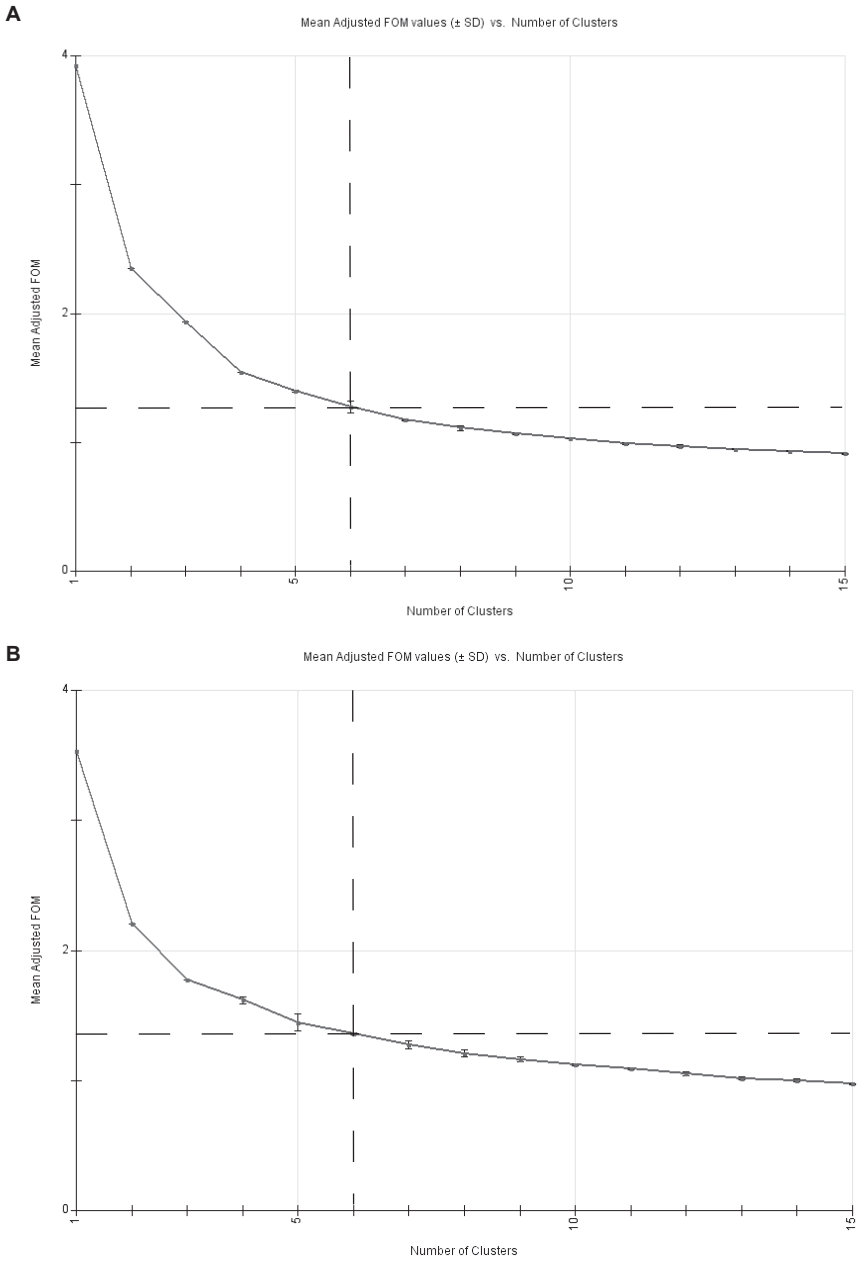

Supplementary Figure III. Figure of merit (FOM) analysis to estimate k-means clustering predictive power in genes differentially expressed by **(A)** CVCs and **(B)** osteoblasts. The lower the adjusted FOM value (y-axis) the higher the predictive power of the k-means algorithm. k = 6 (dashed lines) was used for both cell types.

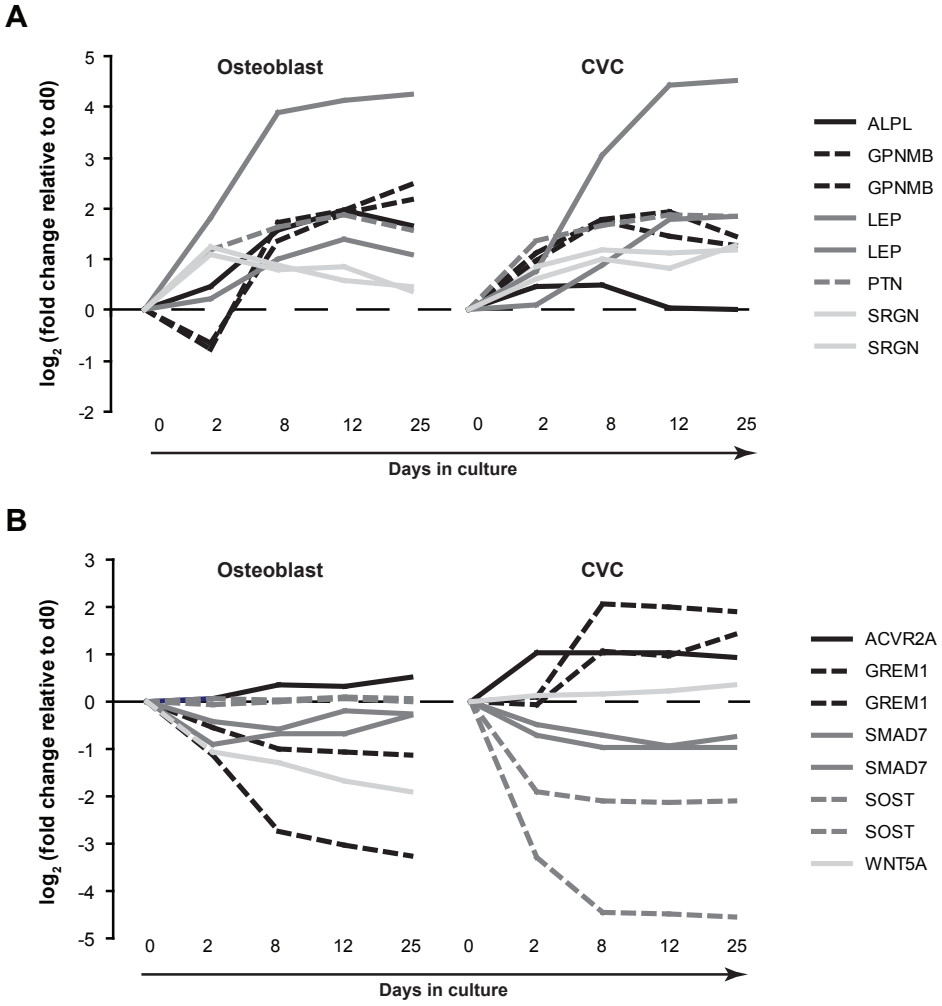

Supplementary Figure IV. Expression profile of a selection of **(A)** correlated biomineral tissue development genes and **(B)** anti-correlated BMP signaling genes during CVC development and osteoblast differentiation. Expression is plotted as $\log_2$ fold change relative to d0. Each line plotted represents a probe set. Probe/gene identifiers are provided in Supplementary Table 4.

Supplementary Table I. Proteins identified by MS/MS in the distinct samples analyzed from differentiating osteoblast cultures at day 5, 10 and 19. Available online at http://pubs.acs.org/doi/suppl/10.1021/pr100400d, filename pr100400d_si_001.xls.

Supplementary Table II. List of 1213 proteins identified in at least 3 out of the 4 bone samples analyzed sorted by emPAI score. Minimum and maximum values obtained for the unique and total peptides identified, the percentage of protein coverage and the Mascot scores in the 4 bone samples analyzed are shown. EmPAI scores are average values of the scores obtained for each of the 4 bone samples. - = detected in less than 3 samples, not accounted for quantification. Available online at http://pubs.acs.org/doi/suppl/10.1021/pr200522n, filename pr200522n_si_002.xls.

Supplementary Table III. Classical bone proteins identified. Several proteins whose expression is commonly associated to osteoblasts, ECM, osteocytes and to bone resorbing osteoclasts were detected. NR = not ranked using emPAI score. - = detected in less than 3 samples, not accounted for quantification. Available online at http://pubs.acs.org/doi/suppl/10.1021/pr200522n, filename pr200522n_si_001.xls.

Supplementary Table IV. Number of probes differentially expressed in CVCs and osteoblasts. Differential expression was calculated independently for both cell types and relative to their initial time point, day 0. The 4782 probes regulated were divided in three categories, identical or opposite regulation in the two cell types and cell-specific regulation. Only significantly regulated probes ($q<0.001$) were considered.

Regulation d2-25 vs. d0	probe #
In osteoblasts & CVC	4782
In osteoblasts	3144
In CVC	3721
Identical regulation	1968
Up in osteoblasts & CVC	978
Down in osteoblasts & CVC	990
Opposite regulation	150
Up in osteoblasts & down in CVC	62
Down in osteoblasts & up in CVC	88
Cell specific regulation	2699
In osteoblasts only	1061
In CVC only	1638

Supplementary Table V. List of extracellular region probe/genes present in cluster 1 and 2 of **(A)** CVCs/osteoblasts, **(B)** CVCs only and **(C)** osteoblasts only.

A #	Probe ID	#	Gene Symbol
1	ILMN_1780170	1	APOD
2	ILMN_1685433	2	COL8A1
3	ILMN_2402392		COL8A1
4	ILMN_1674050		COL8A2
5	ILMN_2102330		COL8A2
6	ILMN_1768227	3	DCN
7	ILMN_1672536	4	FBLN1
8	ILMN_1700541		FBLN1
9	ILMN_1722713		FBLN1
10	ILMN_2207504	5	LEP
11	ILMN_2207505		LEP
12	ILMN_1651958	6	MGP
13	ILMN_2071809		MGP
14	ILMN_1790761	7	POSTN
15	ILMN_2196328		POSTN
16	ILMN_1708934	8	ADM
17	ILMN_1760727	9	ANG
18	ILMN_1677723	10	ANGPT1
19	ILMN_2086890		ANGPT1
20	ILMN_1707727	11	ANGPTL4
21	ILMN_1740938	12	APOE
22	ILMN_1744487	13	C1QTNF5
23	ILMN_1781626	14	C1S
24	ILMN_2396444	15	CD14
25	ILMN_1777190	16	CFD
26	ILMN_1657803	17	CFH
27	ILMN_1810910		CFH
28	ILMN_2412192		CFH
29	ILMN_1789507	18	COL11A1
30	ILMN_1677636	19	COMP
31	ILMN_1800354	20	CST3
32	ILMN_1725090	21	CTHRC1
33	ILMN_2117508		CTHRC1
34	ILMN_1674038	22	CTSD
35	ILMN_1758895	23	CTSK
36	ILMN_1683194	24	DCN
37	ILMN_2347145		DCN
38	ILMN_1708107	25	DPT
39	ILMN_2228938	26	ECM2
40	ILMN_1664176	27	FBLN5
41	ILMN_2223941		FBLN5
42	ILMN_1670899	28	FBN2
43	ILMN_1768260	29	GAS6
44	ILMN_1779558		GAS6
45	ILMN_1784749		GAS6
46	ILMN_1789502	30	GPC4
47	ILMN_1726666	31	GPX3
48	ILMN_1801043	32	GSN
49	ILMN_1676563	33	HTRA1
50	ILMN_1725193	34	IGFBP2
51	ILMN_1788019	35	LAMA2
52	ILMN_2339266		LAMA2
53	ILMN_1790529	36	LUM
54	ILMN_1766914	37	MFAP4
55	ILMN_1756071	38	MFGE8
56	ILMN_1727532	39	OLFML3
57	ILMN_1749846	40	OMD
58	ILMN_1803094	41	PDGFD
59	ILMN_2376859		PDGFD
60	ILMN_2058795	42	PGCP
61	ILMN_1790859	43	PLAC9
62	ILMN_1770800	44	PODN
63	ILMN_1671928	45	PROS1
64	ILMN_1664464	46	PTGDS
65	ILMN_1813753	47	PTN
66	ILMN_2304512	48	SAA1
67	ILMN_1767470	49	SCPEP1
68	ILMN_1785071	50	SEPP1
69	ILMN_1788874	51	SERPINA3
70	ILMN_2141482	52	SERPINF1
71	ILMN_1670305	53	SERPING1
72	ILMN_1796349	54	SMPDL3A
73	ILMN_1795251	55	SPARCL1
74	ILMN_1676213	56	SRPX2
75	ILMN_2112638	57	SVEP1
76	ILMN_1663399	58	TIMP4

B #	Probe ID	#	Gene Symbol
1	ILMN_1745607	1	A2M
2	ILMN_1803686	2	ADA
3	ILMN_1740900	3	BMP4
4	ILMN_1718866	4	C5orf46
5	ILMN_1688242	5	C6
6	ILMN_1687848	6	C7
7	ILMN_1715662	7	CCDC80
8	ILMN_1653028	8	COL4A1
9	ILMN_1724994		COL4A2
10	ILMN_1680624	9	CREG1
11	ILMN_1790689	10	CRISPLD2
12	ILMN_2115125	11	CTGF
13	ILMN_1815673	12	DKK3
14	ILMN_2398159		DKK3
15	ILMN_1735877	13	EFEMP1
16	ILMN_1773125	14	ENTPD1
17	ILMN_1789639	15	FMOD
18	ILMN_1734653	16	FNDC1
19	ILMN_2163873		FNDC1
20	ILMN_1730670	17	FSTL3
21	ILMN_1752965	18	GREM1
22	ILMN_2124585		GREM1
23	ILMN_1702168	19	HSD17B12
24	ILMN_2242900	20	IL1RL1
25	ILMN_2313672		IL1RL1
26	ILMN_2165993	21	ITLN1
27	ILMN_2118129	22	ITLN2
28	ILMN_2167805	23	LUM
29	ILMN_1679391	24	MAMDC2
30	ILMN_1790052	25	MMP23A
31	ILMN_2193325	26	MMP23B
32	ILMN_1685608	27	NPTX2
33	ILMN_2113535	28	PCYOX1
34	ILMN_1801077	29	PLIN2
35	ILMN_2138765		PLIN2
36	ILMN_1773389	30	PLTP
37	ILMN_1781791	31	PRRG1
38	ILMN_1797776	32	PRSS23
39	ILMN_1764754	33	RAMP1
40	ILMN_1810844	34	RARRES2
41	ILMN_1681983	35	RSPO3
42	ILMN_1759910	36	SERPINA5
43	ILMN_1810172	37	SFRP4
44	ILMN_2218208	38	SPARCL1
45	ILMN_1800739	39	SPINT2
46	ILMN_1760347	40	SRGN
47	ILMN_2169152		SRGN
48	ILMN_1686116	41	THBS1
49	ILMN_1676663	42	TNFRSF11B
50	ILMN_1713499	43	WISP1

C #	Probe ID	#	Gene Symbol
1	ILMN_1736178	1	AEBP1
2	ILMN_2166696	2	ANGPTL5
3	ILMN_1664024	3	APOB
4	ILMN_2380237	4	C1QTNF1
5	ILMN_1677198	5	C1R
6	ILMN_1764109		C1R
7	ILMN_1746819	6	C5
8	ILMN_1783593	7	CCL13
9	ILMN_1740015	8	CD14
10	ILMN_1705442	9	CMTM3
11	ILMN_1710124	10	CMTM8
12	ILMN_1672776	11	COL10A1
13	ILMN_2392803	12	COL11A1
14	ILMN_1733756	13	COL12A1
15	ILMN_1751161	14	COL7A1
16	ILMN_2246563	15	COL8A1
17	ILMN_1773337	16	DKK1
18	ILMN_1746763	17	ECM2
19	ILMN_1699022	18	ENDOD1
20	ILMN_1742866	19	F2R
21	ILMN_1777261	20	FAM3C
22	ILMN_1774602	21	FBLN2
23	ILMN_2390919		FBLN2
24	ILMN_1716246	22	FRZB
25	ILMN_1699867	23	IGF2
26	ILMN_2413956		IGF2
27	ILMN_1772869	24	ISM1
28	ILMN_1676265	25	LEPR
29	ILMN_1696391		LEPR
30	ILMN_1731966		LEPR
31	ILMN_2234956		LEPR
32	ILMN_2330570		LEPR
33	ILMN_1657968	26	MAP2K2
34	ILMN_1685403	27	MMP7
35	ILMN_2192072		MMP7
36	ILMN_1761425	28	OLFML2A
37	ILMN_1765557		OLFML2B
38	ILMN_1767934	29	PCSK5
39	ILMN_1680339	30	PDGFRL
40	ILMN_2092077	31	PIP
41	ILMN_1742330	32	PLXNB1
42	ILMN_1714158	33	PON2
43	ILMN_2354381		PON2
44	ILMN_2395156	34	PRELP
45	ILMN_1776602	35	RNASE4
46	ILMN_2408572		RNASE4
47	ILMN_2149164	36	SFRP1
48	ILMN_1756501	37	ST6GAL1
49	ILMN_1662619	38	TFPI
50	ILMN_1707124		TFPI
51	ILMN_1784287	39	TGFBR3
52	ILMN_1726981	40	VEGFB
53	ILMN_1709434	41	VIT
54	ILMN_2111255		VIT
55	ILMN_1812461	42	WISP2

Supplementary Table VI. List of ECM probe/genes **(A)** differentially expressed and **(B)** identically regulated in CVCs and osteoblasts.

A #	Probe ID	#	Gene Symbol
1	ILMN_1673639	1	ABI3BP
2	ILMN_1673566	2	ADAMTS1
3	ILMN_1681886	3	ADAMTS5
4	ILMN_1767362	4	ADAMTS6
5	ILMN_1727084	5	ADAMTSL1
6	ILMN_1687035	6	ADAMTSL4
7	ILMN_1762294		ADAMTSL4
8	ILMN_1696974	7	ANG
9	ILMN_1760727		ANG
10	ILMN_1707727	8	ANGPTL4
11	ILMN_1711899	9	ANXA2
12	ILMN_1755937		ANXA2
13	ILMN_2206746	10	BGN
14	ILMN_1740900	11	BMP4
15	ILMN_1689176	12	C4orf31
16	ILMN_1715662	13	CCDC80
17	ILMN_1803338		CCDC80
18	ILMN_1672776	14	COL10A1
19	ILMN_1789507	15	COL11A1
20	ILMN_2392803		COL11A1
21	ILMN_1733756	16	COL12A1
22	ILMN_2311052	17	COL13A1
23	ILMN_2370624		COL13A1
24	ILMN_1768940	18	COL15A1
25	ILMN_1684554	19	COL16A1
26	ILMN_1806733	20	COL18A1
27	ILMN_1784532	21	COL22A1
28	ILMN_1653028	22	COL4A1
29	ILMN_1724994	23	COL4A2
30	ILMN_1778308	24	COL4A4
31	ILMN_1742534	25	COL4A5
32	ILMN_1706505	26	COL5A1
33	ILMN_1732151	27	COL6A1
34	ILMN_1809928	28	COL6A2
35	ILMN_1751161	29	COL7A1
36	ILMN_1685433	30	COL8A1
37	ILMN_2246563		COL8A1
38	ILMN_2402392		COL8A1
39	ILMN_1674050	31	COL8A2
40	ILMN_2102330		COL8A2
41	ILMN_1677636	32	COMP
42	ILMN_1790689	33	CRISPLD2
43	ILMN_1658384	34	CRTAC1
44	ILMN_1665235	35	CRTAP
45	ILMN_2115125	36	CTGF
46	ILMN_1725090	37	CTHRC1
47	ILMN_2117508		CTHRC1
48	ILMN_1683194	38	DCN
49	ILMN_1768227		DCN
50	ILMN_2347145		DCN
51	ILMN_1791396	39	DGCR6
52	ILMN_1708107	40	DPT
53	ILMN_1658333	41	ECM1
54	ILMN_2329735		ECM1
55	ILMN_1746763	42	ECM2
56	ILMN_2228938		ECM2
57	ILMN_1673880	43	EFEMP1
58	ILMN_1735877		EFEMP1
59	ILMN_2350634		EFEMP1
60	ILMN_1653203	44	EFEMP2
61	ILMN_1654109	45	EGFLAM
62	ILMN_2385672	46	ELN
63	ILMN_1711439	47	EMILIN1
64	ILMN_1697268	48	EMILIN2
65	ILMN_1773125	49	ENTPD1
66	ILMN_1672536	50	FBLN1
67	ILMN_1700541		FBLN1
68	ILMN_1722713		FBLN1
69	ILMN_1774602	51	FBLN2
70	ILMN_2390919		FBLN2
71	ILMN_1664176	52	FBLN5
72	ILMN_2223941		FBLN5
73	ILMN_1670899	53	FBN2
74	ILMN_1789639	54	FMOD
75	ILMN_1778237	55	FN1
76	ILMN_2366463		FN1
77	ILMN_1806667	56	FRAS1
78	ILMN_1789502	57	GPC4
79	ILMN_1678812	58	HAPLN1
80	ILMN_1702168	59	HSD17B12
81	ILMN_2094106		HSD17B12
82	ILMN_2359287	60	ITGA6
83	ILMN_1696434	61	LAMA1
84	ILMN_1788019	62	LAMA2
85	ILMN_2339266		LAMA2
86	ILMN_2406035	63	LAMA3
87	ILMN_1795442	64	LAMA4
88	ILMN_2140059		LAMA4
89	ILMN_1773567	65	LAMA5
90	ILMN_1658709	66	LAMB1
91	ILMN_1664294	67	LEPRE1
92	ILMN_1723978	68	LGALS1
93	ILMN_1772239	69	LOC400406
94	ILMN_1740675	70	LOC649366
95	ILMN_1695880	71	LOX
96	ILMN_1734950	72	LOXL1
97	ILMN_1786444	73	LPL
98	ILMN_1790529	74	LUM
99	ILMN_2167805		LUM
100	ILMN_1679391	75	MAMDC2
101	ILMN_1694840	76	MATN2
102	ILMN_1663171	77	MATN3
103	ILMN_1766914	78	MFAP4
104	ILMN_1733415	79	MFAP5
105	ILMN_1651958	80	MGP
106	ILMN_2071809		MGP
107	ILMN_1726448	81	MMP1
108	ILMN_1741847	82	MMP10
109	ILMN_1655915	83	MMP11
110	ILMN_1762106	84	MMP2
111	ILMN_2317701	85	MMP23A
112	ILMN_2399016	86	MMP28
113	ILMN_1784459	87	MMP3
114	ILMN_1685403	88	MMP7
115	ILMN_2192072		MMP7
116	ILMN_1674719	89	NID1
117	ILMN_1787186	90	NOV
118	ILMN_2113490	91	NTN4
119	ILMN_1790098	92	OGN
120	ILMN_2387105		OGN
121	ILMN_1761425	93	OLFML2A
122	ILMN_1765557	94	OLFML2B
123	ILMN_1749846	95	OMD
124	ILMN_1770800	96	PODN
125	ILMN_1790761	97	POSTN
126	ILMN_2196328		POSTN
127	ILMN_1707380	98	PRELP
128	ILMN_2395156		PRELP
129	ILMN_2294976	99	RNASE4
130	ILMN_2294978		RNASE4
131	ILMN_1812169	100	SERAC1
132	ILMN_1744381	101	SERPINE1
133	ILMN_1655595	102	SERPINE2
134	ILMN_1718807	103	SMC3
135	ILMN_2410938	104	SMOC1
136	ILMN_1719641	105	SMOC2
137	ILMN_1690034	106	SOD3
138	ILMN_1796734	107	SPARC
139	ILMN_1795251	108	SPARCL1
140	ILMN_2218208		SPARCL1
141	ILMN_1746013	109	SPOCK1
142	ILMN_1676099	110	SPON2
143	ILMN_2068104	111	TFPI2
144	ILMN_1812526	112	TGFB2
145	ILMN_1663866	113	TGFBI
146	ILMN_1784287	114	TGFBR3
147	ILMN_1686116	115	THBS1
148	ILMN_1721876	116	TIMP2
149	ILMN_1701461	117	TIMP3
150	ILMN_1663399	118	TIMP4
151	ILMN_1719759	119	TNC
152	ILMN_2145670		TNC
153	ILMN_1676663	120	TNFRSF11B
154	ILMN_1687301	121	VCAN
155	ILMN_1709434	122	VIT
156	ILMN_2111255		VIT
157	ILMN_1694011	123	WNT2
158	ILMN_1740269	124	WNT2B
159	ILMN_1800317	125	WNT5A
160	ILMN_1772824	126	WNT5B

B #	Probe ID	#	Gene Symbol
1	ILMN_1673566	1	ADAMTS1
2	ILMN_1767362	2	ADAMTS6
3	ILMN_1687035	3	ADAMTSL4
4	ILMN_1762294		ADAMTSL4
5	ILMN_1696974	4	ANG
6	ILMN_1760727		ANG
7	ILMN_1707727	5	ANGPTL4
8	ILMN_1711899	6	ANXA2
9	ILMN_1740900	7	BMP4
10	ILMN_1789507	8	COL11A1
11	ILMN_1733756	9	COL12A1
12	ILMN_1768940	10	COL15A1
13	ILMN_1684554	11	COL16A1
14	ILMN_1685433	12	COL8A1
15	ILMN_2246563		COL8A1
16	ILMN_2402392		COL8A1
17	ILMN_1674050	13	COL8A2
18	ILMN_2102330		COL8A2
19	ILMN_1677636	14	COMP
20	ILMN_1665235	15	CRTAP
21	ILMN_2115125	16	CTGF
22	ILMN_1725090	17	CTHRC1
23	ILMN_2117508		CTHRC1
24	ILMN_1683194	18	DCN
25	ILMN_1768227		DCN
26	ILMN_2347145		DCN
27	ILMN_1708107	19	DPT
28	ILMN_1746763	20	ECM2
29	ILMN_2228938		ECM2
30	ILMN_1653203	21	EFEMP2
31	ILMN_1711439	22	EMILIN1
32	ILMN_1672536	23	FBLN1
33	ILMN_1700541		FBLN1
34	ILMN_1722713		FBLN1
35	ILMN_1664176	24	FBLN5
36	ILMN_2223941		FBLN5
37	ILMN_1670899	25	FBN2
38	ILMN_1789639	26	FMOD
39	ILMN_1806667	27	FRAS1
40	ILMN_1789502	28	GPC4
41	ILMN_1702168	29	HSD17B12
42	ILMN_2094106		HSD17B12
43	ILMN_1788019	30	LAMA2
44	ILMN_2339266		LAMA2
45	ILMN_2406035	31	LAMA3
46	ILMN_1658709	32	LAMB1
47	ILMN_1723978	33	LGALS1
48	ILMN_1772239	34	LOC400406
49	ILMN_1790529	35	LUM
50	ILMN_2167805		LUM
51	ILMN_1679391	36	MAMDC2
52	ILMN_1766914	37	MFAP4
53	ILMN_1733415	38	MFAP5
54	ILMN_1651958	39	MGP
55	ILMN_2071809		MGP
56	ILMN_2192072	40	MMP7
57	ILMN_2113490	41	NTN4
58	ILMN_1761425	42	OLFML2A
59	ILMN_1749846	43	OMD
60	ILMN_1770800	44	PODN
61	ILMN_1790761	45	POSTN
62	ILMN_2196328		POSTN
63	ILMN_2294976	46	RNASE4
64	ILMN_2294978		RNASE4
65	ILMN_1719641	47	SMOC2
66	ILMN_1796734	48	SPARC
67	ILMN_1795251	49	SPARCL1
68	ILMN_2218208		SPARCL1
69	ILMN_1676099	50	SPON2
70	ILMN_2068104	51	TFPI2
71	ILMN_1663866	52	TGFBI
72	ILMN_1686116	53	THBS1
73	ILMN_1701461	54	TIMP3
74	ILMN_1663399	55	TIMP4
75	ILMN_1676663	56	TNFRSF11B
76	ILMN_2111255	57	VIT

Supplementary Table VII. List of **(A)** biomineral tissue development and **(C)** BMP signaling probes/genes used for correlation analysis in CVCs and osteoblasts. **(B)** and **(D)** represent differentially expressed genes behind the correlated biomineral tissue development and anti-correlated BMP signaling GO-terms respectively.

A #	Probe ID	#	Gene Symbol
1	ILMN_1701603	1	ALPL
2	ILMN_1724480	2	AXIN2
3	ILMN_1722718	3	BMP2
4	ILMN_1701308	4	COL1A1
5	ILMN_1658333	5	ECM1
6	ILMN_2329735		ECM1
7	ILMN_1724984	6	EIF2AK3
8	ILMN_1700888	7	ENPP1
9	ILMN_1751328	8	FAM83H
10	ILMN_2051972	9	GPC3
11	ILMN_1801205	10	GPNMB
12	ILMN_2407389		GPNMB
13	ILMN_1659122	11	KLF10
14	ILMN_2411897		KLF10
15	ILMN_2207504	12	LEP
16	ILMN_2207505		LEP
17	ILMN_1664994	13	MINPP1
18	ILMN_1663873	14	MMP13
19	ILMN_1677511	15	PTGS2
20	ILMN_2054297		PTGS2
21	ILMN_1795166	16	PTH1R
22	ILMN_1813753	17	PTN
23	ILMN_2081645	18	RSPO2
24	ILMN_1679045	19	SBDS
25	ILMN_1765725	20	SBDSP
26	ILMN_1651354	21	SPP1
27	ILMN_2374449		SPP1
28	ILMN_1760347	22	SRGN
29	ILMN_2169152		SRGN
30	ILMN_2322356	23	STATH
31	ILMN_1672571	24	TFIP11
32	ILMN_1695000		TFIP11
33	ILMN_2408102		TFIP11
34	ILMN_1781374	25	TUFT1

B #	Probe ID	#	Gene Symbol
1	ILMN_1701603	1	ALPL
2	ILMN_1724480	2	AXIN2
3	ILMN_1722718	3	BMP2
4	ILMN_1658333	4	ECM1
5	ILMN_2329735		ECM1
6	ILMN_1801205	5	GPNMB
7	ILMN_2407389		GPNMB
8	ILMN_2207504	6	LEP
9	ILMN_2207505		LEP
10	ILMN_1677511	7	PTGS2
11	ILMN_2054297		PTGS2
12	ILMN_1795166	8	PTH1R
13	ILMN_1813753	9	PTN
14	ILMN_1760347	10	SRGN
15	ILMN_2169152		SRGN

C #	Probe ID	#	Gene Symbol
1	ILMN_1670912	1	ACVR2A
2	ILMN_2152711		ACVR2A
3	ILMN_1807493	2	ACVRL1
4	ILMN_1789095	3	BMPR2
5	ILMN_2070896		BMPR2
6	ILMN_1687583	4	CAV1
7	ILMN_2149226		CAV1
8	ILMN_1760778	5	ENG
9	ILMN_1783182	6	FBN1
10	ILMN_1704418	7	FOXD1
11	ILMN_1789400	8	FOXD2
12	ILMN_2173524	9	FOXD4
13	ILMN_1730670	10	FSTL3
14	ILMN_2051972	11	GPC3
15	ILMN_1752965	12	GREM1
16	ILMN_2124585		GREM1
17	ILMN_1687440	13	HIPK2
18	ILMN_1676563	14	HTRA1
19	ILMN_1727361	15	LEMD3
20	ILMN_2183938		LEMD3
21	ILMN_1652287	16	NOG
22	ILMN_1729161	17	NOTCH1
23	ILMN_1717636	18	RGMA
24	ILMN_1710598	19	SKI
25	ILMN_1767068	20	SMAD6
26	ILMN_2203891	21	SMAD7
27	ILMN_2203896		SMAD7
28	ILMN_1700705	22	SOST
29	ILMN_1781242		SOST
30	ILMN_1682316	23	TRIM33
31	ILMN_2351930		TRIM33
32	ILMN_1726967	24	TWSG1
33	ILMN_2214144		TWSG1
34	ILMN_1800317	25	WNT5A
35	ILMN_1912737		-

D #	Probe ID	#	Gene Symbol
1	ILMN_2152711	1	ACVR2A
2	ILMN_1687583	2	CAV1
3	ILMN_1760778	3	ENG
4	ILMN_1704418	4	FOXD1
5	ILMN_1730670	5	FSTL3
6	ILMN_1752965	6	GREM1
7	ILMN_2124585		GREM1
8	ILMN_1676563	7	HTRA1
9	ILMN_1717636	8	RGMA
10	ILMN_1767068	9	SMAD6
11	ILMN_2203891	10	SMAD7
12	ILMN_2203896		SMAD7
13	ILMN_1700705	11	SOST
14	ILMN_1781242		SOST
15	ILMN_2214144	12	TWSG1
16	ILMN_1800317	13	WNT5A

THANK YOU / DANK U WEL / OBRIGADO....

This is without doubt the most important part of this thesis. Not because of its scientific content but because it gives me the opportunity to acknowledge all the people (sorry in advance if I forgot someone!) that during these years contributed directly or indirectly to this work, making it possible. For a Portuguese this section is also an important part of living since it is when the memories of the past years are recalled with "saudade", a sentiment that has no direct translation to English but that can be (roughly) described as *"A somewhat melancholic feeling due to the absence of particular and desirable experiences and pleasures once lived".*

First of all I would like to thank my promoter. Hans, thank you for trusting in me for this challenging project. It was an excellent experience to work with you, to learn from your enthusiasm, openness to new ideas and always positive critical judgment.

For the current and former members of the bone lab, Andrea, Anke, Bianca, Marco, Bram, Claudia B., Claudia N., Hans, Jeroen, Jess, Katja, Ksenija, Marco, Marijke, Marjoleijn, Mark, Martijn, Nadia, Poom, Ruben, Sander, Tanja, Viola, I would like to thank you for the "gezelligheid" and for the many good moments spend together, in and out of the lab. Regarding work, I would like to thank specifically Marijke and Tanja for the precious help with experiments and Viola for our joint effort to improve the analysis of matrix vesicles.

From the bone group I would also like to thank specially to Marco: thank you for your help during the whole PhD time, from the first experiments to the last checks into my manuscripts and thesis.

To my paraninfs Bram and Jeroen. Bram, it was wonderful to sit together in the same office, to learn from your experience in the bone field and to chat openly about pretty much everything. Jeroen, it was enriching experience to work with you and to learn from your expertise with the array experiments and the data analysis. I really enjoyed talking to you about science. My apologies for not being able to pronounce your name correctly ☺.

Many other “non-bone” people contributed at a certain point to the work presented in this thesis.

Theo Luider and Peter Burgers thank you for introducing me to mass spectrometry-based proteomics and Sigrid Swagemakers for the help with the bioinformatics analysis of my first proteomics data. Wim Klootwijk, thank you for the help provided on trying to resuscitate the old (HP?)LC.

Jeroen Demmers and Karel Bezstarosti, thank you for your input for the proteomics studies and the analysis. I have learned a lot from you in this challenging field as reflected on our co-authored publications.

I also would like to acknowledge all the members of my PhD committee, Prof. Geert Carmeliet, Jeroen Demmers, Prof. Dirk Duncker, Dr. Guido Jenster, Prof. Peter van der Spek and Prof. Harrie Weinans for contributing to the final judgment of my thesis.

Being abroad is a beautiful experience. Like the wine, it is best savored after some years of maturation. Many friends contributed to this experience, making me feel here as well as at home. I would like to mention those who I met initially in Utrecht - Ana, Andy, Heiner, Luckasz, Matt - that helped me forget how difficult it is starting a new life abroad. For the other “allochtonen” like me - Catarina, Dasha, Henrique, Inês, Ivo, João M., João C., Lília, Márcia, Rui M., Rui F., Sandra, Zé - I would like to express my gratitude for the nice moments spent and to be spend together.

Queria também dedicar esta tese a todos os meus amigos de Portugal, especialmente ao Joel, Cuba, Tiago e André Nobre, pela sua amizade intemporal que faz com que cada reencontro seja como se estivéssemos juntos diariamente.

Esta parte da dedicatória vai para todos aqueles que apesar de estar longe da vista não estão longe do coração! A toda a minha família fica aqui o meu sentimento de apreço pelos valores e princípios de que me incutiram e que me fizeram chegar até aqui. A todos eles o meu Muito Obrigado!

Ao meu pai, a minha mãe e as minhas irmãs o meu obrigado pelo vosso apoio incondicional que esteve na génese desta aventura pelo estrangeiro e que me permitiu seguir em frente nos momentos mais difíceis. Um beijo grande e muito especial aos pequenotes da família, ao Afonso e a Mariana, que por hoje ainda não entendem o porquê destas palavras.

Por fim gostaria de agradecer o carinho e apoio da pessoa que a diário me tem de aturar ☺ Leticia, foi, é e continuará a ser uma prazer compartir contigo as coisas boas da vida (e quando tem de ser as menos boas também). Um grande beijo. Amo-te.

PhD PORTFOLIO

Name PhD student:	Rodrigo Dinis Aparício Mendes Alves
Erasmus MC department:	Internal Medicine
PhD period:	2006-2012
Research School:	Postgraduate School Molecular Medicine
Promoter:	Prof.dr. J.P.T.M. van Leeuwen
Co-promoter:	Dr. Marco Eijken

In-depth courses and workshops

2011
- Postdoc Career Development Initiative retreat.

2010
- Basic course on R.

2009
- Ernst Klenk Symposium in Molecular Medicine: "Extracellular Matrix in Health & Disease".

2008
- European Calcified Tissue Society PhD training course.
- Basic data analysis on gene expression arrays.

2007
- Applied bioinformatics workshop.

2006
- Summer school in proteomics basics: "Exploring the diversity of proteins".
- Neuro-Immuno-Endocrinology course and workshop.
- Biomedical research techniques course.

Presentations at national and international conferences

2011
- European Calcified Tissue Society & International Bone and Mineral Society meeting, Athens, Greece. Oral and poster presentation.
- Netherlands Proteomics Centre progress meeting, Utrecht, The Netherlands.
- Molecular Medicine day, Rotterdam, The Netherlands. Poster presentation.
- Science days of the Dept. of Internal Medicine, Antwerpen, Belgium. Poster presentation.

2010
- European Calcified Tissue Society meeting, Glasgow, Scotland. Poster presentation.
- Annual meeting of the Dutch Society for Calcium and Bone Metabolism, Zeist, The Netherlands. Oral presentation.

- Molecular Medicine day, Rotterdam, The Netherlands. Poster presentation.
- Science days of the Dept. of Internal Medicine, Antwerpen, Belgium. Oral presentation.

2009

- Annual meeting of the Dutch Society for Calcium and Bone Metabolism, Zeist, The Netherlands. Oral presentation.
- Science days of the Dept. of Internal Medicine, Antwerpen, Belgium. Poster presentation.

2008

- European Calcified Tissue Society meeting, Barcelona, Spain. Poster presentation.
- Human Proteome Organization meeting, Amsterdam, The Netherlands. Poster presentation.
- European Calcified Tissue Society PhD training course, Rome, Italy.
- Molecular Medicine day, Rotterdam, The Netherlands. Poster presentation.
- Science days of the Dept. of Internal Medicine, Antwerpen, Belgium. Poster presentation.

2007

- Netherlands Proteomics Platform meeting, Amsterdam, The Netherlands. Poster presentation.
- NucSYS consortium meeting, Rotterdam, The Netherlands. Oral presentation.
- Annual meeting of the Dutch Society for Calcium and Bone Metabolism, Zeist, The Netherlands. Oral presentation.
- Science days of the Dept. of Internal Medicine, Goes, The Netherlands. Poster presentation.

Other activities

2006-2009

- Member of the PhD/post-doc committee of the Erasmus Postgraduate School Molecular Medicine. Involved in the organization and evaluation of courses provided to other members of the school, including the 12th Molecular Medicine day.

2011

- Organization of the labday of the Dept. of Internal Medicine.

Awards and Honors

- Netherlands Proteomics Center valorization voucher granted to the project: "Biomarkers for weak bones, from bone-proteome to blood-based biomarkers." Other recipients: Eijken M. and van Leeuwen J.P.T.M.
- Best poster presentation at the 2011 Science days of the Dept. of Internal Medicine, Antwerpen, Belgium.

CURRICULUM VITAE

Rodrigo Dinis Aparício Mendes Alves was born on September 24th, 1982 in Loriga, Portugal. After finishing high school in Escola Secundária de Seia, he studied Biochemistry at Universidade da Beira Interior, Covilhã, Portugal. In 2005, he moved to Utrecht as part of the Erasmus program. At the Endocrinology department of the local university he worked on the characterization of spermatogonial stem cells under the supervision of dr. Ans M.M. van Pelt. Soon after completing this internship he obtained his biochemistry degree and in 2006 he returned to The Netherlands where he started as a PhD student in the department of Internal Medicine at the Erasmus MC in Rotterdam. His PhD project was focused on investigating bone formation from a proteomics perspective under the supervision of dr. Marco Eijken and prof. dr. J.P.T.M van Leeuwen. In 2012 he embraced a new challenge as a post-doc fellow in the team of prof. Thomas Hankemeier and dr. Rob Vreeken at the Netherlands Metabolomics Center in Leiden. He is currently involved in the study of muscle regeneration from a metabolomics perspective.

PUBLICATIONS

Alves R.D.A.M., Eijken M., van de Peppel J. and van Leeuwen J.P.T.M.. *Calcifying vascular cells and osteoblasts: independent cell types exhibiting extracellular matrix and biomineralization-related mimicries.* Submitted.

Alves R.D.A.M., Eijken M., Bezstarosti K., Demmers J.A.A., van Leeuwen J.P.T.M.. *Activin A suppresses osteoblast mineralization capacity by altering extracellular matrix composition and impairing matrix vesicle production.* Submitted.

Alves R.D.A.M., Demmers J.A.A., Bezstarosti K., van der Eerden B.C.J., Verhaar J.A.N., Eijken M. and van Leeuwen J.P.T.M.. *Unraveling the Human Bone microenvironment beyond the classical extracellular matrix proteins: a human bone protein library.* J. Proteome Res., 2011, 10 (10), pp 4725–4733.

Alves R.D.A.M., Eijken M., Swagemakers S.M.A., Chiba H., Titulaer M.K., Burgers P.C., Luider T.M. and van Leeuwen J.P.T.M.. *Proteomic Analysis of Human Osteoblastic Cells: Relevant Proteins and Functional Categories for Differentiation.* J. Proteome Res., 2010, 9 (9), pp 4688–4700.

Woeckel V.J., **Alves R.D.A.M.**, Swagemakers S.M.A., Eijken M., Chiba H., van der Eerden B.C.J. and van Leeuwen J.P.T.M.. *1α,25-(OH)2D3 acts in the early phase of osteoblast differentiation to enhance mineralization via accelerated production of mature matrix vesicles.* J. Cell. Physiol., 2010, 225: 593–600.

osteoblast
mineralization
differentiation
signalling
calcification
expression
formation
proteins
factors
osteoclasts
osteocytes
bone
tissue
function
activity
remodelling
osteoporosis
responsible
proteomics
regulation
studies
metabolism
cells
activin
mechanical
receptor
transcription
calcium
ECM
MVs
quality
matrix
vascular
type
forming
growth
different
vesicles
including
deposition
extracellular
effects
process
complex
mass
structure
detection
used
increased
involved
represents
composition
inhibition
action
binding
phosphate
markers
resorption
production
crucial
osteoprogenitor
specific
biological
development
phosphorylation
important
mesenchymal
hormones
methods
mature
originate
characterize
endocrine
changes
understood
RANKL
Chapter
identified
needed
field
Initially
abundant
contributing
collagen
surrounding
diseases
genes
associated
cytokines
molecules
stimulating
target
known
stages
clinical
modulate
new
result
section
leading
secretion
Smad
BMPs
homeostasis
phenotype
marrow
vasculature
surface
approaches
identification
modelling
ALP
RUNX
stem
skeleton
labelling
peptide
organic
crystal
quantification
pathological
apoptosis